HEC MONTRÉAL
École affiliée à l'Université de Montréal

A Robust Integration of Demand Response into Smart Grid's Capacity Expansion Planning : Considering the Uncertainty of Electric Vehicle's Charging Behavior

par
Sajad Aliakbari Sani

Thèse présentée en vue de l'obtention du grade de Ph. D. en administration
(spécialisation Sciences de la décision)

Janvier 2022

HEC MONTRÉAL
École affiliée à l'Université de Montréal

Cette thèse intitulée :

**A Robust Integration of Demand Response into Smart Grid's Capacity Expansion Planning :
Considering the Uncertainty of Electric Vehicle's Charging Behavior**

Présentée par :

Sajad Aliakbari Sani

a été évaluée par un jury composé des personnes suivantes :

Georges Zaccour
HEC Montréal
Président-rapporteur

Erick Delage
HEC Montréal
Directeur de recherche

Olivier Bahn
HEC Montréal
Codirecteur de recherche

Wei Qi
Desautels Faculty of Management, McGill
Membre du jury

Bissan Ghaddar
Ivey Business School at Western University
Examinatrice externe

Jorge Mendoza Gimenez
HEC Montréal
Représentant du directeur de HEC Montréal

Résumé

Le remplacement des énergies fossiles par des énergies renouvelables (ERs) est la principale solution pour pallier au problème du réchauffement climatique. Cependant, comme certaines ERs sont intrinsèquement intermittents, leur intégration dans les réseaux électriques pose de sérieux défis opérationnels, tels que la réduction de la fiabilité et de la stabilité du réseau. Une solution potentielle est la réponse à la demande (RD), qui consiste en un changement de la consommation en cas de déficit de production. La RD est considérée comme une sorte de réserve de capacité qui permet plus de flexibilité du côté de la demande et, par conséquent, une plus grande intégration des énergies renouvelables dans les réseaux électriques intelligents. D'autre part, l'expansion des véhicules électriques (VEs) dans les systèmes de transport urbain offre aux réseaux électriques la possibilité de mettre en œuvre des programmes de RD à grande échelle. En effet, la plupart des véhicules électriques privés sont garés pendant les heures de travail et la nuit. Par conséquent, leur calendrier de charge peut être décalé en fonction du prix de l'électricité ou des besoins du réseau. De plus, comme les VEs sont alimentés par des batteries, ils peuvent fournir au réseau des capacités de stockage mobiles pour améliorer la fiabilité et la qualité du réseau.

Cette thèse se décline sous la forme de trois articles qui tirent parti des méthodes de recherche opérationnelle pour analyser la future transformation des systèmes énergétiques et analyser les obstacles opérationnels à l'intégration de la RD, en particulier par les VEs, dans les réseaux électriques intelligents. Les trois articles adoptent et améliorent la formulation du modèle Énergie-Technologie-Environnement (ETEM) pour modéliser

l'expansion de la capacité des systèmes énergétiques. En particulier, dans le premier article, nous adoptons ETEM pour modéliser le système énergétique de la grande région de Montréal (GM). Nous analysons l'impact de différentes voies de décarbonation sur l'expansion future du système énergétique dans cette région. Cet article donne un aperçu des principaux changements technologiques, dans les secteurs résidentiel, commercial et des transports, nécessaires à l'atteinte de l'objectif de réduction des émissions de gaz à effet de serre (GES).

Ensuite, dans le deuxième article, nous introduisons l'incertitude de la DR dans ETEM et transformons le modèle en un problème d'optimisation robuste ajustable sur plusieurs périodes. Pour résoudre l'ETEM robuste (R-ETEM), nous approchons le problème de manière conservatrice en utilisant des règles de décision affines et développons une version améliorée de la décomposition de Benders pour résoudre efficacement le problème. Une illustration numérique est présentée pour évaluer les performances de notre approche sur une étude de cas réel qui étudie le système énergétique de la région « Arc Lémanique » en Suisse.

Enfin, dans le dernier article, nous nous intéressons exclusivement à la DR liée à la flotte de VEs connectés au réseau électrique. Dans cet article, le comportement de charge moyen de la batterie des utilisateurs de VEs est simulé à l'aide d'un jeu quadratique linéaire. Ensuite, nous développons une procédure de couplage entre R-ETEM et le modèle de comportement de charge pour ajuster le niveau d'incertitude dans R-ETEM. De cette façon, nous identifions des stratégies d'expansion de capacité robustes et cohérentes sur le plan comportemental. Tout comme dans le second article, l'étude de cas se base sur le système énergétique de la région « Arc Lémanique » pour évaluer la performance de notre approche.

Mots-clés

Réponse à la demande, véhicules électriques, grille intelligente, planification de l'extension de capacité.

Méthodes de recherche

Prise de décision robuste en plusieurs étapes, optimisation robuste, programmation linéaire.

Abstract

Replacing fossil fuels with renewable energies (RE) is the primary solution to overcome the issue of global warming. However, as RE are inherently intermittent, a large integration of them in electricity networks poses serious operational challenges, such as the reduction of reliability and stability of the network. One potential solution is demand response (DR), which is defined as the shifting of demand by consumers, in response to supply-side incentives offered at times of high wholesale market prices or when system reliability is jeopardized. DR is seen as a kind of reserved capacity that improves the demand side flexibility, and consequently, makes possible a larger integration of RE into smart grids. On the other hand, the expansion of electric vehicles (EVs) in urban transportation systems provides the power grids with the opportunity to implement DR programs at large scale. This is because most private EVs are parked during working hours and nights. Therefore, their charging schedule can be shifted in response to the price of electricity or network requirements. In addition, as EVs run on batteries, they can provide the grid with spatially mobile storage capacities to improve network reliability and quality.

This dissertation is a collection of three articles that leverage modern operational research techniques to analyze the expansion of the future energy system, and address operational obstacles on the integration of DR, specifically by EVs, into smart power grids. In all these papers, we have adopted and developed the formulation of the Energy-Technology-Environment-Model (ETEM) to model the capacity expansion of the energy system. In particular, in the first article, we adopt ETEM to model the energy system

of the greater Montreal (GM) region. We analyze the impact of different decarbonization pathways on the future expansion of the energy system in this region. This article provides insight into the main technological shifts, in the residential, commercial, and transportation sectors, to achieve a greenhouse gas (GHG) emission reduction target.

Next, in the second article, we introduce demand response uncertainty (DRU) into ETEM and cast it as a multi-period adjustable robust optimization problem. To solve the robust ETEM (R-ETEM), we conservatively approximate the problem using affine decision rules and develop an enhanced version of Benders decomposition to efficiently solve the approximated problem. A numerical illustration is presented to evaluate the performance of our approach on a real case study that surveys the energy system of the "Arc Lémanique" region in Switzerland.

Finally, in the last article, we exclusively focus on the DR provided by a large fleet of EVs connected to the electricity network. In this article, the average battery charging behavior of EV users is simulated using a linear quadratic game. Then, we propose a coupling algorithm between the R-ETEM and the charging behavior model to adjust the level of uncertainty in R-ETEM. In this way, we identify behaviorally consistent robust capacity expansion strategies. Similar to the second paper, a case study, based on the energy system of the "Arc Lémanique" region evaluates the performance of our approach.

Keywords

Demand response, electric vehicles, smart grid, capacity expansion planning

Research methods

Multi-stage robust decision making model,robust optimization, linear programming, mean-field game theory.

Contents

List of Tables

List of Figures

List of acronyms

DR Demand response

DRU Demand response uncertainty

DLC Desired level of charge

ETEM Energy technology environment model

ETEM-SG Energy technology environment model with smart grid

EV Electric vehicles

GEP Generation expansion planning

LQG Linear quadratic game

MCHF Million Swiss Frank

MFG Mean field game

MILP Mixed integer linear programming

RDRD Relative demand response deviation

RMPCA Robust multi-period conservative approximation

SRM Static robust model

To the loving memory of my father, to my mother, and to my dear wife, for her unconditional love and support.

Acknowledgements

Foremost, I would like to express my sincere gratitude to my advisors: Prof. Erick Delage and Prof. Olivier Bahn, for their patience, support, and mentorship. Their guidance helped me in all the time of research and writing of this thesis. Without their help this Ph.D. would not have been achievable.

I would like to thank Prof. Wei Qi for agreeing to be a part of my thesis committee and providing insightful comments and valuable feed backs. I am also thankful to Prof. Frédéric Babonneau and Prof. Alain Haurie for their valuable discussions and comments to improve my PhD thesis. Thanks are also due to Rinel Foguen, Azadeh Maroufmashat, Normand Mousseau, and Kathleen Vaillancourt, with whom I had the pleasure of collaborating on two of the papers in this thesis.

I am very grateful for the environment at HEC Montréal and at the inter-university research center GERAD, where I had the opportunity to pursue my Ph.D. studies. I also wish to acknowledge the financial support offered by my advisors, HEC Montréal Ph.D. program, and the Canadian IVADO programme (VORTEX Project).

Last but not least, I would like to express my deepest gratitude to my lovely wife and my mother, brother and sister, for their emotional support and encouragement.

General Introduction

Over the last 150 years, the global temperature has increased mainly due to the human activities, especially their greenhouse gas (GHG) emissions (Wuebbles et al., 2017). The emission of GHG, such as carbon dioxide (CO_2), has a long-lasting and devastating effect on our environment. According to an estimation by International Panel on Climate Change (IPCC), 15% to 40% of the total CO_2, emitted by human activities, will remain in the atmosphere longer than 1000 years (DeAngelo et al., 2017). Therefore, there exist a general consensus among environmental scientists about the urgent need for serious actions to mitigate GHG emissions. One strategy is to replace fossil fuels with renewable sources of energy. However, a large-scale adoption of renewables faces serious challenges such as low reliability and high cost of renewable technologies.

The intermittent nature of renewable energies, particularly wind and solar power, poses important operational challenges to ensure the reliability and stability of the electrical networks. In other words, electricity cannot be stored in large scale, therefore, electric power systems need to continuously and perfectly balance their production and consumption. To ensure this balance, traditional power systems relied on the flexibility of the supply side, i.e. adjusting the level of production by spinning reserve and fast ramping power plants. However, with higher penetration levels of renewables, the control over the output of generation technologies decreases. Therefore, modern smart grids incorporate demand side flexibility, through demand response (DR) programs, to achieve the essential balance. DR is defined as the shifting of demand by consumers, in response to supply-side incentives offered at times of high wholesale market prices or when system reliability is jeopardized (DOE, 2006). Unfortunately, implementing DR programs in large scale requires a great penetration of advanced smart metering devices and flexible loads.

Charging electric vehicles (EVs) is a growing and potentially significant load that provides not only large-scale demand response, but also large storage capacity. The duty cycles of most privately owned EVs are limited to only a few hours in the day (mostly mornings and afternoons). Therefore, a large number of these cars are usually parked during working hours and during nights. So, the charging schedule of these vehicles can be shifted in response to the requirements of the electric networks or the price of electricity. In addition, as EVs run on batteries, they can be seen as almost free , spatially mobile storage capacities that can provide the network with sufficient reserved capacity and ancillary services. For example, Montreal consumes around 230 GWh of electricity per day[1]. On the other hand, the capacity of the battery for Tesla Model S is around 100 kwh. This implies that less than 2 million of such EVs can provide enough storage to power the entire city for one day. This amounts to only 75% of the total number of registered vehicles in this city[2]. Nevertheless, integrating this load into the electric network is challenging because the mobility and charging behavior of EV users is not known, and a temporally-spatially imbalanced charging behavior might lead to network failure.

The overall objective of this dissertation is to develop models, analytics and insights to mitigate the operational obstacles of a large scale integration of renewable resources into the electric network by leveraging the opportunities offered by recent socio-economic-technical innovations that occurred in the smart energy-mobility systems, namely the expansion of DR programs and the emergence of EVs. This is achieved by modeling the entire energy chain using a generation expansion planning (GEP) problem, and modeling the DR offered by a large fleet of EVs which are connected to the network. GEP is a classical energy network problem that consists of determining the optimal sizes and types of production facilities to be installed, and the associated times at which they should be available to satisfy the growing demand of energy at a minimum cost (Luss, 1984). In particular, we use, and extend the formulation of an open source GEP problem, called the Energy-Technology-Environment-Model (ETEM) (Babonneau et al., 2017), to model the energy system.

Next, we briefly summarize the three contributions of this dissertation which are written as scientific papers.

The first chapter is an original application of ETEM for the energy database of the Greater Montreal (GM) region. We model the entire energy system of the GM region to analyze different transition pathways to a low-carbon energy system. We adapt the formulation of the ETEM to model the capacity expansion of the generation technologies as well as the penetration of final energy consumption technologies in the residential, commercial and transportation sectors. The planning model covers the years 2020-2050 and quantifies the potential contribution of each sector in the total GHG reduction target. In addition, it provides insights, for each sector, on the main technological transition needed to achieve carbon-neutrality. Finally, the developed model quantifies the optimal share of renewable energies in the total energy consumption of this region. This chapter reveals that the transportation sector plays a significant role in the decarbonizing the energy system. More specifically, the results show that to achieve a deep decarbonization target, all fossil fuel vehicles must be replaced with EVs by 2050. The electrification of the transportation sector not only phases out fossil fuels consumption in this sector, but also results in a larger integration of renewables in the electricity network by offering demand flexibilities.

The second chapter models demand response uncertainty (DRU) in ETEM. In previous work, ETEM had modeled DR as a decision variable which is entirely controlled by the supply side. In other words, the policy maker plans for a target DR in the future. Then, by implementing DR programs, network operators actualize the targeted level of DR. However, in practice there is always a deviation between the planned and the actual DR. In this chapter we model the relative demand response deviation (RDRD) as an implementation error of the DR decision variable. The resulting model takes the form of an adjustable multi-period robust optimization problem. In a first stage, before having any information about the actual level of DR, the planner decides on a robust capacity expansion, as well as, a planned demand response. Afterward, on a season to season basis, the planner decides on the optimal energy procurement, taking into account the actual contribution to DR programs in that season. The performance of the proposed robust ETEM model is evaluated on a real-world case study based on the energy system of the Arc Lémanique region in Switzerland. To solve the problem, we derive a Robust Multi-Period Conservative Approximation (RMPCA) of the problem, and develop a new Benders decomposition algorithm (inspired from Ardestani-Jaafari and Delage, 2018) to solve it. Therefore, this chapter's contribution is summarized as i) introducing DRU in a GEP problem and proposing a robust multi-period formulation of the problem in which the procurement decisions are adjustable to the realized DR, ii) developing a new Benders decomposition algorithm in which we seek Pareto Robustly Optimal (PRO) solutions (see Iancu and Trichakis, 2014) of the master problem in order to accelerate the convergence of the algorithm in large scale instances, and iii) solving a realistic case study whose size, in deterministic setting, is two orders of magnitude larger than the largest instance in the literature. The findings of this chapter reinforces the importance of considering the uncertainty of DR in GEPs. In particular, it shows that an adjustable robust capacity expansion strategy can reduce the average total cost of the system by 33% (equivalent to 9 billion Swiss Frank) compared to a deterministic capacity expansion plan.

In the third chapter, we turn our focus on the DR provided by a large fleet of EVs connected to the electricity network. The objective of this chapter is to seek a *behaviorally consistent*, robust capacity expansion strategy in the sense that it would be immune against the demand response deviations observed in a battery charging behavior model. To do so, we adopt, develop and calibrate the battery charging behavior model introduced in Tchuendom et al. (2019) to estimate the actual DR for the entire fleet of EVs. Then, we propose an original approach to integrate the information provided by this model when adjusting the size of the uncertainty set of the robust ETEM (R-ETEM). The performance of this approach is numerically evaluated on a real case study that surveys the energy system of the "Arc Lémanique" region in Switzerland. The contribution of this chapter is to develop a new coupling algorithm between the R-ETEM and a short-term higher-precision battery charging behavior model. The results show that a behaviorally consistent robust strategy is able to reduce the average total cost of the system by 6.2% compared to a deterministic expansion strategy.

Overall, the proposed approach in this thesis could be used by policy makers to plan the expansion of the energy system while considering the interconnection between the energy sector and the transportation sector. In addition, we provide a framework to deal with the uncertainty in the capacity expansion planning.

Chapter 1

Energy Transition Pathways for Deep Decarbonization of the Greater Montreal Region: An Energy Optimization Framework

Chapter information

This article is a joint work with my supervisors, Olivier Bahn and Erick Delage, and other co-authors: Azadeh Maroufmashat, Frederic Babonneau, Alain Haurie, Normand Mousseau, and Kathleen Vaillancourt. It is under preparation and will be submitted to the journal of Energies.

Abstract

More than half of the world's population are living in cities, and by 2050, it is expected that this number will reach almost 68%. These densely populated cities consume more than 75% of the world's primary energy and are responsible for the emission of around 70% of anthropogenic carbon. Providing sustainable energy for the growing demand

in cities requires multi-faceted planning approach. In this study, we have modeled the energy system of the Greater Montreal region to evaluate the impact of different environmental mitigation policies on the energy system of this region over a long-term horizon (2020-2050). In doing so, we have used the open-source optimization-based model called Energy-Technology-Environment-Model (ETEM). ETEM is a long-term bottom-up energy model that provides insight on the best city's options to procure energy, and satisfy useful demands while reducing carbon dioxide (CO_2) emissions. Results shows that, under a deep decarbonization scenario, the transportation, commercial, and residential sectors will contribute to the emission reduction by 6.9, 1.6, and 1 million ton CO_2-eq in 2050, respectively, compared to their 2020 levels. This is mainly achieved by i) replacing the fossil fuel cars with electric-based vehicles in private and public transportation sectors, ii) replacing fossil fuel furnaces with electric heat pumps to satisfy heating demand in buildings, and iii) improving the efficiency of buildings by isolating walls and roofs.

1.1 Introduction

Human activities in recent years have increased levels of greenhouse gases (GHG), including carbon dioxide (CO_2), resulting in global warming. A projection of the current trends (Masson-Delmotte. et al., 2018) shows that the global temperature may exceed the Paris Accord goal of 1.5°C by 2030. To avoid dangerous disruptions in the climate system, one thus need to implement urgent mitigation measures.

Energy production is among the most important human activities that are responsible for more than three fourths of the global GHG emissions (IEA, 2021). Therefore, the decarbonization of energy systems is one of the most important measures against global warming. On the other hand, cities, as the main consumers of energy commodities, can play an important role in GHG reduction. Currently, over 55% of humans live in urban areas, and it is expected that this number will reach 68% by 2050[1]. The economic activ-

[1] see https://www.un.org/development/desa/en/news/population/2018-revision-of-world-urbanization-prospects.html

ities in cities form nearly 80% of the global gross domestic production (GDP), and they consume more than 75% of the world's primary energy, and emit more than 70% of anthropogenic carbon (Dias et al., 2019; IEA, 2021). Studies show that a proper city-level energy management can potentially reduce emissions from urban buildings and transportation systems up to 90% by 2050 (CFUT, 2019). Therefore, in recent years, significant actions have been taken by many cities, sub-national states, and private sectors to mitigate emissions at an urban scale. A summary of these actions can be found in a study by Coelho et al. (2018) for Portuguese municipalities, in another study by Albana et al. (2016) for European municipalities, and in "Climate Innovation Program"[2] for Canada.

This paper proposes a framework to model and analyze the energy transitions pathways of the Greater Montreal (GM) region in the province of Quebec in Canada. The province of Quebec plans to reduce its GHG emissions to 37.5% of their 1990 level by 2030, and to reach carbon neutrality by 2050 (Municipal, 2020; Whitmore and Pineau, 2019). To this end, Quebec has developed a green economy plan for 2020-2030, with the purpose of stimulating the economy, creating jobs, etc., while reducing GHG emissions. Specifically, the government of Quebec plans to i) spend over 6 billion dollars during the first five years (i.e., 2021-2026) to accelerate the widespread deployment of electrification for infrastructures in transportation, industrial, residential, and commercial sectors, ii) promote the utilisation of bio-energies, renewables, natural gas, and hydrogen for decarbonizing the heating demand in commercial and industrial sectors, and iii) improve the performance of final energy consumption technologies, and energy efficiency (Municipal, 2020; Whitmore and Pineau, 2019). However, these provincial plans need to be broken-down into city-level targets in order to become achievable. The purpose of the current study is to analyze the entire energy system of the GM region to highlight the potentials of GHG reductions by considering different technological options on both the supply and demand sides. Different technological options in the transportation sector include hybrid, electric hybrid, biomass-based and natural-gas vehicles in the private and public transportation sectors. In addition, we have considered different electric and

[2]See https://fcm.ca/en/programs/municipalities-climate-innovation-program

biomass furnaces and plinthes to satisfy the heating and cooling demand in the residential and commercial sectors. Finally we consider installing more capacities of solar and wind turbine power plants as possible future technologies to generate electricity.

Our methodology is to optimize the configuration of energy systems at an urban level. Specifically, we adapt the formulation of the open-source Energy-Technology-Environment-Model (ETEM), proposed by Babonneau et al. (2017), to model the capacity expansion of generation technologies as well as final energy consumption technologies in different sectors. ETEM minimizes the total energy system costs, including investment, fixed and variable operational costs, while satisfying demand and environmental constraints. One salient feature of ETEM is its ability to consider necessary details on the demand side, such as how energy is used by consumers, and how electrical networks perform demand response programs. Such a detailed emphasis on the demand side technologies makes this model well-suited to analyze the energy value chains and different GHG reduction policies at a city level. Finally, we perform a sensitivity analysis to evaluate the impact of different GHG reduction scenarios on the expansion of the energy sector in the GM region. Therefore, the main contribution of this paper is to present an original application of ETEM for analyzing the energy system of the GM region under different decarbonization scenarios.

The structure of the paper is as follows: Section 1.2 provides a literature review on the related studies. In Section 1.3, we present the methodology and the description of ETEM. Section 1.4 elaborates on the definition of scenarios. Section 1.5 describes the results, and Section 1.6 provides further discussion on our major findings. Finally, we conclude in Section 1.7.

1.2 Literature review

In this section, we first review recent publications that study the impacts of environmental policies on energy systems. Specifically, we investigate their methods and their case studies. Then, we give a summary of the history of ETEM, and introduce the most important case studies that have been analyzed using ETEM.

One related stream of research is to study the energy transition and evaluate the environmental impact of a single sector, such as transportation (Forsberg, 2021), buildings (Acha et al., 2018), or power distribution networks (Mehleri et al., 2013). Forsberg and Krook-Riekkola (2021) developed a local energy transition model for transportation sector using the TIMES-City model in Sweden. Yuan et al. (2018) investigated techno-economic impacts of the electrification of transportation systems using energy PLAN for a region in China. Although these studies consider a detailed dynamic of a specific sector, they abstract away the interactions between different energy sectors, so they lack a holistic view point. On the other hand, one stream of research studies the optimal design of urban multi-energy hub networks, including their location, capacity and other technical characteristics (see for example Maroufmashat et al., 2016, 2015; Heinisch et al., 2019), with the purpose of reducing GHG emissions. Although these papers consider the interaction of different energy hubs, they ignore the dynamic of investment, and therefore do not provide insight on the expansion strategies in a long-term horizon planning. Another stream of research is to study the energy transition at a national level. Vaillancourt et al. (2017, 2018) investigate decarbonization pathways for Canada until 2050 using the "North American TIMES Energy Model" (NATEM). Shakouri and Aliakbarisani (2016) developed a framework to consider sustainable development criteria in modeling the energy system at a national level. These national models provide a detailed modeling of the supply technologies, but, in order to avoid the curse of dimensionality, they fail to model the demand side characteristics, such as demand response, detailed description of final energy technologies, and distribution-level electrical network services (e.g., voltage control or reactive power compensations).

Energy planning of an urban scale requires a detailed modeling of how the final energy is used in cities, what are possible options to satisfy energy services, and how the consumption behavior in one section might affect the energy consumption in other sections. To this end, urban energy planning models have a holistic viewpoint that integrates different sectors, such as transportation, residential, commercial, etc. Mirakyan and De Guio

(2013) and Scheller and Bruckner (2019) presented a review of methods and approaches to model the energy system at an urban scale. Dagoumas (2014) explores the interconnection between socioeconomics, energy, and environmental components for the city of London. Xydis (2012) develop an optimization model to identify the optimal strategy to meet the energy requirements of Athens while satisfying techno-economic constraints. Elizondo et al. (2017) evaluates different decarbonization scenarios of the energy system in Mexico City by 2050 using an integrated approach. Finally, Lind and Espegren (2017) use the TIMES model to design an optimal low-carbon pathway for the energy system of the city of Oslo, Norway. But it remains that there is only a limited number of paper at the city level. This paper contributes to this limited body of literature by proposing an application for the city of Montreal.

In this paper, we use ETEM to analyze the energy system of the GM region and evaluate different energy transition pathways. ETEM provides the planner with a decision making framework that not only considers a detailed description of the useful demand technologies, but also models some important characteristics of the demand side, such as demand response in electrical networks. ETEM was first formulated by Andrey, Christopher et al. (2015) and Babonneau et al. (2012) to model the energy system of the Midi-Pyrénées region in France and the Arc Lémanique region in Switzerland. Babonneau et al. (2017) and Babonneau et al. (2016) further developed the ETEM model by introducing a linear approximation of power flow constraints and distribution module. In addition, the new formulation, called ETEM-SG, explicitly modeled the reserve capacities provided by demand response and ancillary services, such as reactive power compensation offered by flexible loads. Babonneau et al. (2017) and Babonneau and Haurie (2019) presented a version of the ETEM-SG that considers the uncertainty of investment costs and of availability of technologies and transmission capacity lines. A static robust optimization approach is used to solve the problem. Aliakbarisani et al. (2020) developed a robust multi-period formulation of ETEM, with uncertain demand response, to better control the level of conservatism in planning. Finally, Babonneau et al. (2020) and Aliakbarisani et al. (2021) linked two robust versions of ETEM to a mean-field-game model that presents the charging behavior of a large fleet of electric vehicles (EVs). This paper is an original application of ETEM for the energy database of the GM region.

1.3 Methodology

This research paper proposes a model for optimal expansion planning of the existing and future technologies in the energy sector of the GM region up to 2050, while meeting GHG emission reduction targets. To do so, we use the formulation of the Energy-Technology-Environment-Model (ETEM). Introduced for the first time by Andrey, Christopher et al. (2015); Babonneau et al. (2012), ETEM is an open-source energy model designed to analyze the energy system at an urban scale. We slightly modify the formulation of ETEM to adapt it to the Montreal database. For example, contrary to the original version which calculates the emission at the process level, we are calculating emissions based on the total primary energy consumption in the entire system. More specifically, we measure the amount of primary energy consumed in the entire energy system (either to generate electricity or to satisfy the useful demand, such as residential heat), and calculate the total emission by multiplying the total consumption of each primary energy with its emission factor.

1.3.1 ETEM model description

ETEM is an open-source, long-term, regional, bottom-up energy model cast as a linear programming problem. ETEM belongs to the MARKAL-TIMES family of models, and in a more general framework is a capacity expansion problem. ETEM models the entire energy sector from primary resources to useful demands and suggests the best combination of the generation and end-user technologies to satisfy the growing demands at a minimum cost. Because of a detailed description of the demand side technologies, ETEM is mostly used to analyze the energy system at regional and urban scales. For example, ETEM has been applied to model the energy system of the Midi-Pyrénées region in France (Andrey, Christopher et al., 2015) or the Arc Lémanique region in Switzerland (Babonneau et al., 2017; Babonneau and Haurie, 2019).

In ETEM, the planning horizon is typically 30 - 50 years which includes several decision making periods. Each decision making period typically represents a duration of 5 years. Moreover, in order to capture the consumption and generation short-term patterns, each year is divided into several time-slices with similar demand loads. For example, Babonneau et al. (2017) and Babonneau and Haurie (2019) divide each year into 3 seasons; and a typical day in each season is divided into 4 load-parts: morning, peak-day, peak-night and night. Therefore, in total, they introduce 12 time-slices in a year that capture different demand load patterns. However, in this research we are modeling higher-resolution time-slices with hourly load parts. In other words, we consider 4 seasons, including winter, spring, summer and autumn. In addition, each season is represented with a typical day with 24 hourly load parts. Therefore, we consider in total 96 time-slices in a year.

The objective function in ETEM is to minimize the total discounted cost of the system over the entire planning horizon. The total cost consists of i) investment cost, ii) fixed and variable operational and maintenance cost, iii) net import and export cost, iv) energy transmission cost and finally v) the salvage value that considers the end-of-life value of the retired technologies. The model provides insights on the optimal capacity expansion and the optimal level of production for each technology as well as the optimal level of import and export for each primary energy or energy resource. In addition, ETEM gives insights on the optimal level of demand response by flexible loads. The demand response, which is defined as shifting the electricity demand from peak to off-peak time-slices, reduces the need to build extra reserved capacity in the system.

Different constraints in ETEM are categorized into technical, network, environmental and economic constraints. Technical constraints guarantee that the solution of the model meet technical characteristics of the generation technologies. For example, technology efficiency and capacity factor constraints limit the level of input and output energy of each technology according to its efficiency and capacity factor. Network constraints guarantee the balance of energy in the entire energy sector. In addition, network constraints limit the energy flow between regions to the capacity of the transmission lines. Environmental constraints limit the total, and annual, GHG emissions of the system to a desired level. And finally the economic constraints refer to a group of constraints that force the solutions of the model to meet realistic economic limitations. For example, market penetration, annual or total constraints on capacity addition, and annual or total constraint on import or export of the energy commodities are among economic constraints that are considered.

1.3.2 Adapting ETEM for the Montreal database

We have modeled the energy system of the GM region in the province of Quebec in Canada. This region consists of 5 main sub-regions, including Montreal agglomeration, Laval, Longueuil, Couronne Nord and Couronne Sud. The planning horizon runs from 2020 to 2050 and is divided into 6 decision making periods with a length of 5 years. Moreover, each year has 96 time-slices. We use 2015 as a base year to calibrate the model. In other words, we have calibrated the input parameters so that the results of ETEM for 2015 (including the total energy consumption, emission, etc.) correspond to the actual statistics in this year. In 2015, the total energy consumption of the GM region was 642 PJ with 20.8 Mt CO_2-eq emissions (Vaillancourt et al., 2017). The region imported 201 PJ of electricity, and generated 34 PJ internally. In the transportation sector, the region consumed 101 PJ, 2.7 PJ and 0.3 PJ of gasoline, diesel and electricity respectively. In total, the transportation sector emitted 6.9 Mt CO_2-eq. In the residential and commercial sectors, there were 67 and 51 PJ of energy consumed respectively, resulting in emissions of 2.9 Mt CO_2-eq.

Fig. 1.1 gives an overview of the reference energy system (RES) in the GM region. In this figure, each horizontal line represents a category of energy commodities, and each box represents a family of conversion technologies. In total, the model includes 51 energy commodities, and 130 conversion technologies in different sectors. We have modeled 13 types of useful demands which are categorized into industrial (IND), agricultural (AGR),

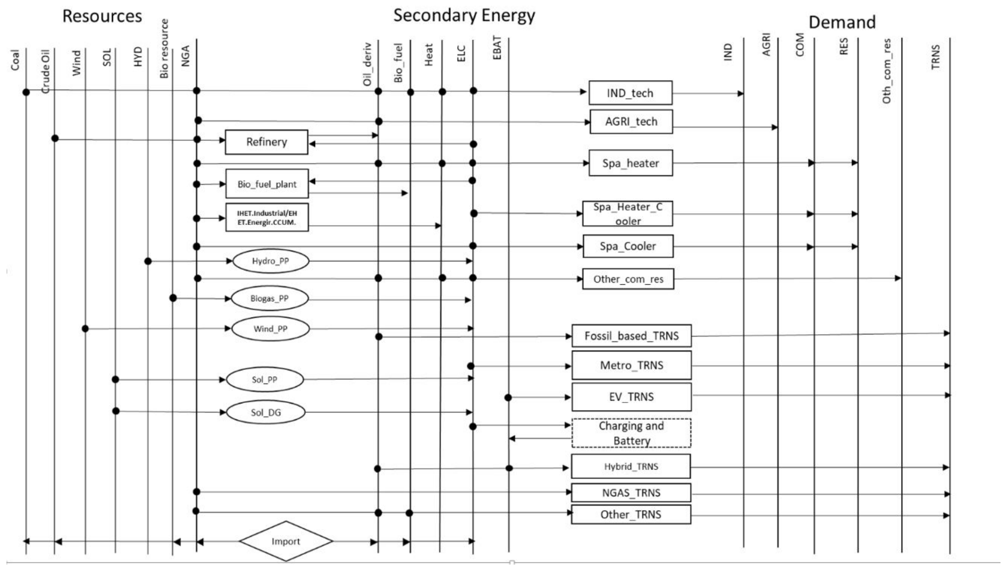

Figure 1.1: Overview of the reference energy system (RES) in the Greater Montreal region. SOL stands for solar, HYD for hydro, NGA for natural gas, PP for power plant, DG for distributed generation, ELC for electricity, EBAT for the electricity of batteries, IND for industry, AGRI for agriculture, Spa for space, TRNS for transportation, EV for electric vehicles, RES for residential, and COM for commercial.

commercial (COM), residential (RES), and transportation (TRNS). The usefull demand in the transportation sector is divided into 5 modes, including i) light duty vehicles, ii) public transportation, iii) trains, iv) metros, and v) other kinds of transportation (including maritime and air transportation). While a generic technology represents the fuel consumption in "other transportation" mode, a detailed breakdown of all current and possible future technologies are considered for light duty vehicles, public transportation trains and metros. Gasoline, natural gas, diesel, and electricity are the main fuels consumed in the transportation sector. Residential and commercial demands include useful energy demand for space heating, space cooling, and "other consumption" (including lighting, electrical appliances, etc.). Similar to transportation, a generic technology represents the energy consumption in the "other consumption" category, but detailed technology choices are modeled for space heating and cooling, including furnaces, different types of heaters, as well as heat pumps. Industrial demand includes coal, natural gas, electricity, heat, diesel, light and heavy fuel oil, propane, and bio fuels. Finally, the agricultural sector consumes natural gas, electricity, gasoline, diesel, light and heavy fuel oil, and propane.

Energy commodities are either generated by the already available generation technologies inside the GM region, or imported from the outside. Specifically, we have modeled two existing hydro-power stations (Beauharnois in Couronne Sud and the Prairies river station in Laval), two existing biogas electricity and heat generation units (one in Couronne Nord and one in the Montreal agglomeration), and the potential to install wind and solar power plants in the north and south of the Montreal island. In addition, we have modeled the Montreal refinery that produces diesel, gasoline, light and heavy fuel oil, propane, and other oil products. Finally, there are two existing bio-ethanol and bio-diesel generation units in Couronne Sud. These generation units can satisfy more than the internal demand and exports part of its production outside the GM region. Beside the internal production, the model also considers the imports of resources and secondary energies. The imported resources include, crude oil, natural gas, and coal. And the imported secondary energies include oil products (gasoline, diesel, light and heavy fuel oil, propane, petroleum coke and jet fuel), ethanol, bio resources (bio diesel, bio gas) and electricity.

Fig. 1.2 provides a summary of the important input and output of the ETEM model calibrated for the GM region. The input data includes energy demand, energy prices, resource availability, technical and economical information for technologies, as well as carbon content of different fuels. The input data are extracted and aggregated from the NATEM database (Vaillancourt et al., 2017). This database includes 475 energy form, 4500 energy conversion technologies, 70 final energy services in the north America. The database provides a periodically prediction of demand and technological characteristics for the period 2010 to 2050 (The periods include 9 decision making intervals of variable length). All costs are transformed to the level of prices in 2011 and are expressed in Canadian dollars. Finally, an annual discount rate of 5% is considered (Vaillancourt et al., 2018). Outputs correspond to optimal capacity expansion plan, optimal import and export of the energy commodities, and the marginal cost of CO_2 emissions.

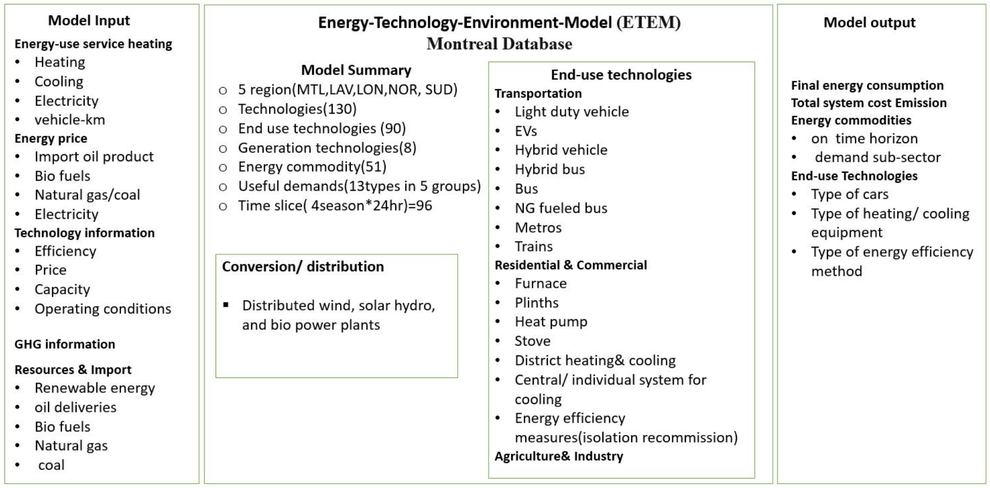

Figure 1.2: A summary of inputs, outputs and the main characteristics of ETEM adapted for the Greater Montreal region.

1.4 Scenarios

Quebec aims at achieving 37.5% GHG emission reduction by 2030 (compared to 1990 levels), and reaching carbon neutrality by 2050 (Municipal, 2020; Whitmore and Pineau, 2019). Motivated by this target, we define four scenarios by imposing different CO_2 emission constraints on the main energy sub-sectors, including secondary energy generation, transportation, commercial, and residential. More specifically, the CO_2 constraint imposes a maximum emission ceiling to the main generation units and final energy consumption sectors. The generation units include power plants, bio-fuel, and oil product generation units. The energy consumption sectors include transportation (light duty vehicles, public transportation, trains, and metros), commercial, and residential (heating and cooling demand). We give below the details of each scenario:

- Business as usual (**BAU**): This scenario is a reference scenario that includes all current provincial policies, such as governmental financial incentives for a large adoption of electric vehicles. But, this scenario imposes no limitation on GHG emissions. In other words, this scenario is a disengagement from the state targets in the sense that no further climate measures are enforced beyond those already in place.

- **GHG1**: A GHG emission reduction scenario with a 37.5% reduction target by 2030, and a 53% reduction target by 2050 (relative to 1990).
- **GHG2**: A more stringent reduction scenario with a 37.5% GHG reduction target by 2030, and continuing the same reduction trend until 2050, which yields a 73% emission reduction (relative to 1990).
- **GHG3**: A deep decarbonization scenario which assumes a linear GHG reduction to achieve a 44% reduction by 2030 and a 93% reduction by 2050 (relative to 1990).

1.5 Results

In this section, we present the main results obtained. Our purpose is to show how each sector contributes to the GHG emission reduction, what are the main technological changes, and how the pattern of primary energy consumption changes.

1.5.1 GHG emission

In this section, we present the total GHG emissions of the transportation, residential and commercial sectors, and evaluate how each sector contributes to the reduction target. Fig. 1.3 shows the total emission of these sectors from 2020 to 2050. In GHG1, GHG2 and GHG3 scenarios, emission reductions follow the emission constraints. Besides, emissions are decreasing in the BAU scenario due to the increasing share of electric-based vehicles in the transportation sector, but partly offset by the growing fossil fuel consumption in the residential and commercial sectors.

Fig. 1.4 gives next the breakdown of emissions by sector. It shows that transportation with 6.9 Mt CO_2-eq has the largest share in 2020 (60% of the total), as the current transportation system mostly relies on petroleum fuels. Over time, the share of the electric vehicles (EVs) increases following an assumed price reduction for these technologies. This price reduction is partly due to governmental incentives to promote the purchase EVs, and partly to a long-term technological price reduction. Consequently, the share of

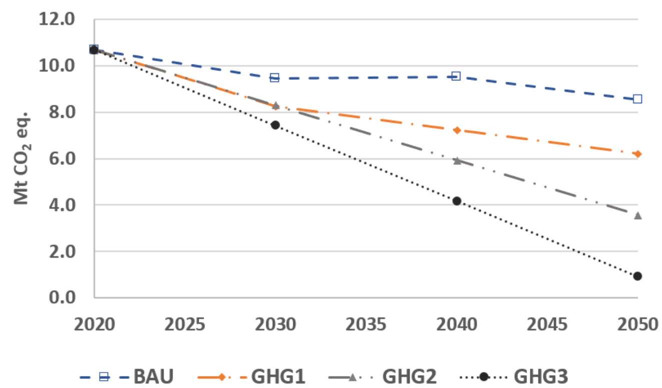

Figure 1.3: Total GHG emissions for different environmental scenarios.

the transportation sector in the total GHG emission, in the BAU scenario, reduces to 15% by 2050. Imposing CO_2 emission constraints further reduces the share of the transportation sector in the total emission by replacing conventional and hybrid cars with plug-in electric vehicles. In particular, emissions of the transportation sector reduce to almost zero in 2050 in GHG3.

Emissions of the residential sector increase in the BAU scenario as ETEM relies mostly on natural gas in order to satisfy the heating and cooling demands. However, imposing environmental constraints forces ETEM to electrify this sector. In particular, emissions of the residential sector reduces from 0.7 in 2020 to 0.3 Mt CO_2-eq in 2050 in GHG3. Finally, the commercial sector is responsible for 23% of the total CO_2 emission in 2020. In the BAU scenario, emissions of this sector increases from 2.2 in 2020 to 2.5 Mt CO_2-eq in 2050. But under a deep decarbonization scenario (GHG3), this sector will only emit 0.6 Mt CO_2-eq in 2050.

Fig. 1.5 depicts how each sector contributes to the total CO_2 emission reduction when a deep decarbonization constraint (in GHG3) is imposed. Specifically, this constraint reduces the total emission to around 3 and 10 Mt CO_2-eq in 2030 and 2050, respectively, compared to the BAU scenario. This figure also reveals that imposing such environmental constraint mostly affects the residential sector. On the other hand, the lower effect is on the transportation sector, as it is already largely decarbonized in the BAU scenario, following an assumed price reduction for EVs.

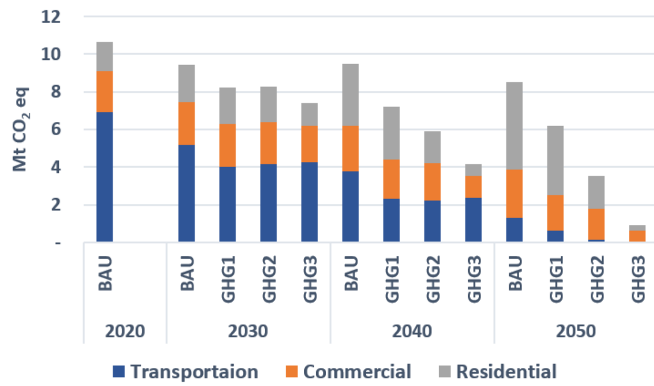

Figure 1.4: Breakdown of GHG emission reductions by sectors and environmental scenarios.

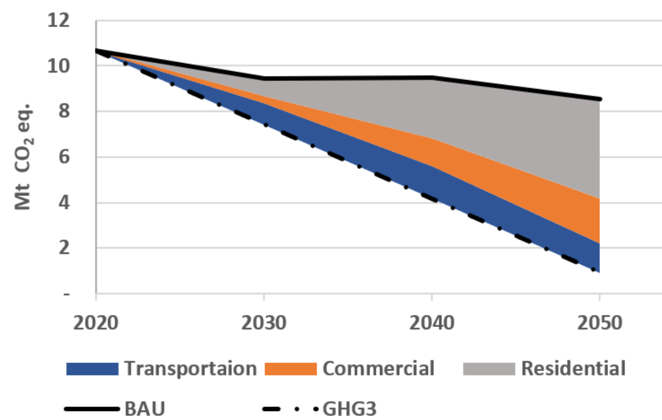

Figure 1.5: Contribution of each sector in the total GHG reductions in the deep decarbonization environmental scenario (GHG3) compared to the reference scenario (BAU).

1.5.2 Final energy consumption

Fig. 1.6 illustrates the final energy consumption by type of fuel in the GM region under different environmental scenarios. While natural gas will be the dominant source of energy in 2050 in the BAU scenario, GHG3 proposes a combination of technologies that mostly consume electricity. Namely, electricity consumption will be tripled in 2050 compared to 2020 in GHG3. In addition, the consumption of gasoline, as one of the most important fuels in the current energy system (2020), will be gradually reduced even in BAU. More specifically, the consumption of gasoline reduces from 101 PJ in 2020 to 19.2 in 2050 in BAU, and to almost zero in GHG1, GHG2 and GHG3. Besides the shift in the primary energy composition, the total level of consumption is also affected by the environmental constraint scenarios. For example, total primary energy used in GHG3 is 13% and 30% less than in BAU in 2030 and 2050, respectively. The reason is that imposing environmental constraints encourages to invest on more efficient technologies. In addition, total primary energy used in the residential and commercial sectors decreases because of investments in buildings insulation.

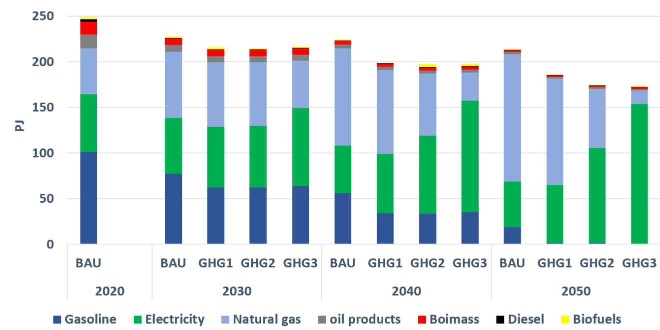

Figure 1.6: Total final energy consumption by type of energy and environmental scenarios.

With around 108 PJ in 2020, the transportation sector is the largest primary energy consumer in the GM region (compared to the residential and commercial sectors). In addition, gasoline, with 101 PJ, is the dominant fuel in this sector in 2020 (see Fig. 1.7). Diesel and ethanol are the second and third fuels with 3 PJ and 2.1 PJ, respectively, in 2020. Finally, light duty vehicles consume the largest amount of energy compared to other transportation vehicles, such as public buses and metros. Fig. 1.7 also indicates that the consumption of gasoline and diesel is gradually reduced over time, as these fuels are substituted by electricity, even in BAU. This is due to i) an assumed increasing cost of fossil-based fuels, and ii) an assumed price reduction of the electric-hybrid vehicles over time, as a consequence of governmental incentives to promote these cars and the long-term lowering in the price of hybrid and electric cars. In addition, stringent environmental constraints (in GHG1, GHG2 and GHG3, respectively) result in bigger electrification rates for the transportation sector. Finally, a transition to electricity reduces total energy consumption in this sector due to the higher efficiency of EVs and electric public buses.

The residential sector is the second largest energy consumer in the GM region in 2020, with a primary energy consumption of around 91 PJ to satisfy heating and cooling

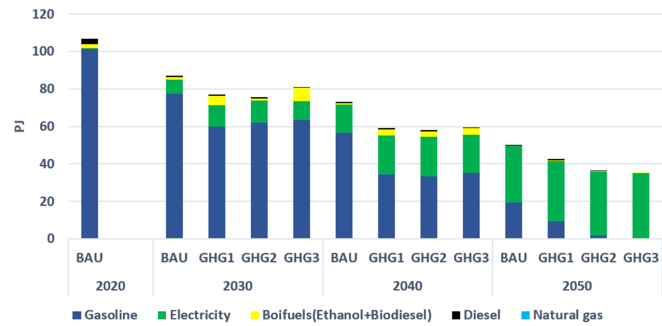

Figure 1.7: Final energy consumption by type in the transport sector.

demands. Electricity corresponds to around 58% of total energy consumption in 2020, followed by biomass, natural gas, and oil products with 15.4%, 14.8%, and 11.5%, respectively (see Fig. 1.8). But by 2050, in BAU, natural gas dominates. More precisely, natural gas-based furnaces and stoves are the main technologies to satisfy heating demands, followed by electrical baseboard heaters. This is due to a lower marginal cost of natural gas compared to electricity. However, imposing more restrictions on CO_2 emissions (in GHG1, GHG2, and GHG3), encourages a higher penetration of electrical baseboard heaters and heat pumps, and consequently reduces further the share of natural gas in total energy consumption. This also triggers larger investments in residential buildings insulation, which reduces final energy consumption. Finally, one can note that the electrification rate is highly sensitive to the severity of the CO_2 reductions, with by 2050 levels of 28%, 63%, and 92%, in GHG1, GHG2, and GHG3, respectively. Transitioning to near-zero emissions in this sector requires thus stringent environmental restrictions.

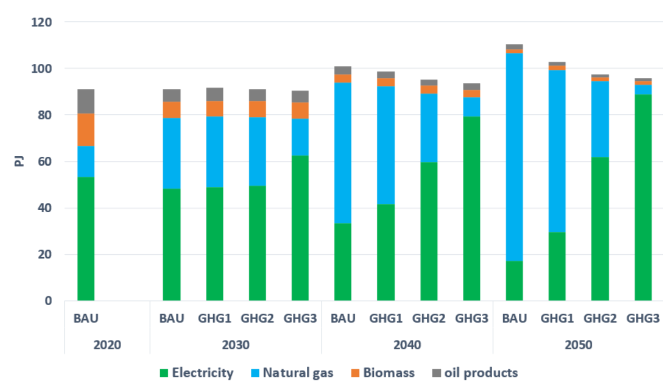

Figure 1.8: Final energy consumption by type in the residential sector.

Concerning the commercial sector, it uses 50.8 PJ of primary energies in 2020. Natural gas, with 73% of total energy consumption, is dominant in 2020. Electricity and oil products are second and third with 18% and 9%, respectively (see Fig. 1.9). With no or less-stringent environmental restrictions (in BAU, GHG1 and GHG2), natural gas remains dominant by 2050. Similarly to the residential sector, this is due to a lower marginal cost for natural gas compared to electricity. However, under a deep decarbonization (GHG3), a transition from fossil-based furnaces to electrical heat pumps takes place to satisfy heating demands. The share of electricity in this scenario thus increases from 18% in 2020 to 71% in 2050. In addition, imposing environmental constraints (in GHG1, GHG2 and GHG3) increases investments in commercial buildings insulation, and thus reduces final energy consumption compared to BAU.

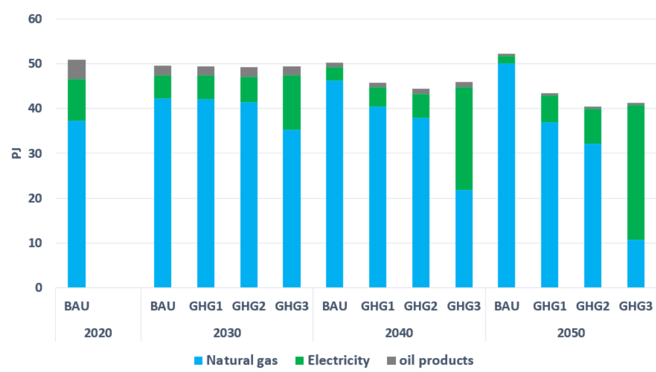

Figure 1.9: Final energy consumption by type in the commercial sector.

1.5.3 Sensitivity Analysis

As seen in Section 1.5.1, the transportation sector plays an important role when decarbonizing the energy sector. On the other hand, total energy consumption in the transportation sector, and accordingly total CO_2 emissions, depend on the mode of transportation. If a larger share of the mobility demand is met by public transportation facilities, the required trip per passenger-kilometer demand reduces, resulting in lower primary energy consumption. In this section, we evaluate the sensitivity of our results to the share of each transportation mode (public and private) in the total mobility demand. To do so, we exogenously shift 20% and 50% of the mobility demand from light-duty vehicles to public transport (buses and metros). These transport modal shifts start in 2030 and continue until 2050.

Fig. 1.10 compares total CO_2-eq emissions of the transportation sector under the different modal shifts. While MS_0% represents the default modal share, MS_20% and MS_50% correspond to the 20% and 50% modal shifts, respectively. This figure relates to the BAU scenario. In 2030, total emissions under MS_50% are 36% lower than in MS_0%. However, this emission gap reduces afterwards following the electrification of light-duty vehicles. In other words, shifting to public transportation can be a temporary strategy to reduce emissions before electrifying the transportation sector.

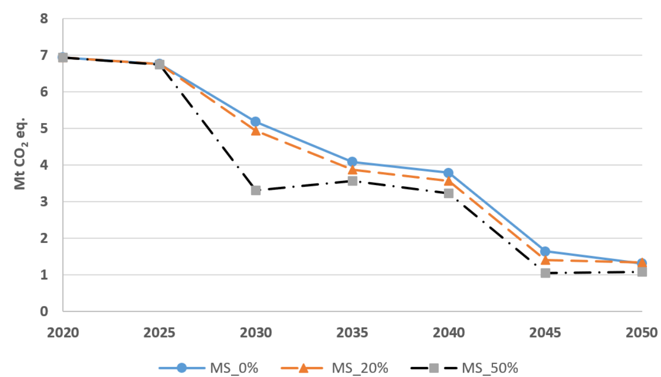

Figure 1.10: GHG emissions from the transportation sector for different modal shifts in BAU, as the mobility demand is partially shifted from light-duty vehicles to public transportation.

Fig. 1.11 compares next final energy consumption of the transportation sector, in 2050, under different scenarios and modal shifts. In general, a shift from private to public transportation not only reduces primary energy consumption, but also increases the share of electricity in final energy consumption. The former trend is because buses and metros are able to move more passengers with a lower energy consumption per passenger. The latter is due to the higher electrification rate in public transportation compared to the private one. Namely, a large portion of public transportation is already electrified thanks to metros. In addition, because the number of buses used is much lower than the one of private cars, electrifying them is faster and easier. Therefore, shifting to public transportation reduces fossil fuels consumption.

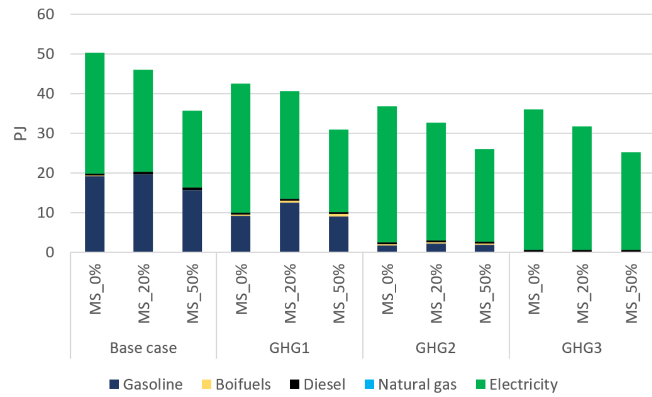

Figure 1.11: 2050 Final energy consumption for the transportation sector under different scenarios and transport modal shifts.

1.6 Discussion

In this paper, we examine different decarbonization pathways for the GM region, and evaluate their impacts on the energy sector. Results show that the GM region can reach a near zero-emission energy sector by electrifying the transportation, commercial and residential sectors, and by increasing the energy efficiency of buildings. This is mainly because i) the majority of electricity produced in Quebec is carbon-free coming from low-cost hydro-power, and ii) there are limited sources of industrial emissions in the region. In addition, when shifting from private to public transportation, final energy consumption can be further reduced.

With 30% of the total energy-related emissions in Quebec, road transportation is currently the largest source of GHG emissions in the GM area (Municipal, 2020; Whitmore and Pineau, 2019). In addition, gasoline is the main primary energy used in this sector with a 94% share. Our findings suggest that promoting the use of EVs reduces the share of gasoline. In particular, under a deep decarbonization scenario (GHG3), this share drops to 78% by 2030, 59% by 2040, and 0% by 2050. In addition, a (partial) shift from private to public transportation can reduce total energy consumption of the transportation sector by up to 30%. Our modal shift scenarios are in line with a city goal to shift around 25% of private transport to public transport. Residential and commercial buildings account for 28% of GHG emissions in the GM area (Municipal, 2020; Whitmore and Pineau, 2019). Our results suggest that lowering emissions can be achieved through electric heating and cooling technologies, in particular baseboard heaters and heat pumps. In parallel, investments in energy efficiency lead to a decrease in total energy consumption. Here again, these findings are in line with the GM plan in terms of energy efficiency improvements for residential and commercial buildings.

Finally, our results are consistent with the main strategies proposed in other related papers. For instance, according to Elizondo et al. (2017), Mexico city plans to reach ambitious GHG emission reductions by using more renewable energies, energy efficiency improvements, and shifting toward cleaner and electrified public transport. Likewise, as presented by Lind and Espegren (2017), the city of Oslo has ambitious decarbonization targets (i.e., 50% GHG emission reduction by 2030, and no fossil fuels by 2050), and it can meet the target by i) shifting from private to public transportation powered by renewable energy, ii) electrification of heating systems, and iii) energy efficiency improvements.

We acknowledge some important limitations of this paper as follows: i) we do not explicitly consider uncertainties in the energy system (uncertainty of prices, demands, technological innovations, etc.); ii) we do not carry out a life-cycle GHG emission assessment; and iii) we abstract away some details of the energy system, such as technological choices in industry, agriculture, and specific consumption in the transportation, residential, and commercial sectors.

1.7 Conclusion

In this paper, we have adopted the formulation of ETEM (Energy-Technology-Environment Model) to assess the long-term energy transition of the greater Montreal (GM) region in Quebec. The proposed model covers the years 2020-2050 and provides insights on the capacity expansion of generation technologies, technological shifts in the demand side, total primary energy consumption, and total energy-related CO_2-eq emissions. We have evaluated the impact of imposing different CO_2-eq emission reduction constraints on energy transition pathways for the GM region. Results show that the transportation sector, with a 6.9 million ton (Mt) emission reduction compared to the 2020 level, plays an important role in a deep decarbonization (GHG3 scenario) of the GM region. This reduction is achieved by electrifying private and public vehicles. Moreover, commercial and residential sectors will contribute to the deep decarbonization by respectively reducing 1.6 Mt and 1 Mt CO_2-eq (compared to their 2020 levels). The most important decarbonization strategies in these sectors include i) replacing fossil fuel-based furnaces with electric-based heat pumps to satisfy heating demands, and ii) reducing energy consumption by increasing buildings insulation.

Several directions could be considered for future work. First, it is worth considering explicitely uncertainty in our analysis. Because of the long-term horizon of planning in ETEM, there are many sources of uncertainties that affect results. Demands, prices of fuels and technologies, efficiency of technologies are among these influential uncertain parameters. Therefore, a first direction is to consider these uncertainties and obtain results that are robust against perturbations of these parameters. Second, our analysis does not model a complete list of hydrogen technologies. Given the potential importance of hydrogen-based technologies in different sectors, it is worthwhile investigating the energy transition considering as well all these technologies. Finally, expanding the boundaries of the energy system to include a detailed description of industrial and agricultural technology choices could also be the subject of a future research.

References

Acha, S., Mariaud, A., Shah, N., and Markides, C. N. (2018). Optimal design and operation of distributed low-carbon energy technologies in commercial buildings. *Energy*, 142:578–591.

Albana, K., Giulia, M., Paolo, Z., Andreea, I., Greet, J.-M., Brigitte, K., Rivas, C. S., Fabio, M.-F., and Paolo, B. (2016). Covenant of mayors: Greenhouse gas emissions achievements and projections. Technical report, European Commission.

Aliakbarisani, S., Bahn, O., and Delage, E. (2020). Affine decision rule approximation to immunize against demand response uncertainty in smart grids capacity planning. *Les Cahiers du GERAD*, G–2020–62.

Aliakbarisani, S., Bahn, O., Delage, E., and Foguen, R. (2021). Robust integration of electric vehicles charging load in smart grid's capacity expansion planning. *Les Cahiers du GERAD*, G-2021-44.

Andrey, Christopher, Babonneau, Frédéric, Haurie, Alain, and Labriet, Maryse (2015). Modélisation stochastique et robuste de l´atténuation et de l´adaptation dans un système énergétique régional. application à la région midi-pyrénées. *Nat. Sci. Soc.*, 23(2):133–149.

Babonneau, F., Caramanis, M., and Haurie, A. (2016). A linear programming model for power distribution with demand response and variable renewable energy. *Applied Energy*, 181:83 – 95.

Babonneau, F., Caramanis, M., and Haurie, A. (2017). ETEM-SG: Optimizing regional smart energy system with power distribution constraints and options. *Environmental Modeling & Assessment*, 22(5):411–430.

Babonneau, F., Foguen, R., Haurie, A., and Malhame, R. (2020). Coupling a power dispatch model with a wardrop or mean-field-game equilibrium model. *Dynamic Games and Applications*.

Babonneau, F. and Haurie, A. (2019). Energy technology environment model with smart grid and robust nodal electricity prices. *Annals of Operations Research*, 274.

Babonneau, F., Haurie, A., Tarel, G., and Thénié, J. (2012). Assessing the future of renewable and smart grid technologies in regional energy systems. *Swiss J Economics Statistics*, 148:229–273.

CFUT (2019). Climate emergency urban opportunity, how national governments can secure economic prosperity and avert climate catastrophe by transforming cities. Technical report, Coalition For Urban Transitions (CFUT).

Coelho, S., Russo, M., Oliveira, R., Monteiro, A., Lopes, M., and Borrego, C. (2018). Sustainable energy action plans at city level: A portuguese experience and perception. *Journal of Cleaner Production*, 176:1223–1230.

Dagoumas, A. (2014). Modelling socio-economic and energy aspects of urban systems. *Sustainable Cities and Society*, 13:192–206.

Dias, L., Simões, S., Gouveia, J., and Seixas, J. (2019). City energy modelling - optimising local low carbon transitions with household budget constraints. *Energy Strategy Reviews*, 26:100387.

Elizondo, A., Pérez-Cirera, V., Strapasson, A., Fernández, J. C., and Cruz-Cano, D. (2017). Mexico's low carbon futures: An integrated assessment for energy planning and climate change mitigation by 2050. *Futures*, 93:14–26.

Forsberg, J. (2021). Energy transition in transportation: Applying times-based energy system optimisation models to sub-national levels. Technical report, Licentiate dissertation, Luleå University of Technology.

Forsberg, J. and Krook-Riekkola, A. (2021). Recoupling climate change and air quality: Exploring low-emission options in urban transportation using the times-city model. *Energies*, 14(11).

Heinisch, V., Göransson, L., Odenberg, M., and Johnsson, F. (2019). Interconnection of the electricity and heating sectors to support the energy transition in cities. *Inter-*

national Journal of Sustainable Energy Planning and Management, 24:57–66. ID: unige:154440.

IEA (2021). Empowering cities for a net zero future. Technical report, IEA, Paris.

Lind, A. and Espegren, K. (2017). The use of energy system models for analysing the transition to low-carbon cities – the case of oslo. *Energy Strategy Reviews*, 15:44–56.

Maroufmashat, A., Elkamel, A., Fowler, M., Sattari, S., Roshandel, R., Hajimiragha, A., Walker, S., and Entchev, E. (2015). Modeling and optimization of a network of energy hubs to improve economic and emission considerations. *Energy*, 93:2546–2558.

Maroufmashat, A., Sattari, S., Roshandel, R., Fowler, M., and Elkamel, A. (2016). Multi-objective optimization for design and operation of distributed energy systems through the multi-energy hub network approach. *Industrial & Engineering Chemistry Research*, 55(33):8950–8966.

Masson-Delmotte., P.Zhai, Pörtner, H.-O., Roberts, D., Skea, J., Shukla, P., Pirani, A., Moufouma-Okia, W., Péan, C., Pidcock, R., Connors, S., Matthews, J., Chen, Y., Zhou, X., Gomis, M., Lonnoy, E., T. Maycock, M. T., , and Waterfield, T. (2018). Summary for policymakers. in: Global warming of 1.5°c. an ipcc special report on the impacts of global warming of 1.5°c above pre-industrial levels and related global greenhouse gas emission pathways, in the context of strengthening the global response to the threat of climate change, sustainable development, and efforts to eradicate poverty. Technical report, Intergovernmental Panel on Climate Change.

Mehleri, E., Sarimveis, H., Markatos, N., and Papageorgiou, L. (2013). Optimal design and operation of distributed energy systems: Application to greek residential sector. *Renewable Energy*, 51:331–342.

Mirakyan, A. and De Guio, R. (2013). Integrated energy planning in cities and territories: A review of methods and tools. *Renewable and Sustainable Energy Reviews*, 22:289–297.

Municipal, M. (2020). Plan climat 2020-2030, pour une ville inclusive, résiliente et carboneutre. Technical report, Montreal Municipal.

Scheller, F. and Bruckner, T. (2019). Energy system optimization at the municipal level: An analysis of modeling approaches and challenges. *Renewable and Sustainable Energy Reviews*, 105:444–461.

Shakouri, H. and Aliakbarisani, S. (2016). At what valuation of sustainability can we abandon fossil fuels? a comprehensive multistage decision support model for electricity planning. *Energy*, 107:60 – 77.

Vaillancourt, K., Bahn, O., Frenette, E., and Sigvaldason, O. (2017). Exploring deep decarbonization pathways to 2050 for canada using an optimization energy model framework. *Applied Energy*, 195:774–785.

Vaillancourt, K., Bahn, O., and Sigvaldason, O. (2018). *The Canadian Contribution to Limiting Global Warming Below 2 °C: An Analysis of Technological Options and Regional Cooperation*, pages 227–244. Springer International Publishing, Cham.

Whitmore, J. and Pineau, P.-O. (2019). The state of energy in quebec -2019. Technical report, Chair of energy sector management, HEC Montreal.

Xydis, G. (2012). Development of an integrated methodology for the energy needs of a major urban city: The case study of athens, greece. *Renewable and Sustainable Energy Reviews*, 16(9):6705–6716.

Yuan, X.-C., Lyu, Y.-J., Wang, B., Liu, Q.-H., and Wu, Q. (2018). China's energy transition strategy at the city level: The role of renewable energy. *Journal of Cleaner Production*, 205:980–986.

Chapter 2

Affine Decision Rule Approximation to Address Demand Response Uncertainty in Smart Grids' Capacity Planning

Chapter information

This article is a joint work with my supervisors, Olivier Bahn and Erick Delage. It is submitted to European Journal of Operational Research, and after a major revision, it is under the second round of review.

Abstract

Generation expansion planning is a classical problem that determines an optimal investment plan for the expansion of electricity network. With the advent of demand response as a reserved capacity in smart power systems, recent versions of this class of problems model demand response as an alternative for the expansion of the network. This adds uncertainties, since the availability of this resource is not known at the planning phase. In this paper, we model demand response uncertainty in a multi-commodity energy model, called ETEM, to address the generation expansion planning problem. The resulting model

takes the form of an intractable multi-period adjustable robust problem which can be conservatively approximated using affine decision rules. To tackle instances of realistic size, we propose a Benders decomposition that exploits valid inequalities and favors Pareto robustly optimal solutions at each iteration. The performance of our new robust ETEM is evaluated in a realistic case study that surveys the energy system of the Swiss "Arc Lémanique" region. Results show that an adjustable robust strategy can potentially reduce the expected cost of the system by as much as 33% compared to a deterministic approach when accounting for electricity shortage penalties. Moreover, an adjustable procurement strategy can be responsible for a 9 billion Swiss francs cost reduction compared to a naive static robust strategy. The proposed decomposition scheme improves the run time of the solution algorithm by 40% compared to the traditional Benders decomposition. To conclude, we provide a discussion on other possible problem formulations and implementations.

2.1 Introduction

Generation expansion planning (GEP) is a classical energy problem that aims at determining the required power capacity to satisfy demand over a long-term horizon at minimum cost, while satisfying economic, environmental and technical constraints (see Koltsaklis and Dagoumas, 2018, for a recent review). For this, one must consider existing and future electricity generation technologies to determine an optimal investment and retirement plan for the power sector. Computationally speaking, in a deterministic setting, the GEP problem is a large-scale optimization problem that typically accounts for more than hundreds of thousands of decision variables and constraints in order to identify realistic solutions. Motivated by advances in the structure of smart grids, recent versions of GEP problems have become even more complex as they attempt to model the notion of demand response (DR) (see e.g. Babonneau et al., 2017; Lohmann and Rebennack, 2017). DR can be defined as the shifting of demand by consumers, in response to supply-side incentives offered at times of high wholesale market prices or when system reliability is jeopardized (DOE, 2006). Development of sophisticated data-gathering devices such as smart meters and voltage sensors, as well as increasing penetration of flexible loads such as electric vehicles (EV) and heating pumps, provide the technical possibility of implementing DR programs through utilities. In the wholesale capacity market, the participants bid on providing DR resources as an alternative for expensive generation and transmission expansion strategies. DR resources can drastically reduce marginal production costs, as they are substitutes for technologies that help meet peak loads. However, including DR in the GEP problem is challenging. Indeed, DR is a price-sensitive resource, whose availability is not fully known, especially in the capacity expansion planning phase. As the planning horizon in a GEP problem is typically several decades, any planning or prediction of the availability of DR resources will be affected by two sources of uncertainties: i) errors in the prediction of total demand; and ii) changes in the response behavior. Failure to properly consider DR uncertainty (DRU) is likely to lead to situations in which there are insufficient capacity resources to satisfy realized demands.

Robust Optimization (RO) and Stochastic Programming (SP) are the two main methodologies to address uncertainty. The underlying assumption in SP is that the probability distribution of an uncertain parameter is known (Birge and Louveaux, 2011). Conversely, RO does not assume information about the distribution of an uncertain parameter, but instead assumes that uncertain parameters lie in a user-defined uncertainty set. RO aims at finding solutions that are immunized to all perturbations of the uncertain parameters in the uncertainty set (Bertsimas et al., 2011). In multi-stage versions of SP and RO, it is assumed that decisions are taken at different points of time. The simplest form, known respectively as two-stage SP or Adjustable RO (ARO), considers *here-and-now* decisions that need to be made before having any information about the uncertain parameters and *wait-and-see* decisions that can be adjusted according to the realized uncertain parameters at a later time. It is generally known that ARO (Ben-Tal et al., 2004) provides less conservative optimal solutions than RO, since it has more flexibility to adjust the decisions with respect to the uncertain parameters. However, the better performance comes at the price of problem intractability. To circumvent this issue, Ben-Tal et al. (2004) propose using affine decision rules for the delayed decisions, a technique also referred as the affinely adjustable robust counterpart (AARC). Following Ben-Tal et al. (2004), other types of decision rules have been proposed for ARO problems (Bertsimas and Georghiou, 2018; Georghiou et al., 2020). For a review of the ARO approach, we refer the reader to Yanıkoğlu et al. (2019).

A number of different multi-stage robust or stochastic approaches have been previously used in the literature to address uncertainties in GEP problems (Dehghan et al., 2014; Mejía-Giraldo and McCalley, 2014; Domínguez et al., 2016; Amjady et al., 2018; Baringo and Baringo, 2018; Han et al., 2018; Zou et al., 2018). Because of the inherent computational challenges that emerge with these models, there should be a compromise between the level of details and the size of the problem. For example, Han et al. (2018) propose a two-stage stochastic program that only considers a single-period planning horizon, while the multi-stage model proposed in Domínguez et al. (2016) is only implemented in a case study involving four periods. It therefore appears that tackling uncertainty in long-term industrial-size GEP problems is out of reach for currently available methods. Improving the computational efficiency of algorithms for solving such problems is also crucial in helping to understand better the interactions between demand and supply side, as such studies can require iterating through the resolution of a number of GEP problems to identify market equilibria (see Babonneau et al., 2016, 2020, for examples of this approach).

In this paper, we propose a numerical method for addressing DRU on a realistic large-scale GEP problem. To do so, we use the Energy-Technology-Environment Model (ETEM) proposed in Babonneau et al. (2017) to model the market mechanism that matches flexible load and supply, where we introduce for the first time DRU as an implementation error of the DR decision variable. We formulate the problem as a robust multi-period linear program. In a first stage, the policy-maker decides how to invest in the capacity of each generation technology and plans for a target DR for each future time period. Then, periodically, depending on the actual level of contribution in DR programs for this period, the planner decides on optimal energy procurement based on available resources.

We evaluate the performance of the proposed *robust ETEM* model on a real-world case study based on the energy system of the "Arc Lémanique" region in Switzerland. To solve the problem, we derive a Robust Multi-Period Conservative Approximation (RMPCA) of the problem, and develop a Benders decomposition algorithm (inspired from Ardestani-Jaafari and Delage, 2018) to solve it. In order to focus on the effects of DRU on the design of smart electricity networks, we have limited the model in this paper to only consider the uncertainty of DR. However, the proposed methodology could be extended to accommodate supply-side uncertainties, such as availability of intermittent resources, or investment costs. We however leave this as the subject of future work as discussed in Section 2.7.

Overall, the contributions of this paper can be summarized as follows:

1. We introduce DRU in a GEP problem, addressed using the ETEM energy model, and propose a robust multi-period linear program in which the procurement decisions are adjustable to the actual DR. The approach that we propose is flexible in the sense that, with minor modifications, it could accommodate other sources of uncertainties in GEP problems such as uncertainty of intermittent energy resources and investment costs.

2. We propose, for the first time, to seek Pareto Robustly Optimal (PRO) solutions (see Iancu and Trichakis, 2014) of the master problem in a Benders decomposition algorithm in order to accelerate convergence. When combined with the valid inequalities proposed in Ardestani-Jaafari and Delage (2020), solution time is improved by 40% on average in our randomly generated instances. Note that this idea differs from the idea of Pareto optimal cut, introduced by Magnanti and Wong (1981), in the way that the latter seeks a Pareto optimal solution among multiple optimal solutions of the sub-problems. In contrast, we seek a PRO solution in the master problem, i.e., a solution that is guaranteed not to be dominated by any other optimal solutions in terms of its constraint margin profile.

3. Compared to previous work in the literature, we solve an adjustable robust multi-commodity GEP problem whose size, in deterministic form, is two orders of magni-

tudes larger than the largest instance addressed in previous case studies. Moreover, our case study confirms in a simulation that adjustable robust policies can significantly improve (i.e., around 33%) the expected total cost of the energy system compared to the solution of the deterministic version when accounting for electricity shortage penalties. Furthermore, it shows that the flexibility of energy procurement decisions can be responsible for a reduction of 9 billion Swiss francs (CHF) in expected total expansion planning costs.

The remainder of the paper is organized as follows. In the next section, we present an overview of different approaches to model DRU, and summarize studies that use a multi-stage approach to model uncertainties in GEP problems. In Section 2.3, we introduce briefly the ETEM model. In Section 2.4, we present how we have modeled DRU in ETEM and derive the multi-period robust optimization problem as well as its conservative approximation. In Section 2.5, the Benders decomposition is detailed. Section 2.6 presents the case study and provides numerical results. Finally, Section 2.7 provides concluding remarks.

2.2 Literature Review

In this section, we first review papers that use a multi-period approach to model a robust or stochastic GEP problem. We specifically summarize their solution method and the size of the instances they solve. Usually, the size of a GEP problem is dependent on the number of time periods, load duration curve (LDC) steps, technologies, and commodities. Hence, we will summarize the size of studied instances with the product of these quantities, referred as the Deterministic Size Indicator (DSI) index. In a second part, we review recently proposed strategies to model DRU in different energy-related problems. Finally, we review the literature on the ETEM model.

Bloom (1983) and Bloom et al. (1984) are among the first papers that propose a two-stage stochastic programming formulation for GEP problems with uncertain demand and supply. They propose a general Benders decomposition, where a master problem accounts for investment decisions, and a set of subproblems represent the annual operation cost and reliability level of the installed capacities while enforcing probabilistic reliability constraints. Han et al. (2018) develop a two-stage stochastic program to model the uncertainty of load demand and wind output in a GEP problem. Using affine decision rules, they reformulate the problem as a deterministic second-order cone optimization problem. They solve an instance with 1 period, 5 LDC steps, and 32 technologies to test their algorithm (DSI=160). Mejía-Giraldo and McCalley (2014) propose an adjustable robust optimization framework to address the uncertainty of fuel price, demand, and transmission capacities in a GEP problem. In this setting, investment decisions are set as an affine function of fuel price, whereas voltage angle (decision) is parameterized as an affine function of demand and transmission capacities. They reformulate the problem as an LP and test it on a simplified version of the US power system with 20 periods, 3 LDC steps, and 13 technologies (DSI=780). Domínguez et al. (2016) use linear decision rules to reformulate a multi-stage GEP problem and cast it as a tractable LP. They solve a GEP problem with 4 decision periods, 18 technologies and 100 LDC steps (DSI=7200). Zou et al. (2018) propose a partially adaptive multi-stage stochastic GEP problem. In this setting, the capacity expansion plan is adaptive to the uncertain parameter up to a certain point. Fuel price and demand are two sources of uncertainties in this study. They test their algorithm on a case study with 10 periods, 3 LDC steps, and 6 technologies (DSI=180). Dehghan et al. (2014) develop a two-stage robust optimization problem in which the load demand and investment cost are uncertain. They solve their problem, using a cutting plane method. The case study is a 10-period planning of a network with 120 technologies and 3 LDC steps (DSI=3600). None of the above studies model neither DR nor DRU. In addition, all of them are a single-commodity GEP problem, meaning that they only model the electricity network and account for an aggregated electricity demand over the planning horizon. By contrast, in a multi-commodity energy model such as ETEM, one also models the interactions of the electricity sector with other sectors of the energy system (e.g., heat, transportation sectors), as well as the demands for final energy services (such as heat and lighting). This increases the size of the deterministic problem. In this paper, we solve a case study with 10 decision-making periods, 12 LDC steps, 142 technologies, and 57 energy commodities (DSI=971,280).

DR is also modeled in other power system planning problems such as unit commitment, transmission or distribution expansion planning, and wholesale electricity market problems. In general, there are two strategies one can follow to implement DR programs: dispatchable and non-dispatchable. In the former, the utility directly controls the timing of some loads of the customers who voluntarily participate in the program. More precisely, the utility cuts down the consumption during peak periods to ensure system reliability, and in return, remunerates participants with annual payments. In non-dispatchable strategies, the utility sends to customers a price signal with the purpose of flattening the demand curve. Automatic price-responsive devices adjust the timing of the consumption. While developing an optimal consumption schedule is the focus of some research (Liu et al., 2019), another stream studies the conditions under which the dynamic price signals improve social welfare (see, e.g., Adelman and Uçkun, 2019; Venizelou et al., 2018). Elaboration on the different strategies to implement DR and an overview on the success of these programs in the US electricity market is presented in Shariatzadeh et al. (2015).

The effect of DR on the wholesale and capacity market is another stream of research. Vatani et al. (2017) introduce DR to a capacity market problem in which the cost-minimizer capacity planner trades off between new generation and transmission capacity expansion and DR expenses. Arasteh et al. (2015) model a trade-off between DR expenses and distribution expansion costs. Zhang and Zhang (2019) model DR as an alternative procurement strategy for an electricity retailer. Namely, the electricity retailer must procure energy in a day-ahead wholesale market. Given that the prices in this market are highly uncertain, DR is introduced as a leverage to manage the retailer's risk. In this approach, the retailer solves its problem to determine a procurement strategy as well as DR incentive prices. Then, consumers respond to the signaled price in order to minimize their consumption cost. Babonneau et al. (2016) model DR in a capacity expansion planning problem considering distribution constraints. They develop a game framework between the retailer and many small consumers. The retailer solves a minimization model to determine his desired DR and capacity expansion plan. Then, using marginal cost of production, which corresponds to dual variables, he signals consumers to adjust their consumption. They argue that, if the price function, with which the retailer signals consumers, is convex with respect to both demand and required level of reserved capacity, their approach can be cast as a linear programming problem. Finally, Lohmann and Rebennack (2017) model DR in a long-term capacity expansion planning problem.

In all the above research, DR was mostly modeled in a deterministic way. In other words, when DR was modeled using a price elastic demand curve, no uncertainty affected this curve. Alternatively, when it was modeled as a decision variable, no implementation error was affecting optimal DR decisions. However, due to a variety of reasons, including demand prediction errors and changes in response behavior, in practice DR necessarily ends up different from what the supply side expected. According to Chatterjee et al. (2018), a lack of DR forecasting and estimation tools is one of the most important barriers to wider adoption of DR. On this regard, an active stream of literature has proposed a number of statistical learning methods for predicting demand response associated to storage-like flexible loads such as residential and industrial air conditioning (see, e.g., Dyson et al., 2014; Qi et al., 2020), and a stand-alone micro-grid with the presence of photovoltaic and wind generation units (see Amrollahi and Bathaee, 2017). Another stream of research investigates the influence of DRU on its integration to the network. Li et al. (2015) model incentive-based DR as an alternative for transmission upgrade investments and consider consumer's bid for load reduction uncertainty. They develop a stochastic programming model and use Monte Carlo simulation and Benders decomposition for resolution. Ströhle and Flath (2016) model DRU in a local online market to match flexible load and uncertain electricity supply. Gärttner et al. (2018) formulate DRU in a demand aggregator's problem where the scheduling of demand and the optimal dispatch are optimized at the same time. He et al. (2019) develop a two-stage distributionally robust problem to model DRU in a distribution network expansion problem. Prices are modeled as a decision variable to optimally shape the desired demand response. However, the price elasticity is considered to be a random parameter. Moreover, distributed generation resources are also affected by uncertainty. They propose a column and constraint generation approach to solve the resulting problem. Zhao et al. (2013) model the uncertainty of DR and wind generation in a unit commitment problem. DR is modeled through a price-elastic demand curve with price uncertainty. They propose a three-stage robust optimization formulation. First stage decisions consider unit commitment planning, i.e., turning on and off the generators. Second stage decisions include the dispatch of electricity and are implemented after the actual wind power output is realized. Finally, in a third stage, the demand response is observed. Moreover, they propose a Benders decomposition to solve the three-stage problem. An overview of the different techniques to model ancillary services in unit commitment problems is presented in Knueven et al. (2020). Asensio et al. (2018) model the DRU through a price-sensitive demand curve in a distribution network expansion problem and use a scenario-tree approach to solve the resulting stochastic programming model. Roveto et al. (2020) develop a data-driven distributionally robust optimization model of the demand response auction, where the risk of the retailer is controlled using value-at-risk and conditional value-at-risk measures. They model DRU by considering DR bid uncertainty. In other words, the aggregator receives bids from consumers to reduce their consumption at a specific time. However, consumers might not actually reduce their consumption to this full amount. The aggregator aims to ensure a certain level of demand response procurement at minimum cost. Huang et al. (2020) develop a multi-stage stochastic programming model to optimally schedule power generation assets when the system operator has access to the ancillary service market. In this paper, we model DRU in a multi-commodity energy planning model, called ETEM (Babonneau et al., 2017), to address a GEP problem. In ETEM, DR is modeled through a decision variable which is optimized by the supply-side. It is assumed that the supply-side can shape consumer's response behavior through different long-term DR programs. For the first time, we model DRU as an implementation error of the DR decision in ETEM, and develop an adaptive robust multi-period conservative approximation formulation of the problem.

ETEM first was formulated by Babonneau et al. (2012). Although the developed formulation is deterministic, they also provide a stochastic programming model with different scenarios for the electricity import cost. As an extension to the primary ETEM model, Babonneau et al. (2016) propose a linear approximation of distribution system and power flow constraints in ETEM. The new formulation, called ETEM-SG, accounts for provision of reserved capacities provided by demand response in smart grids. Babonneau et al. (2017) and Babonneau and Haurie (2019) propose robust versions of ETEM to address the uncertainty of investment costs and of availability of technologies and transmission capacity of electricity transmission lines. In both papers, a static robust version of ETEM is developed and a relaxed version of the model is solved to reduce conservatism of the solution. Babonneau et al. (2020) is the first version of ETEM that employs robust optimization to handle uncertain demand response. Specifically, it proposes a robust ETEM model coupled with a mean-field game equilibrium model that represents the charging behavior of electric vehicle owners. The paper models the uncertainty of DR by introducing in ETEM two upper and lower bounding constraints on the sum of DR over all time periods. The bounding constraints are calibrated based on the confidence intervals of the random demand which is simulated using a mean-field game model. We note that Babonneau et al.'s way of accounting for DRU in ETEM is fundamentally different from ours. First, they again only involve static decisions and focus on a single-period investment problem. More importantly, a careful analysis of their approach reveals that it effectively offers no protection against the DR deviations in our setting. A more detailed demonstration of this weakness is presented in Appendix 2.8.1. Our paper should therefore be seen as presenting a significant extension of ETEM that identifies adaptive long term strategies to immunizes for the first time the energy system against DR deviations.

2.3 The ETEM Energy Model

As proposed in Babonneau et al. (2012), ETEM is a long-term, bottom-up energy model cast as a linear programming problem. It is a member of the *MARKAL-TIMES* family of models, and represents the entire energy sector from primary resources to useful energy demands. ETEM is a demand-driven model in which the objective is to provide energy services at minimum cost. The planning horizon is typically more than 50 years and the model gives insights on both long-term strategic and short-term operational decisions. While the long-term decisions include capacity expansion and strategic targeting for a desired demand response, short-term decisions consist of energy procurement planning, which includes optimal generation, import, export and regional transmissions. ETEM can also account for technical, economic and market constraints (see Babonneau et al., 2017).

ETEM is based on the concept of a reference energy system (see Figure 2.1 for the depiction of the energy system of the Arc Lémanique region in Switzerland considered in our case study). The model considers different energy commodities (captured by vertical lines in the figure) namely “resources" (i.e., a mix of primary energy resources and some imported secondary energy forms), selected secondary forms (i.e., electricity and heat), and useful energy demands. More precisely, resources correspond to coal, oil products, gas, hydro, intermittent renewables (wind and solar), as well as other sources such as municipal solid waste and wood. Useful energy demands belong to four categories: industry, residential electricity, residential heat, and transportation. The boxes correspond to the different energy technologies, from generators to technologies providing energy services to end-users. In our implementation, we also add an energy resource (denoted “ExR") with a high cost that represents the cost of shortage in the system. A dummy technology (denoted “EXT") links this expensive resource to the useful demands (see Assumption 1 and following discussion for more details).

The planning horizon in ETEM spans over several decades to simulate the long investment cycles typical of the energy sector. We denote by $t \in \mathbb{T} := \{1, \ldots, |\mathbb{T}|\}$ the index representing the decision-making periods. In addition, to capture short-term operational patterns of the demand load, each period is divided into smaller time-slices $s \in \mathbb{S}$, representing load duration curve steps. In ETEM, 12 time-slices are assumed ($\mathbb{S} = \{1, \cdots, 12\}$), which are partitioned among a set $\mathbb{J}$ of 3 typical seasons (winter, summer, and intermediate), and each day of these seasons is divided into 4 time slots (morning, midday, mid-

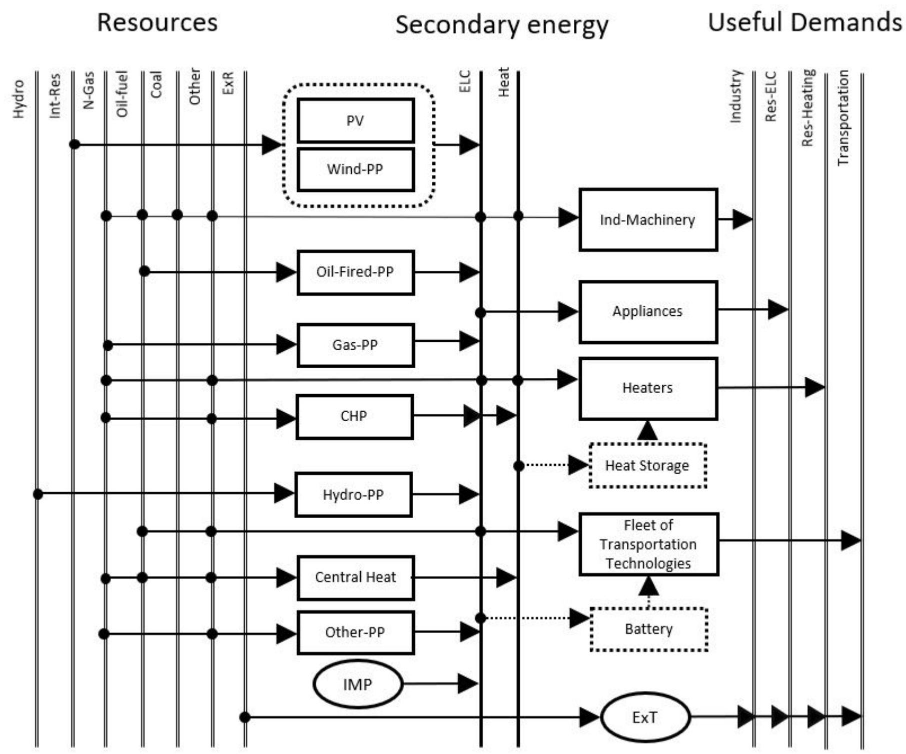

Figure 2.1: Arc Lémanique reference energy system, where Int-Res stands for intermittent resources (solar and wind), N-Gas for natural gas, Oil-fuel for processed oil products, Other for hydrogen and additional sources of energy (such as solid waste and wood and geothermal), ELC for electricity, RES for residential, PP for power plant, CHP for combined heat and power plant, IMP for electricity import, Ind-Machinery for industrial machinery, ExR for a dummy expensive resource added to avoid in-feasibility, ExT for a dummy expensive technology used to avoid in-feasibility. Other-PP includes geothermal, fuel-cell and municipal waste power plants.

night, and night), as shown in Figure 2.2.

Before describing ETEM's mathematical formulation, it is worth introducing our nomenclature. Let $\mathbb{C}$ be the set of energy commodities and let $\mathbb{P}$ be the set of energy technologies. The set of indices $\mathbb{F}$ identifies the different input-output energy flows associated to each technology. For instance, in Figure 2.1, Combined Heat and Power (CHP) uses natural gas, solid waste and wood as input to generate both electricity and heat. Finally, let $\mathbb{L}$ be a set of buses in different geographical zones. A full nomenclature is presented in Table 2.1. Below, we present the main elements of ETEM. Interested readers can refer to Babonneau et al. (2017) for more details:

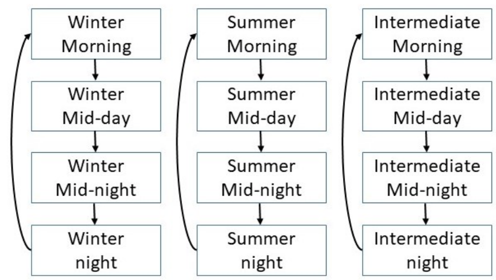

Figure 2.2: Sequence of time-slices

$$W^* := \min \sum_{t,l} \rho^t \cdot \Bigg(\sum_p \alpha_{t,p} \boldsymbol{C}_{t,l,p} + \pi_{t,p} \Big(\sum_{k=0}^{l_p-1} \boldsymbol{C}_{t-k,l,p} + \Omega_{t,l,p} \Big) + \sum_{s,c} \nu_{t,p} \boldsymbol{P}_{t,s,l,p,c} + \sum_{s,c} (\lambda_{t,s,c} \boldsymbol{I}_{t,s,l,c} - \lambda'_{t,s,c} \boldsymbol{E}_{t,s,l,c}) + \sum_{s,l',c} \lambda''_{t,s,l,l',c} \boldsymbol{T}_{t,s,l,l',c} \Bigg), \tag{2.1a}$$

s.t.

$$\Big(\sum_{p \in \mathbb{P}^P_c} \boldsymbol{P}_{t,s,l,p,c} + \boldsymbol{I}_{t,s,l,c} \Big) \eta_c + \sum_{l' \neq l} (\eta_c \boldsymbol{T}_{t,s,l',l,c} - \boldsymbol{T}_{t,s,l,l',c}) \geq \sum_{p \in \mathbb{P}^C_c} \boldsymbol{P}_{t,s,l,p,c} + \boldsymbol{E}_{t,s,l,c} \quad \forall\, t,s,l,c \in \mathbb{C}/\mathbb{C}^{\mathscr{D}} \tag{2.1b}$$

$$\Big(\sum_{l,p \in \mathbb{P}^c} \theta^c_p \cdot \beta_{t,s,p} \Big(\sum_{k=0}^{l_p-1} \boldsymbol{C}_{t-k,l,p} + \Omega_{t,l,p} \Big) + \sum_{l,p \in \mathbb{P}^P_c / \mathbb{P}_c} \theta^c_p \cdot \boldsymbol{P}_{t,s,l,p,c} + \boldsymbol{I}_{t,s,l,c} \Big) \cdot \rho_{t,s,c} \geq \sum_{l,p \in \mathbb{P}^C_c} \boldsymbol{P}_{t,s,l,p,c} + \boldsymbol{E}_{t,s,l,c} \quad \forall t, s \in \mathbb{S}^{\mathscr{G}}, c \in \mathbb{C}^{\mathscr{G}} \tag{2.1c}$$

$$\eta_c \sum_{p \in \mathbb{P}^{P_c}} \boldsymbol{P}_{t,s,l,p,c} = \sum_{p \in \mathbb{P}^{C_c}, s' \in \mathbb{S}^s} \boldsymbol{P}_{t,s',l,p,c} \quad \forall t,s,l,c \in \mathbb{CS} \tag{2.1d}$$

$$\sum_{p \in \mathbb{P}^P_c} \boldsymbol{P}_{t,s,l,p,c} \geq \Theta_{t,l,c} \boldsymbol{V}_{t,s,c} \qquad \forall t,s,l,c \in \mathbb{C}^{\mathscr{D}} \tag{2.1e}$$

$$\upsilon_{t,s,c}(1 - \nu_{t,s,c}) \leq \boldsymbol{V}_{t,s,c} \leq \upsilon_{t,s,c}(1 + \nu_{t,s,c}) \quad \forall t,s,c \in \mathbb{C}^{\mathscr{D}} \tag{2.1f}$$

$$\sum_{s \in \mathscr{S}_j} \boldsymbol{V}_{t,s,c} = \sum_{s \in \mathscr{S}_j} \upsilon_{t,s,c} \qquad \forall t, c \in \mathbb{C}^{\mathscr{D}}, j \in \mathbb{J} \tag{2.1g}$$

$$\sum_{c : p \in \mathbb{P}^P_c} \boldsymbol{P}_{t,s,l,p,c} \leq \beta_{t,s,p} \left(\sum_{k=0}^{l_p-1} \boldsymbol{C}_{t-k,l,p} + \Omega_{t,l,p} \right) \qquad \forall t,s,l,p \notin \mathbb{P}^R, \tag{2.1h}$$

Table 2.1: Nomenclature for ETEM formulation

Indices		**Parameters**	
$t \in \mathbb{T}$	Index for time period	$\alpha_{t,p}$	Investment cost
$s \in \mathbb{S}$	Index for time-slices	$\beta_{t,s,p}$	Capacity factor
$p \in \mathbb{P}$	Index for technologies	η_c	Network efficiency
$c \in \mathbb{C}$	Index for energy commodities	$\eta^t_{f,f'}$	Technology efficiency
$c_s \in \mathbb{CS}$	Index for energy storage	$\lambda''_{t,s,l,l',c}$	Transmission cost
$f \in \mathbb{F}$	Index for energy flows	$\lambda'_{t,s,c}$	Export cost
$l \in \mathbb{L}$	Index for buses (geographical zones)	$\lambda_{t,s,c}$	Import cost
$j \in \mathbb{J}$	Index for seasons	$\nu_{t,s,c}$	Maximum deviation from
$i \in \mathbb{I}$	Index for period-seasons (t,j)		nominal demand response
Sets		$\nu_{t,p}$	Variable cost
$\mathbb{P}^C_c \subseteq \mathbb{P}$	Set of technologies consuming c	$\Omega_{t,l,p}$	Available capacity of technology p
$\mathbb{P}^P_c \subseteq \mathbb{P}$	Set of technologies producing c	$\pi_{t,p}$	Fixed production cost
$\mathbb{P}^R \subseteq \mathbb{P}$	Set of intermittent technologies	ρ	Discount factor
$\mathbb{C}^I \subseteq \mathbb{C}$	Set of imported commodities	θ^c_p	Proportion of output c from technology
$\mathbb{C}^{\mathscr{D}} \subseteq \mathbb{C}$	Set of useful demands		p that can be used in peak period
$\mathbb{C}^{EX} \subseteq \mathbb{C}$	Set of exported commodities	l_p	Life duration of technology p
$\mathbb{C}^{TR} \subseteq \mathbb{C}$	Set of transmitted commodities	$\Theta_{t,l,d}$	Annual final demand
$\mathbb{C}_f \subseteq \mathbb{C}$	Set of commodities linked to flow f	$\upsilon_{t,s,c}$	Nominal demand response
$\mathbb{C}^{\mathscr{G}} \subseteq \mathbb{C}$	Set of commodities with margin reserve	$\rho_{t,s,c}$	Required reserve for commodity $c \in \mathbb{C}^{\mathscr{G}}$
$\mathbb{S}^j \subseteq \mathbb{S}$	Set of time-slices s in season j	**Variables**	
$\mathbb{S}^s \subseteq \mathbb{S}$	Set of successive time-slices of s	$\boldsymbol{C}_{t,l,p}$	Variable for new capacity addition
$\mathbb{S}^{\mathscr{G}} \subseteq \mathbb{S}$	Set of time-slices in peak period	$\boldsymbol{P}_{t,s,l,p,c}$	Variable for activity of technology p
$\mathbb{FI}_p \subseteq \mathbb{F}$	Set of inputs to technology p	$\boldsymbol{I}_{t,s,l,c}$	Variable for import
$\mathbb{FO}_p \subseteq \mathbb{F}$	Set of outputs from technology p	$\boldsymbol{E}_{t,s,l,c}$	Variable for export
		$\boldsymbol{T}_{t,s,l,l',c}$	Variable for regional transmission
		$\boldsymbol{V}_{t,s,l,d}$	Variable for demand response

$$\sum_{c \in \mathbb{C}^P_m} \boldsymbol{P}_{t,s,l,p,c} = \beta_{t,s,p} \left(\sum_{k=0}^{l_p-1} \boldsymbol{C}_{t-k,l,p} + \Omega_{t,l,p} \right) \qquad \forall t,s,l,p \in \mathbb{P}^R \tag{2.1i}$$

$$\sum_{c \in \mathbb{C}_{f'}} \boldsymbol{P}_{t,s,l,p,c} = \eta^t_{f,f'} \cdot \sum_{c \in \mathbb{C}_f} \boldsymbol{P}_{t,s,l,p,c} \quad \forall f \in \mathbb{FI}_p, f' \in \mathbb{FO}_p, t,s,l,p \tag{2.1j}$$

$$LB_{t,j,c} \leq \sum_{s \in \mathbb{S}^j, l, p \in \mathbb{P}^P_c} \boldsymbol{P}_{t,s,l,p,c} \leq UB_{t,j,c} \quad \forall t,j,c \in \mathbb{C} \tag{2.1k}$$

$$LB_{t,j,c} \leq \sum_{l, s \in \mathbb{S}^j} \boldsymbol{I}_{t,s,l,c} \leq UB_{t,j,c} \quad \forall t,j,c \in \mathbb{C}^I \tag{2.1l}$$

$$\sum_{s \in \mathbb{S}^j, l} \big(\sum_{p \in \mathbb{P}^P_c} \boldsymbol{P}_{t,s,l,p,c} + \boldsymbol{I}_{t,s,l,c} - \sum_{p \in \mathbb{P}^C_c} \boldsymbol{P}_{t,s,l,p,c} - \boldsymbol{E}_{t,s,l,c} \big) \leq UB_{t,j,c} \quad \forall t,j,c \in \mathbb{C} \tag{2.1m}$$

$$(\boldsymbol{P},\boldsymbol{I},\boldsymbol{E},\boldsymbol{T}) \in \mathscr{Y}\ ,\ \boldsymbol{C} \in \mathscr{X}\ ,\ \boldsymbol{P} \geq 0, \boldsymbol{I} \geq 0, \boldsymbol{E} \geq 0, \boldsymbol{T} \geq 0, \boldsymbol{C} \geq 0, \boldsymbol{V} \geq 0\,. \tag{2.1n}$$

The objective function (2.1a) minimizes a discounted sum of all costs of the system over all regions ($l \in \mathbb{L}$) and time periods ($t \in \mathbb{T}$), where parameters $\alpha_{t,p}$, $\pi_{t,p}$, $\nu_{t,p}$, $\lambda_{t,s,c}$, $\lambda'_{t,s,c}$, and $\lambda''_{t,s,l,l',c}$ are unit costs of investment, fixed, variable, import, export, and regional transmission respectively .

Constraint (2.1b) is a commodity balance constraint. It ensures that the regional procurement of each energy commodity c is greater or equal than its total consumption at each period t and time-slice s. Specifically, the left-hand side of this constraint consists of i) total production of commodity c in region l by all technologies producing it ($\mathbb{P}_c^P$) ii) import of commodity c, and, iii) net transmission of commodity c into region l. It is worth mentioning that in ETEM, import (and similarly export) of energy refers to amount of input (output) energy to (from) the energy system from outside of it, but energy transmission refers to amount of energy which is produced in one region and transmitted to another region inside energy system. Parameter η_c is the network efficiency with respect to commodity c, e.g., the efficiency of electricity transmission lines. On the right-hand side, the consumption is equal to the total consumption by technologies consuming the commodity, i.e., $\mathbb{P}_c^C$, added to the amount of commodity that is exported.

Constraint (2.1c) introduces a safety margin in procurement of commodity $c \in \mathbb{C}^{\mathscr{G}}$, mostly electricity, during peak time-slices $s \in \mathbb{S}^{\mathscr{G}}$, to protect against random events not explicitly represented in the model. Parameter $\rho_{t,s,c} \in [0,\ 1]$ represents the fraction of reserved capacity needed to ensure covering the peak load. The left-hand side of this constraint models the maximum amount of commodity $c \in \mathbb{C}^{\mathscr{G}}$ that can be procured in period t and time-slice s. This amount is equal to the sum of i) the maximum production capacity of commodity c by technologies that produce it as their main output ($\mathbb{P}_c$), ii) the production of commodity c by technologies that produce c as their by-product of their main activity, and iii) the import of commodity c. The left-hand side is the total consumption similar to constraint (2.1b). Parameter θ_p^c is the proportion of technology production that can be used during the peak period. Constraint (2.1d) models the balance of energy storage between consecutive time-slices. Amount of storage at time-slice c can be consumed at subsequent time-slice s'. The notion of subsequency of time-slices is presented in Figure 2.2. Constraints (2.1e) - (2.1g) are the key constraints that model the use of demand response. Parameter $\Theta_{t,l,c}$ is the total demand of service $c \in \mathbb{C}^{\mathscr{D}}$ in the period t and zone l. Variable $\boldsymbol{V}_{t,s,c}$ is the demand response which optimally distributes the total demand of period t into all time-slices s inside period t. Constraint (2.1f) limits the demand response to vary between an interval around the nominal value, i.e., $\upsilon_{t,s,c}$. In addition, the sum of the demand response must be equal to the sum of the nominal values in each season, according to constraint (2.1g).

Constraint (2.1h) limits the maximum production or consumption of each technology to the available capacity of that technology. The parameter $\beta_{t,s,p}$ is the capacity factor. The capacity factor of technology p is defined as the average power generated divided by the rated peak power. This simply represents the fraction of the total capacity which is available at each time-slice. In addition, since renewable generation is usually given priority in dispatch over conventional forms of generation (see for example Knueven et al., 2020; Lohmann and Rebennack, 2017), their production is imposed to take its maximum production capacity in constraint (2.1i). Constraint (2.1j) models the efficiency of technology p. In ETEM, the efficiency of a technology is modeled through the annual parameter $\eta^t_{f,f'}$ that links each output flow $f' \in \mathbb{FO}_p$ to an input flow $f \in \mathbb{FI}_p$. The constraint ensures that the sum of all output energy commodity c which is linked to output flow f', i.e., $\mathbb{C}_{f'}$, is equal to a fraction of the sum of all input energy commodities c which is linked to input flow f, i.e., $\mathbb{C}_f$.

We note that constraints (2.1k) and (2.1l) impose upper and lower bounds for seasonal production of technology p in region l, and seasonal import of energy commodity c in region l. Moreover, in constraint (2.1m) the seasonal procurement of commodity c, over all regions in $\mathbb{L}$, is imposed an upper bound. This departs slightly from the original ETEM formulation, which only imposed annual bounds but is reasonable and enables the decomposition scheme presented in Section 2.5. We will discuss later that seasonally independent procurement decisions enable us to decompose the problem into several independent sub-problems where one decides on the optimal procurement given a capacity plan and demand response. This structure benefits the efficiency of the solution method. Finally, space $\mathscr{X}$ and $\mathscr{Y}$ represent other operational, technical, and economical constraints that define a desirable space for capacity and procurement decisions. Moreover, $\mathscr{X}$ and $\mathscr{Y}$ contain constraints that define the structure of the energy network. In particular, these constraints enforce energy productions, $\boldsymbol{P}_{t,s,l,p,c}$, that do not exist in the energy network to be zero. Since these constraints do not affect our analysis, we omit to report them and refer the reader to Babonneau et al. (2017) for a complete list of constraints.

2.4 A Demand Response Robust Version of ETEM

The ETEM model presented in Section 2.3 optimizes the future evolution of the energy system by assuming full information. However, in reality, there is always uncertainty. In particular, demand response is an important source of uncertainty. ETEM assumes that demand response is completely controlled by the supply side. From a decentralized electricity market point of view, this structure can be interpreted as a situation where the supply side targets an optimal level of DR, and encourages the actual demand load to be close to target DR using DR programs such as incentive real-time pricing. But, one must expect some realized deviations from the plans. Such deviations can either be caused by differences in the actual overall daily demand loads, as time evolves over a 50-year horizon, or by the level of participation and compliance of consumers in DR programs. In this paper, we model both types of uncertainties as implementation errors of the planned demand response $\boldsymbol{V}$ and we immunize ETEM against such error (see Ben-Tal et al., 2015, for a seminal work on robust optimization with implementation error). Specifically, given a set $\mathbb{C}^{\mathscr{U}} \subseteq \mathbb{C}^{\mathscr{D}}$ of useful demand, such as residential electricity, with error-prone demand response, the demand $\Theta_{t,l,c}\boldsymbol{V}_{t,s,c}$ for time period $t \in \mathbb{T}$, time-slice $s \in \mathbb{S}$, region $l \in \mathbb{L}$, and commodity $c \in \mathbb{C}^{\mathscr{U}}$, is replaced with $\Theta_{t,l,c}(\boldsymbol{V}_{t,s,c} + \boldsymbol{\delta}_{t,s,c})$, where $\boldsymbol{\delta}_{t,s,c}$ captures the Relative Demand Response Deviations (RDRD) from the planned response. In a general presentation, we will consider the vector of relative deviations $\boldsymbol{\delta} \in \mathbb{R}^d$, to be the vector that is obtained from arranging the parameters $\boldsymbol{\delta}_{t,s,c}$ for all $t \in \mathbb{T}, s \in \mathbb{S}$ and $c \in \mathbb{C}^{\mathscr{U}}$ into a vector. For simplicity of exposure, we assume that the vector of each seasonal subset of RDRD lies in a scaled budgeted uncertainty set (as introduced in Bertsimas and Sim, 2004) defined as:

$$\Delta = \left\{ \boldsymbol{\delta} \in \mathbb{R}^d \,\middle|\, \begin{array}{c} \exists \boldsymbol{\zeta} \in [-1, 1]^d \\ \boldsymbol{\delta}_{t,s,c} = \beta_{t,s,c} \boldsymbol{\zeta}_{t,s,c}, \ \forall t, s, c \in \mathbb{C}^U \\ \sum_{s \in \mathbb{S}^j} \sum_{c \in \mathbb{C}^U} |\boldsymbol{\zeta}_{t,s,c}| \leq \Gamma_{t,j} \ \forall t, j \in \mathbb{J} \end{array} \right\}, \tag{2.2}$$

where $d := |\mathbb{T}| \cdot |\mathbb{S}| \cdot |\mathbb{C}^{\mathscr{U}}|$, $\beta_{t,s,c}$ captures the maximum possible RDRD, while $\Gamma_{t,j}$ is a seasonal budget that represents the fact that we expect a maximum of $\Gamma_{t,j}$ RDRD to take on their extreme values in season j of time period t. The idea of decomposing the uncertainty information structure over each season has three important advantages. First, from a numerical perspective, it will help by enabling us to employ decomposition schemes based on Benders decomposition. Second, it is also attractive from a statistical perspective as it allows us to calibrate the size of each seasonal uncertainty set using seasonal data which is usually readily available, while data over joint realizations over many seasons can be scarce. Finally, imposing uncertainty budgets on subsets of perturbed parameters is known to lead to less conservative solutions in robust optimization as it enforces the worst-case scenario to distribute the damage over parameters of different subsets instead of focusing on a single one (see Bertsimas and Thiele, 2006, where similar techniques are used).

In what follows, we present first, in Section 2.4.1, how we modify ETEM in order to identify capacity and demand response plans that are immunized against RDRD. The modified model is cast as a robust multi-period linear program. Unfortunately, this class of problems is known to be generally intractable. To address this issue, Section 2.4.2 presents a tractable conservative approximation that can be reformulated as a large-scale linear program.

2.4.1 A Robust Multi-Period Linear Programming Formulation

With the introduction of the RDRD in ETEM, the problem has the potential of turning into a multi-stage decision-making problem where different decisions are allowed to depend

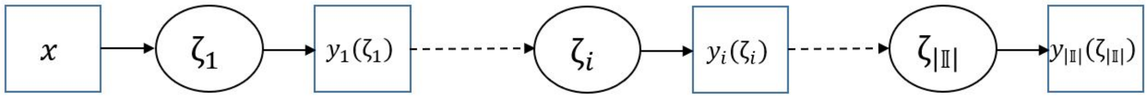

Figure 2.3: Sequence of decisions and uncertainty observations in our multi-period problem

on the observed realization of RDRD. Indeed, we will assume that in the first stage the energy network planner decides on the capacity expansion of the system (variable $\boldsymbol{C}$) and the planned demand response (variable $\boldsymbol{V}$). Then, in later stages, on a season-by-season basis, the seasonal RDRD are revealed to the planner who responds by deciding on the optimal energy production, energy transfers between regions, and energy imports and exports. To simplify the analysis of such a multi-stage model, we will further assume that the planner's response only depends on the current seasonal RDRD instead of reacting to all the observations made since the first season.

To be mathematically precise and help with presentation, decision variable $\boldsymbol{x} \in \mathbb{R}^m$, with $m = |\mathbb{T}| \cdot |\mathbb{L}| \cdot |\mathbb{P}| + |\mathbb{T}| \cdot |\mathbb{S}| \cdot |\mathbb{C}^{\mathscr{D}}|$, will capture the vector of all first stage decisions $(\boldsymbol{C}, \boldsymbol{V})$ in the demand response robust version of ETEM. Furthermore, for each time period t and season j, let $i \in \mathbb{I}$ denote the seasonal period (t, j), and consider that $\boldsymbol{y}_i \in \mathbb{R}^{k_i}$, with $k_i = |\mathbb{S}^j| \cdot |\mathbb{L}| \cdot |\mathbb{P}| \cdot |\mathbb{C}| + |\mathbb{S}^j| \cdot |\mathbb{L}| \cdot |\mathbb{C}^I| + |\mathbb{S}^j| \cdot |\mathbb{L}| \cdot |\mathbb{C}^{EX}| + |\mathbb{S}^j| \cdot |\mathbb{L}|^2 \cdot |\mathbb{C}^{TR}|$, captures all adaptive "procurement" decisions $(\boldsymbol{P}_{t,s,l,p,c}, \boldsymbol{I}_{t,s,l,c \in \mathbb{C}^I}, \boldsymbol{E}_{t,s,l,c \in \mathbb{C}^{EX}}, \boldsymbol{T}_{t,s,l,l',c \in \mathbb{C}^{TR}})_{t, s \in \mathbb{S}_j, l \in \mathbb{L}, l' \in \mathbb{L}}$ implemented in season j and time period t. For simplicity, we will refer to seasonal periods as $i \in \mathbb{I}$ instead of $(t, j) \in \mathbb{T} \times \mathbb{J}$ and consider $\mathbb{A}_i := \{(t,s)\}_{s \in \mathbb{S}_j}$ as the set of all (t,s) pairs associated to seasonal period i. Finally, we refer to $\boldsymbol{\zeta}_i \in [-1,1]^{d_i}$ as the vector of seasonal RDRD perturbances $\{\boldsymbol{\zeta}_{t,s,c}\}_{(t,s) \in \mathbb{A}_i, c \in \mathbb{C}^{\mathscr{U}}}$.

The chronology of our multi-period decision-making model is depicted in Figure 2.3. In particular, this model can be shown to take the following form:

$$\min_{\boldsymbol{x}, \{\boldsymbol{y}_i\}_{i=1}^{|\mathbb{I}|}} \max_{\{\boldsymbol{\zeta}_i \in \mathscr{Z}_i\}_{i=1}^{|\mathbb{I}|}} f^\top \boldsymbol{x} + \sum_{i=1}^{|\mathbb{I}|} h_i^\top \boldsymbol{y}_i(\boldsymbol{\zeta}_i) \tag{2.3a}$$

$$\text{s.t.} \quad A_i \boldsymbol{x} + B_i \boldsymbol{y}_i(\boldsymbol{\zeta}_i) \leq b_i + C_i \boldsymbol{\zeta}_i \quad \forall \boldsymbol{\zeta}_i \in \mathscr{Z}_i(\Gamma_i), \forall i \in \{1 \ldots |\mathbb{I}|\} \tag{2.3b}$$

$$D\boldsymbol{x} \leq e, \tag{2.3c}$$

where constraint (2.3c) describes the polyhedral feasible set for $\boldsymbol{C}$ and $\boldsymbol{V}$ based on $\mathscr{X}$ and constraints (2.1f) and (2.1g), while constraint (2.3b) describes for each i the constraints imposed on $\{\boldsymbol{P}_{t,s,l,p,c}, \boldsymbol{I}_{t,s,l,c\in\mathbb{C}^I}, \boldsymbol{E}_{t,s,l,c\in\mathbb{C}^{EX}}, \boldsymbol{T}_{t,s,l,l',c\in\mathbb{C}^{TR}}\}_{(t,s)\in\mathbb{A}_i,(l,l')\in\mathbb{L}^2}$. Namely, the latter include the constraints in $\mathscr{Y}$, which in Babonneau et al. (2017) decompose over each season, and constraints (2.1b)-(2.1e), (2.1h)-(2.1m). Finally, $\mathscr{Z}_i(\Gamma_i) := \{\boldsymbol{\zeta}_i \in \mathbb{R}^{d_i} \,|\, \|\boldsymbol{\zeta}_i\|_\infty \leq 1,\ \|\boldsymbol{\zeta}_i\|_1 \leq \Gamma_i\}$ is the traditional budgeted uncertainty set while $C_i \in \mathbb{R}^{n_i \times d_i}$ models the linear effect of the standardized perturbances on each constraint. For completeness, we note that $f \in \mathbb{R}^m$, $h_i \in \mathbb{R}^{k_i}$, $A_i \in \mathbb{R}^{n_i \times m}$, $B_i \in \mathbb{R}^{n_i \times k_i}$, and $b_i \in \mathbb{R}^{n_i}$.

2.4.2 Affinely Adjustable Approximation

Given the known numerical intractability of problem (2.3) (see Ben-Tal et al., 2004), one can instead solve a conservative approximation model obtained by enforcing that adjustable variables $\boldsymbol{y}_i(\boldsymbol{\zeta}_i)$ be affine functions of $\boldsymbol{\zeta}_i$; i.e., $\boldsymbol{y}_i(\boldsymbol{\zeta}_i) = \boldsymbol{y}_i + \boldsymbol{Y}_i \bar{\boldsymbol{\zeta}}_i$, where $\boldsymbol{y}_i \in \mathbb{R}^{k_i}$ and $\boldsymbol{Y}_i \in \mathbb{R}^{k_i \times r_i}$ become the decision variables. We follow this approach after employing a commonly used lifting of the uncertainty set:

$$\mathscr{Z}_i = P_i \bar{\mathscr{Z}}_i,$$

where

$$\bar{\mathscr{Z}}_i = \left\{ \bar{\boldsymbol{\zeta}}_i \in \mathbb{R}^{r_i} \,\middle|\, W_i \bar{\boldsymbol{\zeta}}_i \leq v_i, \bar{\boldsymbol{\zeta}}_i \geq 0 \right\},$$

with

$$W_i := \begin{bmatrix} I_{d_i} & I_{d_i} \\ \mathbf{1}_{1\times d_i} & \mathbf{1}_{1\times d_i} \end{bmatrix}, \qquad v_i := \begin{bmatrix} \mathbf{1}_{d_i \times 1} \\ \Gamma_i \end{bmatrix}, \qquad P_i := \begin{bmatrix} I_{d_i} & -I_{d_i} \end{bmatrix},$$

and I_{d_i} is the $d_i \times d_i$ identify matrix, $r_i = 2d_i$. In other words, problem (2.3) is conservatively approximated by the following robust linear program (referred as the Robust Multi-Period Conservative Approximation model):

$$\text{(RMPCA)} \qquad \min_{\boldsymbol{x}, \{\boldsymbol{Y}_i, \boldsymbol{y}_i\}_{i=1}^{|\mathbb{I}|}} \ \max_{\{\bar{\boldsymbol{\zeta}}_i \in \bar{\mathscr{Z}}_i\}_{i=1}^{|\mathbb{I}|}} f^\top \boldsymbol{x} + \sum_{i=1}^{|\mathbb{I}|} h_i^\top \left(\boldsymbol{y}_i + \boldsymbol{Y}_i \bar{\boldsymbol{\zeta}}_i \right) \tag{2.4a}$$

$$\text{s.t.} \quad A_i \boldsymbol{x} + B_i \Big(\boldsymbol{y}_i + \boldsymbol{Y}_i \bar{\boldsymbol{\zeta}}_i \Big) \leq b_i + C_i P_i \bar{\boldsymbol{\zeta}}_i \quad \forall \bar{\boldsymbol{\zeta}}_i \in \bar{\mathscr{Z}}_i \, \forall i \in \{1 \ldots |\mathbb{I}|\} \tag{2.4b}$$

$$D\boldsymbol{x} \leq e \,. \tag{2.4c}$$

Applying standard robust reformulation techniques, we obtain the following tractable linear program:

$$\min_{\boldsymbol{x}, \{\boldsymbol{\psi}_i, \boldsymbol{\Phi}_i, \boldsymbol{Y}_i, \boldsymbol{y}_i\}_{i=1}^{|\mathbb{I}|}} \; f^\top \boldsymbol{x} + \sum_{i=1}^{|\mathbb{I}|} v_i^\top \boldsymbol{\psi}_i + h_i^\top \boldsymbol{y}_i \tag{2.5a}$$

$$\text{s.t.} \quad D\boldsymbol{x} \leq e \tag{2.5b}$$

$$W_i^\top \boldsymbol{\psi}_i \geq (h_i^\top \boldsymbol{Y}_i)^\top \quad \forall i \in \{1, .., |\mathbb{I}|\} \tag{2.5c}$$

$$\boldsymbol{\Phi}_i v_i \leq b_i - A_i \boldsymbol{x} - B_i \boldsymbol{y}_i \quad \forall i \in \{1, .., |\mathbb{I}|\} \tag{2.5d}$$

$$\boldsymbol{\Phi}_i W_i \geq B_i \boldsymbol{Y}_i - C_i P_i \quad \forall i \in \{1, .., |\mathbb{I}|\} \tag{2.5e}$$

$$\boldsymbol{\Phi}_i, \boldsymbol{\psi}_i \geq 0 \,, \tag{2.5f}$$

where $\boldsymbol{\psi}_i \in \mathbb{R}^{(d_i+1)\times 1}$ and $\boldsymbol{\Phi}_i \in \mathbb{R}^{n_i \times (d_i+1)}$ are new variables added to the model to guarantee the feasibility of the decision variables in the worst-case scenario. It is worth mentioning that problem (2.5) provides an upper-bound and feasible first-stage decision for problem (2.3) as the space of decision rule has been reduced to affine functions.

2.5 Improving Numerical Efficiency using Benders Decomposition

Because of the capacity expansion decisions with a horizon of several decades, alongside with the procurement decisions with daily resolution, ETEM is already in its deterministic form a large-scale LP model. The size of LP that needs to be solved is further exacerbated when considering the robust reformulation presented in (2.5). In this regard, Section 2.6 will consider instances where the number of decisions and constraints is increased twenty-fold and nine-fold respectively. For this reason, we propose here a decomposition scheme to reduce the computational burden.

Specifically, we start by reformulating problem (2.4) as follows:

$$\min_{\boldsymbol{x},\boldsymbol{\rho},\{\boldsymbol{y}_i\}_{i=1}^{|\mathbb{I}|}} f^\top \boldsymbol{x} + \sum_{i=1}^{|\mathbb{I}|} h_i^\top \boldsymbol{y}_i + \boldsymbol{\rho}_i \tag{2.6a}$$

$$\text{s.t.} \quad D\boldsymbol{x} \le e \tag{2.6b}$$

$$\boldsymbol{\rho}_i \ge g_i(\boldsymbol{x},\boldsymbol{y}_i) \quad \forall i \in \{1...|\mathbb{I}|\} \tag{2.6c}$$

$$A_i\boldsymbol{x} + B_i\boldsymbol{y}_i \le b_i \quad \forall i \in \{1...|\mathbb{I}|\}, \tag{2.6d}$$

with

$$g_i(\boldsymbol{x},\boldsymbol{y}_i) := \min_{\boldsymbol{Y}_i} \max_{\{\bar{\boldsymbol{\zeta}}_i \in \bar{\mathscr{Z}}_i\}_{i=1}^{|\mathbb{I}|}} h_i^\top \boldsymbol{Y}_i \bar{\boldsymbol{\zeta}}_i \tag{2.7a}$$

$$\text{s.t.} \quad (2.4\text{b}),$$

where constraint (2.6d) is a redundant constraint that describes the fact that (2.4b) must be satisfied for $\bar{\boldsymbol{\zeta}}_i = 0$ since $0 \in \bar{\mathscr{Z}}_i$. Given that $g_i(\boldsymbol{x},\boldsymbol{y}_i)$ is jointly convex, we identify a supporting plane representation that will enable the use of a constraint generation approach, also commonly referred to as a Benders decomposition scheme, which relies on iteratively solving a master and set of subproblems until convergence. Note that constraint (2.6c) should be considered violated if $\boldsymbol{x}$ and $\boldsymbol{y}_i$ are such that problem (2.7) is infeasible.

In what follows, we start by describing the algorithm, then present two schemes that can be employed to improve its numerical efficiency by refining the quality of the upper and lower bounding process. In the latter case, the refinement will make use for the first time of the notion of Pareto robustly optimal solution (Iancu and Trichakis, 2014) in decomposition schemes for robust optimization.

Remark 1. *It is worth noting that our scheme is strongly inspired by the one used in Ardestani-Jaafari and Delage (2018) and Ardestani-Jaafari and Delage (2020), yet we depart from that work in three ways. First, unlike this prior work we choose to keep in problem* (2.6) *the $\boldsymbol{y}_i$ variables, which describe what the affine strategy prescribes for the nominal scenario $\bar{\boldsymbol{\zeta}} = 0$. This allows us to more easily interpret the optimal solution.*

We also observed empirically that this led to a significant reduction in the number of iterations. Second, we derive conditions that are specific to this application under which we can ensure that the solution of the master's problem always leads to a set of feasible subproblems. Third, we identify a new scheme, which is based on the theory of Pareto robust optimality, to identify optimal solutions of the master problem that accelerate the convergence of the algorithm.

2.5.1 The Benders Decomposition Algorithm

To simplify the presentation of this algorithm we make the following assumption.

Assumption 1. *(Uncapacitated technology) ETEM includes a technology* $p_x \in \mathbb{P}_c^P/\mathbb{P}^R$ *with* $c \in \mathbb{C}^{\mathscr{U}}$ *generated from a resource* $c_x \in \mathbb{C}^I/\mathbb{C}^{\mathscr{D}}$*, with infinite capacity, i.e.,* $\Omega_{t,l,p_x} = \infty$*. Furthermore,* $\mathscr{X}$ *and* $\mathscr{Y}$ *do not impose additional constraints on* $\boldsymbol{P}_{t,s,l,p_x,c}$ *and* $\boldsymbol{I}_{t,s,l,c_x}$*.*

The role of the above assumption is to ensure that when removing constraint (2.6c) from problem (2.6), we do not end up with solutions for $(\boldsymbol{x}, \{\boldsymbol{y}_i\}_{i=1}^{|\mathbb{I}|})$ that make problem (2.7) infeasible. Note also that in our description of ETEM, the EXT technology and ExR energy resource respectively play the role of p_x and c_x.

Lemma 1. *Given that an uncapacitated technology exists (i.e., Assumption 1), problem* (2.7) *is feasible for any* $\boldsymbol{x}$ *and* $\{\boldsymbol{y}_i\}_{i=1}^{|\mathbb{I}|}$ *that satisfy* (2.6d).

Proof. One needs to show that for any given $\boldsymbol{x}$ and $\boldsymbol{y}_i$, $i = 1, \cdots, |\mathbb{I}|$, that satisfy (2.6b) and (2.6d), there exists a $\boldsymbol{Y}_i$ so that the constraint (2.4b) is feasible. To do so, given that we already now that $\boldsymbol{x}$ and $\boldsymbol{y}_i$ are such that they can cover the nominal demand response, i.e., $\boldsymbol{\zeta}^+ = \boldsymbol{\zeta}^- = 0$, we will show how to construct a $\boldsymbol{Y}_i$ that will simply cover any deviation of the demand coming from the RDRDusing the uncapacited technology. Specifically, we let all values of $\boldsymbol{Y}$ equal to zero except for the terms that model the influence of $\boldsymbol{\delta}^+$ on $\boldsymbol{P}_{t,s,l,p_x,c}$ with $c \in \mathbb{C}^{\mathscr{U}}$, $\boldsymbol{P}_{t,s,l,p_x,c_x}$, and $\boldsymbol{I}_{t,s,l,c_x}$. In particular, when setting all other terms to zero, most constraints reduce exactly to the constraints imposed in (2.6d) and are straightforwardly satisfied. The only constraints that need to be verified consist of a few members of (2.1b), (2.1e), (2.1h) and (2.1j), which can be described as follows:

$$\begin{aligned}(2.1\text{b}) \rightarrow &\Big(\sum_{p\in\mathbb{P}^{P_{c_x}}} \bar{\boldsymbol{P}}_{t,s,l,p,c_x} + \bar{\boldsymbol{I}}_{t,s,l,c_x} + \sum_{c\in\mathbb{C}^{\mathscr{U}}} \boldsymbol{I}^{+}_{t,s,l,c_x,c}\boldsymbol{\delta}^{+}_{t,s,c}\Big)\eta_{c_x} + \sum_{l'\neq l}(\eta_{c_x}\bar{\boldsymbol{T}}_{t,s,l',l,c_x} - \bar{\boldsymbol{T}}_{t,s,l,l',c_x})\\ &\geq \sum_{p\in\mathbb{P}^{C}_{c}} \bar{\boldsymbol{P}}^{+}_{t,s,l,p,c} + \sum_{c\in\mathbb{C}^{\mathscr{U}}} \boldsymbol{P}^{+}_{t,s,l,p_x,c_x,c}\boldsymbol{\delta}^{+}_{t,s,c} + \bar{\boldsymbol{E}}_{t,s,l,c_x} \qquad \begin{array}{l}\forall(\boldsymbol{\delta}^{+}_{i},\boldsymbol{\delta}^{-}_{i}) \in \bar{\mathscr{Z}_i}, \forall l \in \mathbb{L}\\ \forall(t,s) \in \mathscr{A}_i, \forall i \in \mathbb{I}\end{array}\end{aligned} \tag{2.8}$$

$$\begin{aligned}(2.1\text{e}) \rightarrow &\sum_{p\in\mathbb{P}^{P}_{c}} \bar{\boldsymbol{P}}_{t,s,l,p,c} + \boldsymbol{P}^{+}_{t,s,l,p_x,c}\boldsymbol{\delta}^{+}_{t,s,c} \geq \Theta_{t,l,c}\big(\bar{\boldsymbol{V}}_{t,s,c} + \boldsymbol{\delta}^{+}_{t,s,c} - \boldsymbol{\delta}^{-}_{t,s,c}\big)\\ &\forall(\boldsymbol{\delta}^{+}_{i},\boldsymbol{\delta}^{-}_{i}) \in \bar{\mathscr{Z}_i}, \forall c \in \mathbb{C}^{\mathscr{U}}\\ &\forall(t,s) \in \mathscr{A}_i, \forall i \in \mathbb{I}\end{aligned} \tag{2.9}$$

$$(2.1\text{h}) \rightarrow \quad \sum_{c:p_x\in\mathbb{P}^{P}_{c}} \bar{\boldsymbol{P}}_{t,s,l,p_x,c} + \sum_{c\in\mathbb{C}^{\mathscr{U}}} \boldsymbol{P}^{+}_{t,s,l,p_x,c}\boldsymbol{\delta}^{+}_{t,s,c} \leq \infty \qquad \begin{array}{l}\forall(\boldsymbol{\delta}^{+}_{i},\boldsymbol{\delta}^{-}_{i}) \in \bar{\mathscr{Z}_i}, \forall l \in \mathbb{L}\\ \forall(t,s) \in \mathscr{A}_i, \forall i \in \mathbb{I}\end{array} \tag{2.10}$$

$$\begin{aligned}(2.1\text{j}) \rightarrow &\sum_{c\in\mathbb{C}_{f'}} \bar{\boldsymbol{P}}_{t,s,l,p_x,c} + \sum_{c\in\mathbb{C}^{\mathscr{U}}} \boldsymbol{P}^{+}_{t,s,l,p_x,c}\boldsymbol{\delta}^{+}_{t,s,c} = \eta^{t}_{f,f'}\Big(\sum_{c\in\mathbb{C}_f} \bar{\boldsymbol{P}}_{t,s,l,p_x,c} +\\ &\sum_{c'\in\mathbb{C}^{\mathscr{U}}} \boldsymbol{P}^{+}_{t,s,l,p_x,c_x,c'}\boldsymbol{\delta}^{+}_{t,s,c'}\Big) \qquad \begin{array}{l}\forall(\boldsymbol{\delta}^{+}_{i},\boldsymbol{\delta}^{-}_{i}) \in \bar{\mathscr{Z}_i}, \forall l \in \mathbb{L}\\ \forall(t,s) \in \mathscr{A}_i, \forall i \in \mathbb{I}\end{array} \quad ,\end{aligned} \tag{2.11}$$

where $\bar{\boldsymbol{P}}$, $\bar{\boldsymbol{V}}$, $\bar{\boldsymbol{C}}$, $\bar{\boldsymbol{I}}$, $\bar{\boldsymbol{T}}$, and $\bar{\boldsymbol{E}}$ refer to the assignments made through the fixed $\boldsymbol{x}$ and $\boldsymbol{y}_i$'s, while $\boldsymbol{P}^{+}_{t,s,l,p_x,c}$, $\boldsymbol{P}^{+}_{t,s,l,p_x,c_x,c}$, and $\boldsymbol{I}^{+}_{t,s,l,c_x,c}$ model the influence of $\boldsymbol{\delta}^{+}_{t,s,c}$ on $\boldsymbol{P}_{t,s,l,p_x,c}$, $\boldsymbol{P}_{t,s,l,p_x,c_x}$, and $\boldsymbol{I}_{t,s,l,c_c}$ respectively, for $c \in \mathbb{C}^{\mathscr{U}}$. In order to get a feasible assignment for $\boldsymbol{Y}$, for all t, s, $c \in \mathbb{C}^{\mathscr{U}}$, we let $\boldsymbol{P}^{+}_{t,s,l,p_x,c} := \Theta_{t,l,c}$, $\boldsymbol{P}^{+}_{t,s,l,p_x,c_x,c} := \boldsymbol{P}^{+}_{t,s,l,p_x,c}/\eta^{t}_{f,f'}$, and $\boldsymbol{I}^{+}_{t,s,l,c_x,c} = \boldsymbol{P}^{+}_{t,s,l,p_x,c_x,c}/\eta_{c_x}$. One can readily verify that constraints (2.8), (2.10), and (2.11) reduce to the constraint already accounted for in (2.6d). On the other hand, constraint (2.9) reduces to:

$$\sum_{p\in\mathbb{P}^{P}_{c}} \bar{\boldsymbol{P}}_{t,s,l,p,c} \geq \Theta_{t,l,c}\big(\bar{\boldsymbol{V}}_{t,s,c} - \boldsymbol{\delta}^{-}_{t,s,c}\big) \qquad \begin{array}{l}\forall(\boldsymbol{\delta}^{+}_{i},\boldsymbol{\delta}^{-}_{i}) \in \bar{\mathscr{Z}_i}, \forall c \in \mathbb{C}^{\mathscr{U}}\\ \forall(t,s) \in \mathscr{A}_i, \forall i \in \mathbb{I}\end{array} \quad ,$$

which is necessarily satisfied since $\Theta_{t,l,c} \geq 0$ and $\boldsymbol{\delta}_i^- \geq 0$. A similar argument can be used to confirm that all non-negative constraints on $\bar{\boldsymbol{P}}_{t,s,l,p_x,c} + \boldsymbol{P}^+_{t,s,l,p_x,c}\boldsymbol{\delta}^+_{t,s,c}$, $\bar{\boldsymbol{P}}_{t,s,l,p_x,c_x} + \sum_{c\in\mathbb{C}^{\mathscr{U}}} \boldsymbol{P}^+_{t,s,l,p_x,c_x,c}\boldsymbol{\delta}^+_{t,s,c}$, and $\bar{\boldsymbol{I}}_{t,s,l,c_x} + \sum_{c\in\mathbb{C}^{\mathscr{U}}} \boldsymbol{I}^+_{t,s,l,c_x,c}\boldsymbol{\delta}^+_{t,s,c}$ are also satisfied. $\square$

In practice, if Assumption 1 is not satisfied, a few remedies exist. First, one can create an artificial technology with either infinite or very large capacity, whose price is set to an arbitrarily large amount. One can interpret the price of this artificial technology as the marginal cost of shortages in the system. If this technology is not used in the optimal solution that is identified, then shortages do not occur and the solution is optimal for the problem without this artificial technology. Alternatively, one could also modify the algorithm that is presented below to have it identify "feasibility cuts" when the current candidate solution makes (2.7) infeasible (see Rahmaniani et al., 2017, for details).

We now focus on presenting a support plane representation of $g(\boldsymbol{x},\boldsymbol{y}_i)$.

Theorem 2. *Given that Assumption 1 is satisfied,*

$$g_i(\boldsymbol{x},\boldsymbol{y}_i) = \max_{\boldsymbol{\theta}_i\geq 0,\bar{\boldsymbol{\zeta}}_i\geq 0,\boldsymbol{\lambda}_i\geq 0} (-b_i + A_i\boldsymbol{x} + B_i\boldsymbol{y}_i)^\top \boldsymbol{\theta}_i - Tr(C_iP_i\boldsymbol{\lambda}_i) \tag{2.12a}$$

$$s.t. \quad \boldsymbol{\theta}_i v_i^\top - \boldsymbol{\lambda}_i W_i^\top \geq 0 \tag{2.12b}$$

$$B_i^\top \boldsymbol{\lambda}_i = -h_i\bar{\boldsymbol{\zeta}}_i^\top \tag{2.12c}$$

$$W_i\bar{\boldsymbol{\zeta}}_i \leq v_i\,, \tag{2.12d}$$

where $\boldsymbol{\theta}_i \in \mathbb{R}^{n_i\times 1}, \boldsymbol{\lambda}_i \in \mathbb{R}^{n_i\times r_i}$ *and* $\bar{\boldsymbol{\zeta}}_i \in \mathbb{R}^{r_i\times 1}$.

Proof. In the first step, we identify the robust counterpart of constraint (2.4b). For each $i\in\mathbb{I}$, given that $\bar{\mathscr{Z}_i}$ is non-empty, LP duality applies on each robust constraint thus introducing auxiliary variables that we denote in matrix form in $\boldsymbol{\Phi}_i$. Namely, constraint (2.4b) can be said equivalent to

$$\exists \boldsymbol{\Phi}_i \in \mathbb{R}^{n_i\times(d_i+1)}, \quad \forall i \in \{1\cdots|\mathbb{I}|\}$$

$$\boldsymbol{\Phi}_i v_i \leq b_i - A_i\boldsymbol{x} - B_i\boldsymbol{y}_i \qquad \forall i \in \{1\cdots|\mathbb{I}|\} \tag{2.13}$$

$$\boldsymbol{\Phi}_i W_i \geq B_i\boldsymbol{Y}_i - C_iP_i \quad \forall i \in \{1\cdots|\mathbb{I}|\}\,. \tag{2.14}$$

Therefore, problem (2.7) can be reformulated as:

$$\begin{aligned} \min_{\boldsymbol{Y}_i, \boldsymbol{\Phi}_i} \quad & \max_{\bar{\boldsymbol{\zeta}}_i \in \bar{\mathscr{Z}}_i} \left(h_i^\top \boldsymbol{Y}_i \bar{\boldsymbol{\zeta}}_i \right) \\ \text{s.t.} \quad & (2.13), (2.14), \end{aligned}$$

which is a feasible minimization problem according to Lemma 1 since we assumed that Assumption 1 holds. In the next step, since $\bar{\mathscr{Z}}_i$ is a compact and convex set, Sion's minmax theorem (Sion, 1958) holds and one can reverse the order of minimization over $\{\boldsymbol{Y}_i, \boldsymbol{\Phi}_i\}$ and maximization over $\bar{\boldsymbol{\zeta}}_i$'s. Finally, since the set defined by (2.13) and (2.14) is feasible, one can employ LP duality to replace the inner minimization problem with its dual maximization problem to obtain:

$$\begin{aligned} g(\boldsymbol{x}, \boldsymbol{y}_i) = \max_{\bar{\boldsymbol{\zeta}}_i \in \bar{\mathscr{Z}}_i, \boldsymbol{\theta}_i, \boldsymbol{\lambda}_i} \quad & (-b_i + A_i \boldsymbol{x} + B_i \boldsymbol{y}_i)^\top \boldsymbol{\theta}_i - Tr(C_i P_i \boldsymbol{\lambda}_i) \\ \text{s.t.} \quad & \boldsymbol{\theta}_i \nu_i^\top - \boldsymbol{\lambda}_i W^\top \geq 0 \\ & B_i^\top \boldsymbol{\lambda}_i = -h_i \bar{\boldsymbol{\zeta}}_i^\top \\ & \boldsymbol{\theta}_i \geq 0,\ \boldsymbol{\lambda}_i \geq 0, \end{aligned}$$

where $\boldsymbol{\lambda}_i \in \mathbb{R}^{n_i \times r_i}$, $\boldsymbol{\theta}_i \in \mathbb{R}^{n_i \times 1}$ are dual variables associated with constraints (2.13) and (2.14) respectively. □

Equipped with Theorem 2, we can define the following Benders decomposition algorithm. Intuitively, the procedure consists in solving a so-called master problem in which constraint (2.6c) is removed thus producing a sequence of lower bounds for problem (2.4). Given a current optimal solution of the master problem, the latter is refined by progressively reintroducing the constraints that are the most violated from the set:

$$\boldsymbol{\rho}_i \geq (-b_i + A_i \boldsymbol{x} + B_i \boldsymbol{y}_i)^\top \boldsymbol{\theta}_i - Tr(C_i P_i \boldsymbol{\lambda}_i),$$

$$\forall (\boldsymbol{\lambda}_i, \boldsymbol{\theta}_i) \in \{(\boldsymbol{\lambda}_i, \boldsymbol{\theta}_i) \in \mathbb{R}_+^{n_1 \times r_i} \times \mathbb{R}_+^{n_i} \,|\, \exists \bar{\boldsymbol{\zeta}}_i \in \bar{\mathscr{Z}}_i, \text{(2.12b), (2.12c)}\}, \forall i \in \mathbb{I}.$$

For each i, the most violated constraint can be found by solving the LP presented in (2.12), which optimal value can be used to update an upper bound problem (2.4). We refer the reader to the pseudo-code presented in Algorithm 1.

Algorithme 1 : Benders Decomposition (BD) algorithm

Set $UB = \infty, LB = -\infty, v = 0$;
Let i be the index for each subproblem;
Let $v = v+1$ and solve the deterministic problem, i.e., problem (2.4) when $\bar{\mathscr{Z}}_i = \{0\}$, and store the value of $\boldsymbol{x}$ as $\overline{\boldsymbol{x}}^{(v)}$ and $\boldsymbol{y}_i$ as $\overline{\boldsymbol{y}}_i^{(v)}$;
while $(UB - LB)/LB \geq \varepsilon$ **do**
    $\forall i = \{1 \cdots |\mathbb{I}|\}$ solve problem (2.12) with $(\overline{\boldsymbol{x}}^{(v)}, \overline{\boldsymbol{y}}_i^{(v)})$ and store the optimal value in $\boldsymbol{\rho}_i^*$ and decision variables in $\overline{\boldsymbol{\theta}}_i^v, \overline{\boldsymbol{\lambda}}_i^v, \overline{\boldsymbol{\zeta}}_i^v$;
    Update upper bound $UB = \min(UB, f^\top \overline{\boldsymbol{x}}^v + \sum_{i=1}^{|\mathbb{I}|} \boldsymbol{\rho}_i^* + h_i^\top \overline{\boldsymbol{y}}_i^v)$;
    Solve the updated master problem :

$$\min_{\boldsymbol{x}, \{\boldsymbol{\rho}_i, \boldsymbol{y}_i\}_{i=1}^{|\mathbb{I}|}} f^\top \boldsymbol{x} + \sum_{i=1}^{|\mathbb{I}|} h_i^\top \boldsymbol{y}_i + \boldsymbol{\rho}_i \tag{2.15a}$$

$$\text{s.t.} \quad (2.6\text{b}), (2.6\text{d}),$$

$$\boldsymbol{\rho}_i \geq (-b_i + A_i \boldsymbol{x} + B_i \boldsymbol{y}_i)^\top \overline{\boldsymbol{\theta}}_i^{v'} - Tr(C_i P \overline{\boldsymbol{\lambda}}_i^{v'}), \quad \forall v' \leq v, \forall i \in \{1 \cdots |\mathbb{I}|\}. \tag{2.15b}$$

    Let $v = v+1$ and store the optimal value of the master problem variables in $\overline{\boldsymbol{x}}^v, \overline{\boldsymbol{y}}_i^v$ and $\overline{\boldsymbol{\rho}}^v$;
    Update the lower bound: $LB = f^\top \overline{\boldsymbol{x}}^v + \sum_i h_i^\top \overline{\boldsymbol{y}}_i^v + \overline{\boldsymbol{\rho}}^v$.
end

2.5.2 Improving the Algorithm's Convergence

In order to improve the algorithm convergence, we apply two strategies. First, as proposed in Ardestani-Jaafari and Delage (2018) and Ardestani-Jaafari and Delage (2020), we add a set of valid inequalities to the master problem (2.15) based on violated scenarios from previous iterations in order to tighten the lower bounding problem. Specifically, for any $i \in \mathbb{I}$ and finite set of scenarios $\{\bar{\boldsymbol{\zeta}}_i^l\}_{l \in \Omega} \subset \bar{\mathscr{Z}}_i$, the following constraint necessarily holds in problem (2.6):

$$\forall l \in \Omega, \exists \boldsymbol{y}_i^l \in \mathbb{R}^{d_i},\ \boldsymbol{\rho}_i \geq h_i^\top (\boldsymbol{y}_i^l - \boldsymbol{y}_i)\ \&\ A_i \boldsymbol{x} + B_i \boldsymbol{y}_i^l \leq b_i + C_i P_i \bar{\boldsymbol{\zeta}}_i^l,$$

given that for all $l \in \Omega$:

$$\boldsymbol{\rho}_i \geq g(\boldsymbol{x}, \boldsymbol{y}_i) = \min_{\boldsymbol{Y}_i : (2.4\text{b})} \max_{\bar{\boldsymbol{\zeta}}_i \in \bar{\mathscr{Z}}_i} h_i^\top \boldsymbol{Y}_i \bar{\boldsymbol{\zeta}}_i \geq \min_{\boldsymbol{Y}_i : A_i \boldsymbol{x} + B_i \left(\boldsymbol{y}_i + \boldsymbol{Y}_i \bar{\boldsymbol{\zeta}}_i^l\right) \leq b_i + C_i P_i \bar{\boldsymbol{\zeta}}_i^l} h_i^\top \boldsymbol{Y}_i \bar{\boldsymbol{\zeta}}_i^l$$

$$= \min_{\boldsymbol{y}_i^l, \boldsymbol{Y}_i : \boldsymbol{y}_i^l = \boldsymbol{y}_i + \boldsymbol{Y}_i \bar{\boldsymbol{\zeta}}_i^l, A_i \boldsymbol{x} + B_i \boldsymbol{y}_i^l \le b_i + C_i P_i \bar{\boldsymbol{\zeta}}_i^l} h_i^\top (\boldsymbol{y}_i^l - \boldsymbol{y}_i)$$

$$\ge \min_{\boldsymbol{y}_i^l : A_i \boldsymbol{x} + B_i \boldsymbol{y}_i^l \le b_i + C_i P_i \bar{\boldsymbol{\zeta}}_i^l} h_i^\top (\boldsymbol{y}_i^l - \boldsymbol{y}_i),$$

where $\boldsymbol{y}_i^l$ plays the role of an adjustable plan specifically designed for scenario $\bar{\boldsymbol{\zeta}}_i^l$ and which can depart from the affine decision rule. Finally, In our implementation, we choose to set $\{\bar{\boldsymbol{\zeta}}_i^l\}_{l\in\Omega}$ to be the violated scenarios in the last v iterations of the algorithm. For completeness, we include the new master problem below:

$$\min_{\boldsymbol{x}, \{\boldsymbol{\rho}_i, \boldsymbol{y}_i, \boldsymbol{y}_i^l\}_{i=1}^{|\mathbb{I}|}} \quad f^\top \boldsymbol{x} + \sum_{i=1}^{|\mathbb{I}|} h_i^\top \boldsymbol{y}_i + \boldsymbol{\rho}_i \tag{2.16a}$$

$$\text{s.t.} \quad (2.6\text{b}), (2.6\text{d}), (2.15\text{b}),$$

$$\boldsymbol{\rho}_i \ge h_i^\top (\boldsymbol{y}_i^l - \boldsymbol{y}_i) \quad \forall l \in \Omega, \forall i \in \{1 \cdots |\mathbb{I}|\} \tag{2.16b}$$

$$A_i \boldsymbol{x} + B_i \boldsymbol{y}_i^l \le b_i + C_i P_i \bar{\boldsymbol{\zeta}}_i^l \quad \forall l \in \Omega, \forall i \in \{1 \cdots |\mathbb{I}|\}. \tag{2.16c}$$

The second proposed improvement has to do with how the upper bound is obtained. In particular, this bound comes from evaluating the true worst-case cost of the current best candidate based on the master problem (2.15), or its tighter version (2.16). Yet, since the master problem is itself a robust optimization problem, we can expect based on the findings of Iancu and Trichakis (2014) that at each iteration there exists a large set of optimal solutions for (2.15). In a traditional Benders decomposition approach (such as in Ardestani-Jaafari and Delage, 2018), the candidate that is used to calculate the upper bound and generate an optimality cut is arbitrarily chosen by the LP solver used to solve (2.15). While such a solution is optimal for (2.15), it could have a much worst performance in problem (2.12) compared to other optimal solutions. We therefore recommend, after solving (2.15), to identify a Pareto robustly optimal solution of (2.15) by solving the following LP:

$$\min_{\boldsymbol{x}, \{\boldsymbol{\rho}_i', \boldsymbol{\rho}_i, \boldsymbol{y}_i\}_{i=1}^{|\mathbb{I}|}} f^\top \boldsymbol{x} + \sum_{i=1}^{|\mathbb{I}|} h_i^\top \boldsymbol{y}_i + \boldsymbol{\rho}_i' \tag{2.17a}$$

$$\text{s.t.} \quad (2.6\text{b}), (2.6\text{d}), (2.15\text{b}), (2.16\text{b}), (2.16\text{c}),$$

$$f^\top \boldsymbol{x} + \sum_{i=1}^{|\mathbb{I}|} h_i^\top \boldsymbol{y}_i + \boldsymbol{\rho}_i \leq (1+\varepsilon)\mathscr{M}_v^* \tag{2.17b}$$

$$\boldsymbol{\rho}_i' \geq \sum_{v' \leq v} \frac{1}{v}((-b_i + A_i \boldsymbol{x} + B_i \boldsymbol{y}_i)^\top \overline{\boldsymbol{\theta}}_i^{v'} - Tr(C_i P \overline{\boldsymbol{\lambda}}_i^{v'})) \quad \forall i \in \{1 \cdots |\mathbb{I}|\}, \tag{2.17c}$$

where $\mathscr{M}_v^*$ is the optimal solution of the master problem (2.15) in iteration v of Algorithm 1, and $\varepsilon > 0$ allows for some small ε sub-optimality in order to help numerically. The new candidate $(\overline{\boldsymbol{x}}^v, \overline{\boldsymbol{y}}_i^v)$ remains approximately optimal for (2.15) yet is guaranteed to not be Pareto dominated by other solutions of (2.15). This follows from the fact that constraint (2.17c) is equivalent to:

$$\boldsymbol{\rho}_i' \geq (-b_i + A_i \boldsymbol{x} + B_i \boldsymbol{y}_i)^\top (\sum_{v' \leq v} \frac{1}{v} \overline{\boldsymbol{\theta}}_i^{v'}) - Tr(C_i P(\sum_{v' \leq v} \frac{1}{v} \overline{\boldsymbol{\lambda}}_i^{v'})) \quad \forall i \in \{1 \cdots |\mathbb{I}|\},$$

and that $((\sum_{v' \leq v} \frac{1}{v} \overline{\boldsymbol{\theta}}_i^{v'}), (\sum_{v' \leq v} \frac{1}{v} \overline{\boldsymbol{\lambda}}_i^{v'}))$ is in the relative interior of the convex hull of $\{(\overline{\boldsymbol{\theta}}_i^{v'}, \overline{\boldsymbol{\lambda}}_i^{v'})\}_{v' \leq v}$. Hence, Corollary 1 in Iancu and Trichakis (2014) can be applied to obtain the Pareto non-dominance guarantee.

We refer the reader to Iancu and Trichakis (2014) for more details about how to identify Pareto robustly optimal solutions.

2.6 Computational Results

In this section, we evaluate the performance of the proposed robust ETEM approximation model (i.e., RMPCA) on a case study based on the energy system of the Arc Lémanique region in Switzerland. To do so, we compare the performance of the RMPCA formulation with a static robust model (SRM), which considers all decisions as *here-and-now* decisions, and a deterministic model (DET), which disregards demand response uncertainty. The purpose of these computational experiments is to empirically show that: i) considering DRU in a capacity expansion planning problem and solving it using robust optimization can decrease both worst-case and expected total costs of the system compared to a deterministic formulation of the problem; and ii) assuming flexibility of the procurement decisions with respect to observed actual DR decreases the level of conservatism of the model and consequently the expected total cost of the system. Recall that in RMPCA the planner first decides on the capacities and planned DR, then in seasonal periods, after observing the actual DR, he decides on the optimal procurement of energy. Theoretically, it is known that the policies proposed by SRM are more conservative compared to policies proposed by RMPCA. In addition, we present a detailed comparison of the structure of the RMPCA, SRM, and DET policies. The purpose is to understand how considering the uncertainty of the demand response affects the long-term capacity expansion strategies. Finally, we provide a computational analysis to compare the performance of the different decomposition algorithms presented in Section 2.5. All numerical studies are performed on a 64-bit computer with 128 GB of RAM and Intel(R) Xeon(R) 3.1 GHz (40 CPUs). The deterministic version of ETEM is originally written in AMPL. However, we extract the standard form matrices from AMPL and carry out robust optimization using the YALMIP toolbox and GUROBI solver in a MATLAB R2019a environment.

2.6.1 A Swiss Case Study

The ETEM model describing the Arc Lémanique region (Cantons of Geneva and Vaud, in Switzerland) encompasses 142 different technologies, including centralized electricity and heat production plants, decentralized electricity production, conventional and flexible loads, and end-use transportation technologies. In addition, 57 energy commodities, including 21 types of useful demand, are modeled. We choose to immunize ETEM against residential electricity demand response deviations (i.e., Res-ELC in Figure 2.1), which implies that the robust model is subject to 120 independent sources of perturbations. This choice is motivated by the fact that the response behavior of residential electricity is more prone to uncertainty in the long-run compared to industrial and large-scale electricity consumers, as the former corresponds to a larger and more diverse group of consumers. Table 2.2 presents techno-economic features of both presently available and expected future electricity generation technologies in the Arc Lémanique region. As we

Table 2.2: Characteristics of electricity generation technologies considered in the Arc Lémanique region model

Category[1]	Technology	Status	Input[2]	Output[3]	Investment cost (MCHF/GW)	Fixed cost (MCHF/GW)	Variable cost (MCHF/PJ)	Efficiency	Life (year)
Gas-PP	Gas Turbine	existing	NGA	ELC,CO2	300	25	0.22	0.3	4
	Gas CC	new	NGA	ELC,CO2	450	25	0.55	0.6	5
Hydro-PP	Veytaux (turbine)	existing	HYD	ELC	-	130	0	0.89	10
	Hydroelectric VAUD	existing	HYD	ELC	-	130	0	0.39	10
	Hydroelectric GENEVA	existing	HYD	ELC	-	130	0	0.39	10
PV	Photovoltaic	new	SOL	ELC	6000-2000	25	0	0.39	6
Wind-pp	Wind	new	WND	ELC	1500-1250	40	0	0.4	5
Oil-Fired-PP	Oil-Fired Steam-Cycle	new	DSL	ELC,CO2	-	92	0.52	0.39	6
	Oil-Fired Steam-Cycle (CPD)	new	NGA,DSL	ELC,CO2	1100	68	0.55	0.4	7
CHP	Gas CC (CHP)	new	NGA	ELC,CO2	1000	46	0.55	0.85	7
	Centrale de Cheneviers (heat and electricity)	existing	MSW	ELC,CO2	1200	30	0.0	0.38	10
	Enerbois (Vaud)	existing	WOR	ELC,CO2	-	0	0.0	1	10
	Pierre-de-Plan (heat+electricity)	existing	NGA	ELC,CO2	450	25	0.55	0.9	5
	Industrial Cogen. Gas Turbine (5 MW)	existing	NGA	ELC,CO2	800	78	0	0.28	5
	Industrial Cogen. STEAM Turbine (5 MW)	existing	NGA	ELC,CO2	1000	208	0	0.15	5
	Industrial Combined Cycle CC (5 MW)	existing	NGA	ELC,CO2	1200	68	0	0.37	5
	Cogeneration INDustry (Motor)	existing	NGA	ELC,CO2	4160	104	0	0.35	3
	Cogeneration COMM (Motor)	existing	NGA	ELC,CO2	5434	65	0	0.53	3
	Cogeneration RESID (Motor)	existing	NGA	ELC,CO2	6136	92	0	0.53	3
	Chatillon Plant (heat)	existing	WOR	ELC,CO2	-	-	-	1	10
	CHP combined heat production	new	NGA	ELC,CO2	1800	15	0.71	0.9	4
	CHP combined heat production	new	NGA	ELC,CO2	1200	12	0.71	0.9	4
Other-PP	Geothermie (Vaud)	existing	HTH	ELC	-	-	-	1	10
	Tridel (Vaud) Electricity	existing	MSW	ELC,CO2	-	-	-	0.38	10
	Gas fuel cell	new	NGA	ELC	2000-1250	78	4.78	0.42	6

[1] Definition of technology categories is presented in Fig 2.1.
[2] NGA: Natural gas, HYD: Hydro power, SOL: Solar, WND: Wind, DSL: Diesel, MSW: Municipal solid waste, WOR: Wood residential, HTH: High temperature heat.
[3] ELC: Electricity, CO2: CO_2 emissions.

wish to avoid as much as possible energy shortages in the system, we set the cost of the additional energy source (ExR) high enough so that there is no capacity shortage in the optimal solution of RMPCA model when the largest amount of deviations are assumed. Finally, in order to better investigate the influence of robust optimization on the solutions, no upper bound limits the installation of renewable technologies (wind and photovoltaic power plants) in the model. For interested readers, we note that our deterministic version of ETEM presents 171,620 variables and 431,652 constraints while the LP reformulation of RMPCA, i.e., problem (2.5), presents 3,540,720 variables and 3,708,658 constraints.

While we refer the reader to Babonneau et al. (2017) for a complete description of all input parameters and assumptions, it is worth mentioning that we consider here a case where CO_2 emissions are curbed to 2.5 Mt in 2050, a 45% reduction compared to 2010 levels (5.48 Mt).

2.6.2 Performance Analysis

In this section, we study the performance of strategies proposed by RMPCA, SRM, and DET in the average and worst-case scenarios. For a specific budget size Γ and box size β, $\boldsymbol{x}^{\Gamma,\beta}_{RMPCA}$ represents the RMPCA strategy obtained by solving problem (2.5). Similarly, $\boldsymbol{x}^{\Gamma,\beta}_{SRM}$ is the static robust strategy obtained by solving problem (2.5) when forcing $\boldsymbol{Y}_i = 0 \; \forall i \in \{1 \cdots |\mathbb{I}|\}$. It should be noted that, because problem (2.5) is computationally demanding and cannot be solved in a 72-hour time limit, we have used the PRO-BD-VI algorithm proposed in Section 2.5. Finally, the DET strategy $\boldsymbol{x}_{DET}$ is obtained by solving the deterministic model, i.e., problem (2.4) when $\bar{\mathscr{Z}_i} = \{0\} \; \forall i \in \{1 \cdots |\mathbb{I}|\}$. After obtaining all the strategies from the different models, in a next step, we generate a set of 1000 DR random scenarios $\boldsymbol{\zeta}^j_i$ $(\forall i \in \{1, \cdots, |\mathbb{I}|\}, j \in [1, \cdots, 1000])$ using a uniform distribution on the $[-\beta, \beta]$ interval. For each scenario, we then re-optimize problem (2.4) with the value of $\boldsymbol{x}$ and $\boldsymbol{\zeta}_i$ fixed to the corresponding strategy and random scenario. In the first period (i.e., $t = 1$), we have no uncertainty given that a full information about the level of DR is available. If, for a specific policy and scenario, problem (2.4) becomes infeasible, this implies a capacity shortage. Table 2.3 reports the proportion of scenarios with capacity shortage for the different strategies and different budget sizes (expressed in percentage of $|d_i|$ and denoted as $\Gamma\%$). When the budget size increases, the chances of capacity shortage of RMPCA and SRM reduces. This is because a larger budget size increases the conservatism of the model, and consequently, the model installs more capacity to avoid shortage, which obviously is more expensive. Nevertheless, for budget sizes in the range of [50%, 60%], the capacity shortage of RMPCA can be as low as 2%. To have a fair comparison between the expected total cost of different strategies, we report the average total cost both over all scenarios and over the scenarios without capacity shortage.

Figure 2.4a presents statistics of the total cost for the RMPCA and SRM strategies, over all scenarios, for different budget sizes and $\beta = 0.6$. Figure 2.4b gives similar results when the average costs are taken over only scenarios without capacity shortage. We can first note that the average cost for the SRM strategy remains fixed for budget sizes greater

Table 2.3: Proportion of random scenarios with capacity shortage when $\beta = 0.6$.

$\Gamma\%$[1]	RMPCA	SRM	DET
10%	100%	100%	100%
20%	98%	96%	100%
30%	29%	0%	100%
40%	9%	0%	100%
50%	4%	0%	100%
60%	2%	0%	100%
70%	10%	0%	100%
80%	0%	0%	100%
90%	0%	0%	100%
100%	0%	0%	100%

[1] $\Gamma\%$ denotes that the units are in percent of $|d_i|$.

than 25%. This is because when $\Gamma\% = 25\%$, $|d_i| = 1$, the SRM already considers each constraint to be maximally perturbed due to the fact that each one only involves one demand deviation. Second, we note that Figures 2.4 (a) and (b) show that the average RMPCA cost is considerably lower than the SRM cost for all budget sizes. This already suggests that the flexibility of energy procurement decisions can significantly reduce the expected total cost. More precisely, the maximum difference occurs when $\Gamma\% = 30\%$ yet this difference comes at the price of 29% chances of capacity shortage (see again Table 2.3). A better trade-off is achieved when $\Gamma\% = 50\%$, where the average total cost of RMPCA is around 4% less than for SRM (i.e., a 9 billion CHF reduction) while the chances of capacity shortage are estimated at only 4% . In comparison, the average total cost (including shortage penalties) from implementing the DET strategy is around 256 billion CHF, which is about 33% more than the total cost of RMPCA. Overall, this evidence supports the importance of: i) accounting of uncertainty of the demand response in ETEM; and ii) the importance of considering that the procurement is adjustable with respect to the actual DR.

Figure 2.5 is similar to Figure 2.4, but we have fixed the budget size to 50% and let the box size β vary. For example, $\beta = 0.2$ means that the actual demand response at each time-slice can deviate from the planned demand response by up to 20% of the total

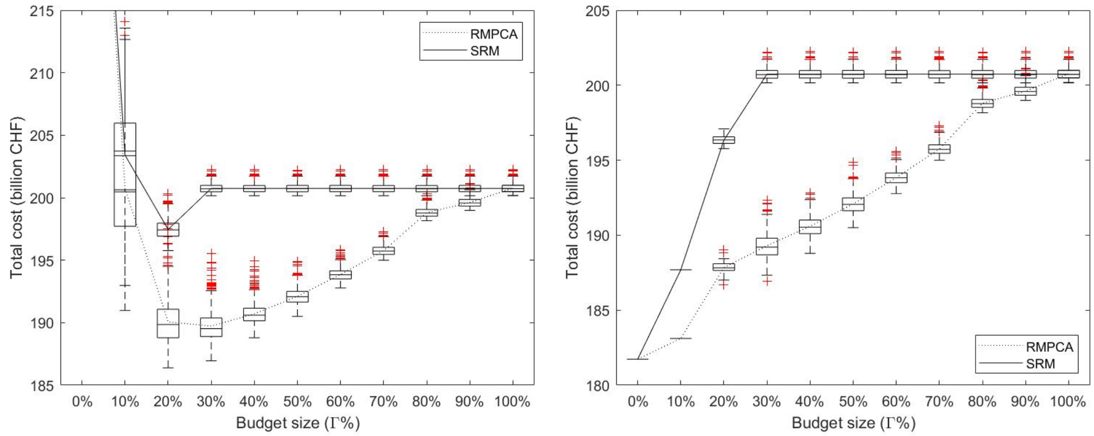

(a) (b)

Figure 2.4: Statistics of the total cost of RMPCA and SRM strategies for different budget sizes and $\beta = 0.6$. (a) presents the distribution of the total cost over all 1000 random scenarios, whereas (b) presents the conditional distributions given that no shortages occurred. The curves present the mean values while each box presents the min, max, 25th and 75th percentile and some extreme realizations (+).

demand. As expected, increasing the support of $\boldsymbol{\zeta}$ leads to an increase of the average total cost of the system. Interestingly, the rate of increase of the DET cost is larger than for RMPCA and SRM. Indeed, as SRM and RMPCA are sensitive to worst-case values of DR, more capacity is built under these strategies. This gives more production flexibility with cheaper prices for the system when the actual DR is lower than planned DR. Finally, the figure also illustrates that the average total cost (~192.5 billion CHF) of preventing 96% of shortages when $\beta = 0.6$ is only about 5% more expensive than the cost estimated by the deterministic model (i.e. ~182.5 billion CHF).

Figure 2.6 corresponds to the Cumulative Distribution Function (CDF) diagram of the simulated total cost of RMPCA, SRM and DET strategies when $\Gamma\% = 50\%$ and $\beta = 0.6$. We can note that RMPCA stochastically dominates SRM, while SRM stochastically dominates DET. In fact, the maximum cost of the RMPCA strategy over all random scenarios is less than the minimum cost of the SRM strategy, and similarly for the DET strategy. Again, this figure shows the importance of considering uncertainty of the DR in capacity expansion models.

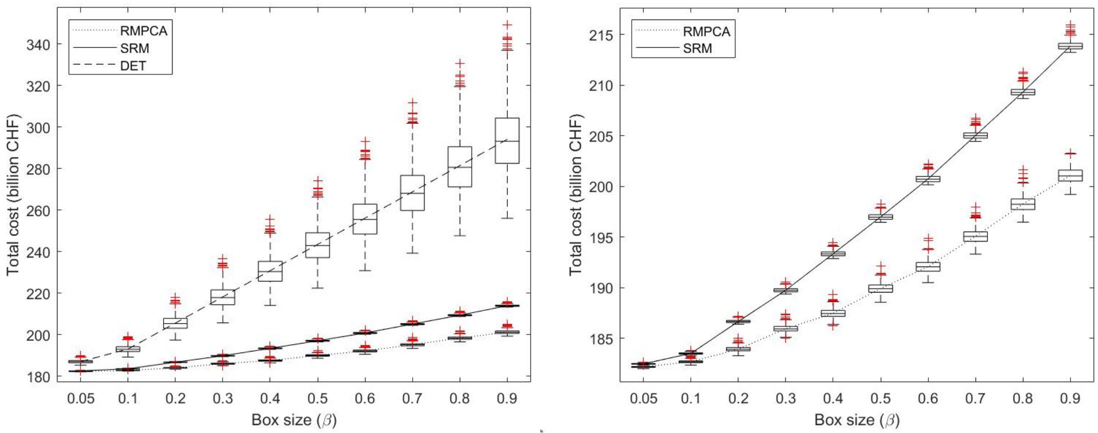

(a) (b)

Figure 2.5: Statistics of the total cost of RMPCA, SRM and DET strategies for different box sizes and $\Gamma\% = 50\%$. (a) presents the distribution of the total cost over all 1000 random scenarios, whereas (b) presents conditional distributions given that no shortages occurred.

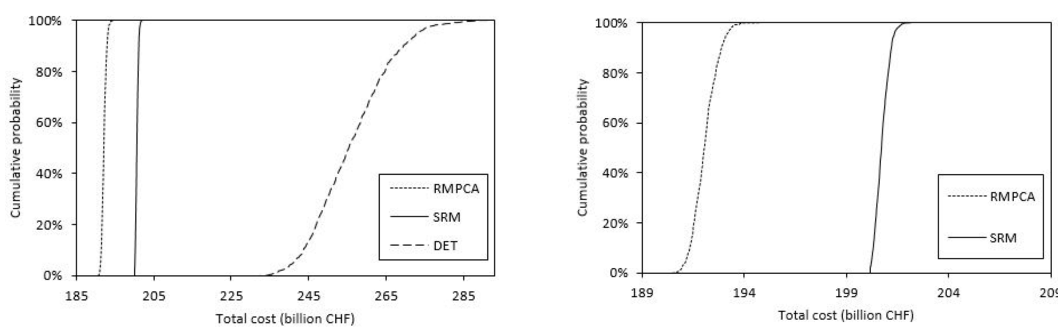

(a) (b)

Figure 2.6: Comparison of the cumulative distribution functions of simulated total cost associated with RMPCA, SRM and DET policies when $\Gamma\% = 50\%$ and $\beta = 0.6$. (a) presents the distribution for all 1000 random scenarios, while (b) presents the distribution for the scenarios without capacity shortage.

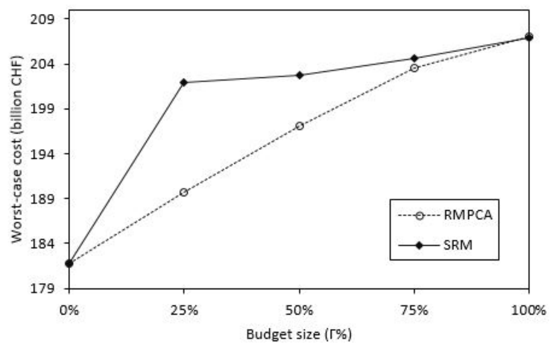

Figure 2.7: Worst-case performance of RMPCA and SRM as a function of budget size (for $\beta = 0.6$)

Next, Figure 2.7 shows the worst-case total cost of the system when implementing the RMPCA and SRM strategies for different budget sizes. As this figure shows, RMPCA performs up to 6% better than SRM which is equivalent to approximately 12 billion CHF over the entire planning horizon.

Figure 2.8 provides finally an analysis on the trade-off between rate of capacity shortage and the average total cost for RMPCA and SRM strategies when the budget size varies from 10% to 100% and the box size $\beta = 0.6$. As it is also shown in Table 2.3, for budget sizes greater than 30%, the rate of capacity shortage for SRM is 0%. However, this zero-shortage comes at the cost of building too much capacity (see Figure 2.9, below). As Figure 2.8 suggests, allowing a certain degree of shortage can reduce the total cost drastically. For example, for $\Gamma\% = 60\%$ allowing a 2% chance of capacity shortage reduces the average total cost by around 7 billion CHF (equivalent to 4% of the total system cost).

2.6.3 Electricity Generation Structure

In this section, we discuss how the different modeling schemes impact the evolution over time of electricity generation. Figure 2.9 presents first the total installed capacity for the different strategies. SRM is the most conservative approach, as it yields more capacity than RMPCA and DET (around 1.5 times more than RMPCA, and 3 times more than DET). It is indeed reasonable that RMPCA is less conservative than SRM, as it enjoys the

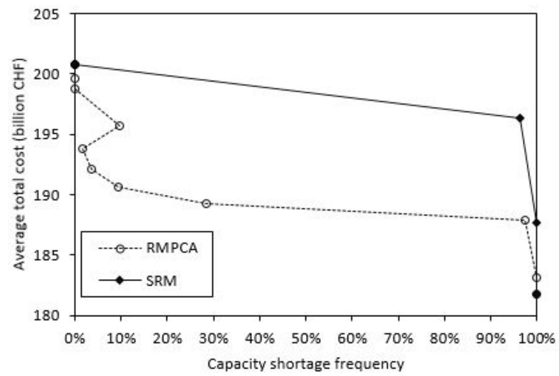

Figure 2.8: Trade-off between capacity shortage frequency and average total cost of RMPCA and SRM for different budget sizes and $\beta = 0.6$.

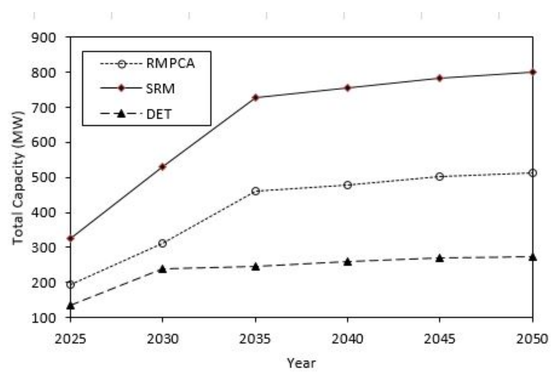

Figure 2.9: Total installed capacity for RMPCA, SRM and DET.

flexibility of the energy procurement decisions to adjust for the actual (observed) demand response.

Figure 2.10 presents next the installed capacity by type of technology for the RMPCA, SRM and DET strategies. It highlights the importance of wind power to decarbonize the electricity generation sector. Specifically, wind power will form around 88% of the total installed capacity by 2050. It is followed by hydro power plant with 8%, and other technologies (including CHP, PV, geothermal, fuel-cell, and municipal-waste power plants) with less than 4% share in the total installed capacity. In addition, Figure 2.11 reports on the average annual electricity generation by different technology types for RMPCA, SRM, and DET policies. A more detailed description of the installed capacity and the average annual electricity generation is presented in Appendix 2.8.2.

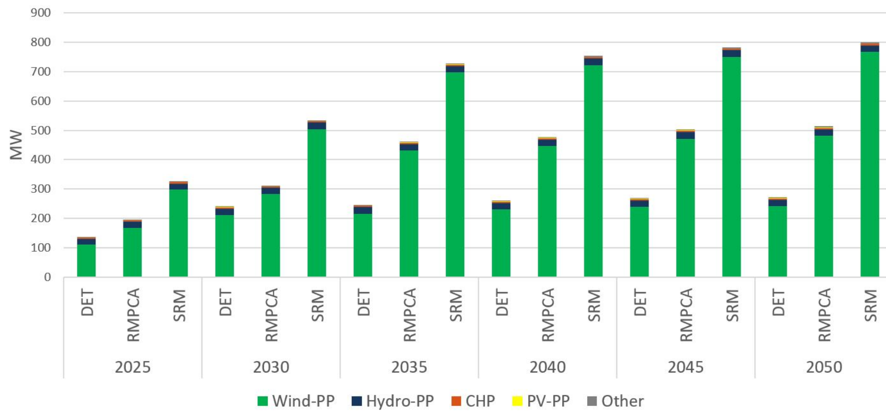

Figure 2.10: Total installed capacity (in MW) by type of technology for DET, RMPCA, and SRM models. Other technologies include geothermal,fuel-cell and municipal-waste power plant.

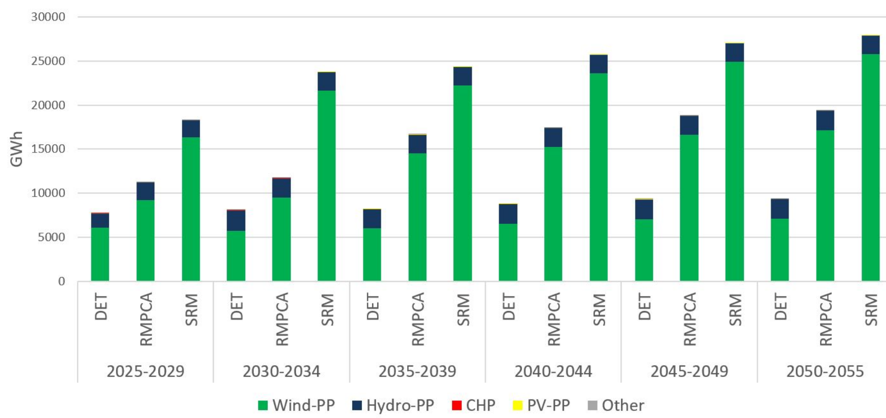

Figure 2.11: Average annual electricity generation (in GWh) by type of technology for DET, RMPCA, and SRM models over 1000 random scenarios. Other technologies include geothermal,fuel-cell and municipal-waste power plant

2.6.4 Computational Analysis

In this section, we numerically evaluate the performance of the decomposition algorithms presented in Section 2.5. Specifically, we investigate how considering PRO and valid inequalities can improve the solution time and the number of iterations of Algorithm 1. In order for our results to be more general, we have designed smaller versions of *ETEM* with 16 technologies and 9 energy commodities, in which parameters (including different costs, demand, nominal demand response, technological capacity factor, availability

Table 2.4: Solution time (ST) in seconds, number of iterations (It), percentage of improvement (% impr.) with respect to BD for different versions of the decomposition algorithms. Four problem sizes are considered, for which the number of variables (VAR) and constraints (CON) are reported together with the solution time of solving (2.5) with CPLEX.

$\mathbb{T}$	DET (2.1) size		RMPCA (2.5) size		CPLEX	BD		PRO-BD			PRO-BD-VI		
	VAR	CON	VAR	CON	ST	ST	It	ST	It	% impr.	ST	It	% impr.
3	4,644	11,830	97,112	103,095	71.8	47.0	15	37.5	10	20%	26.0	4	45%
5	7,740	19,718	161,860	171,837	227.5	92.8	15	78.1	11	16%	68.9	5	26%
7	10,836	27,601	226,583	240,534	519.2	78.0	10	68.0	7	13%	48.0	3	39%
9	13,932	35,486	291,316	309,249	1242.8	97.0	9	82.1	6	15%	81.3	3	16%
11	17,028	43,380	356,094	378,045	2336.4	141.8	11	90.5	7	36%	58.6	3	59%
13	20,124	51,263	420,817	446,742	4350.4	154.4	10	105.6	7	32%	69.7	3	55%
Average					1458.0	101.8	12	77.0	8	22%	58.75	4	40%

of technologies, etc.) are randomly assigned. Moreover, the size of the model changes with different problem horizons $\mathbb{T} \in \{3, 5, 7, 9, 11, 13\}$. Then, for each problem size, we generate 20 random instances and solve these random instances for different budget sizes $\Gamma\% \in \{20\%, 40\%, 60\%, 80\%\}$. Table 2.4 reports, for different problem sizes, the average solution time (ST) of CPLEX for solving the RMPCA problem (2.5), together with the average solution time and the number of iterations (It) for different versions of our decomposition algorithm. Specifically, BD refers to the traditional Benders decomposition, i.e., Algorithm 1. PRO-BD refers to the algorithm with improved upper bound based on PRO solutions while PRO-BD-VI additionally exploits valid inequalities. It is worth mentioning that based on our numerical experiments, restricting Ω to the last 4 worst-case scenarios led to the best solution time. Results show that PRO-BD improves the solution time of the BD by up to 36%, whereas PRO-BD-VI is able to improve it by up to 59%. On average, PRO-BD improves the solution time by 22% and PRO-BD-VI improves by 40%. Finally, a considerable improvement in terms of the number of iterations is observed when comparing PRO-BD-VI and BD.

2.7 Concluding Remarks

In this paper, we model demand response uncertainty in an adjustable multi-period robust generation capacity expansion problem. In a first stage, the planner decides on capacity expansion, as well as, planned demand response. Then, in sequence of seasonal stages, the actual DR is revealed, and accordingly, the optimal procurement decisions are taken. As the resulting adjustable model is intractable, we use a conservative approximation scheme based on affine decision rules to solve the problem. We present a general formulation of the problem, where with slight modifications of the formulation one could accommodate other sources of uncertainty such as the level of production one can achieve from intermittent resources. We test our algorithm on a real-world case study based on the energy system of the Arc Lémanique region (Cantons of Geneva and Vaud, in Switzerland). Numerical results reinforce the importance of adjustable robust formulation. Namely, RMPCA can reduce the average total cost of the system by 33% compared to the solution of the deterministic problem, while keeping the chances of shortage near 4%. RMPCA also performs 4% better than a more naive static robust counterpart (SRM). Finally, we develop a Benders type of decomposition to solve our large-scale RMPCA problem. In this algorithm, the speed of convergence is improved through i) adding valid inequalities to the master problem, and ii) identifying PRO solutions of the master problem. One alternative strategy to calculate the optimal investment decisions is to sequentially solve forward-shifting horizon RMPCA problems, and provide the investment plan over the entire horizon by assembling the capacity addition decisions made at the beginning of each forward-shifting horizon. However, this practical implementation of RMPCA problem is beyond the scope of this paper and shall be considered as future work. Moreover, it is worth mentioning that although this paper has focused on the uncertainty of demand response, one can easily introduce a group of supply-side uncertainties, such as availability of intermittent resources, or uncertainty of investment costs, to the general formulation of the problem (2.4). In this case, matrices A_i and vector f will be affected by these uncertainties. As our problem still preserves the “fixed recourse" condition, the approach presented in Sections 2.4.2 and 2.5 remains valid. Conversely, considering another group of supply-side uncertainties, such as fuel cost, or efficiency uncertainties, will affect matrices h_i and B_i, and thus consists of more significant changes to the structure of the decision model. In conclusion, here follows some interesting directions to expand on this paper. One idea is to consider investment decisions to be adaptive to the evolution of the uncertainty. Another extension is to consider other sources of uncertainties, especially the ones that do not preserve the fixed recourse characteristic of the problem. One could also control the loss of loads through reliability constraints. Finally, another possible extension would be to link the robust ETEM with a collective behavior demand model to more precisely adjust the size of the specific uncertainty sets of each period.

2.8 Appendix

2.8.1 Comparison with robust ETEM from Babonneau et al. (2020)

In this section, we first summarize the technique proposed in Babonneau et al. (2020) to model the demand response uncertainty in ETEM. Then, we discuss issues that arise when using their proposed approach to account for demand response uncertainty that is present in our case study. Namely, we will show that Babonneau et al. (2020)'s approach ends up simply adding redundant constraints to the deterministic problem (2.1). We also encourage interested readers to have a look at Appendix B in Aliakbarisani et al. (2021), which additionally argues that the constraints proposed in Babonneau et al. (2020) to model demand response uncertainty fail to offer protection against observed demand response deviations.

A summary of the method used in Babonneau et al. (2020)

In Babonneau et al. (2020), the authors propose an iterative procedure to robustify the deterministic version of ETEM presented in (2.1) in context of uncertainty. They first recommend solving the deterministic version of ETEM to obtain an initial demand response plan $\Theta_{t,l,c}\overline{V}_{t,s,c}$. This plan can then be used to produce distributions of realized demand responses $\tilde{V}_{t,l,s,c}$ for each period, time slice, region, and commodity. Descriptive statistics of each $\tilde{V}_{t,l,s,c}$ are then extracted in the form of a mean value $\hat{\Delta}^{l,c}_{t,s}$ and a confidence region $[\Delta^{l,c,-}_{t,s}, \Delta^{l,c,+}_{t,s}]$. Finally, they use arguments based on moment inequalities to suggest "robustifying" the ETEM by adding the following constraints:

$$\Delta^{\min}_{l,c} \leq \sum_{t\in\mathbb{T}}\sum_{s\in\mathbb{S}} \Theta_{t,l,c}\boldsymbol{V}_{t,s,c} \leq \Delta^{\max}_{l,c}, \forall l \in \mathbb{L}, c \in \mathbb{C}^{\mathscr{U}}, \tag{2.18}$$

with

$$\Delta^{\min}_{l,c} := \sup_{\xi \in [0,1]^{\mathbb{T}\times\mathbb{S}}} \quad \sum_{(t,s)\in\mathbb{T}\times\mathbb{S}} \Delta^{l,c,-}_{t,s} + (\hat{\Delta}^{l,c}_{t,s} - \Delta^{l,c,-}_{t,s})\xi_{t,s}$$
$$\text{s.t.} \quad \sum_{(t,s)\in\mathbb{T}\times\mathbb{S}} \xi_{t,s} \leq \Gamma,$$

and

$$\Delta^{\max}_{l,c} := \inf_{\xi \in [0,1]^{\mathbb{T}\times\mathbb{S}}} \quad \sum_{(t,s)\in\mathbb{T}\times\mathbb{S}} \Delta^{l,c,+}_{t,s} + (\hat{\Delta}^{l,c}_{t,s} - \Delta^{l,c,+}_{t,s})\xi_{t,s}$$
$$\text{s.t.} \quad \sum_{(t,s)\in\mathbb{T}\times\mathbb{S}} \xi_{t,s} \leq \Gamma.$$

This iterative process is repeated until the robustified model starts producing the same solutions in two consecutive iterations.

Implementing Babonneau et al. (2020)'s approach in our Swiss Case study

In the Swiss case study presented in Section 2.6, the random demand response is modeled as the summation of the planned demand and the relative demand response deviations (RDRDs), i.e., $\tilde{V}_{t,l,s,c} := \Theta_{t,l,c}(\overline{V}_{t,s,c} + \delta_{t,s,c})$, where each $\delta_{t,s,c}$ follows a uniform distribution over the interval $[-\beta_{t,s,c}, \beta_{t,s,c}]$. Therefore, in the first iteration of Babonneau et al. (2020)'s, $\overline{V}$ is the solution of the deterministic ETEM (i.e. problem (2.1)) and the following descriptive statistics are obtained from the observed realized demand responses:

$$\Delta^{l,c,-}_{t,s} := \Theta_{t,l,c}\left[\overline{V}_{t,s,c} - (1-\varepsilon)\beta_{t,s,c}\right], \tag{2.19}$$

$$\Delta^{l,c,+}_{t,s} := \Theta_{t,l,c}\left[\overline{V}_{t,s,c} + (1-\varepsilon)\beta_{t,s,c}\right], \tag{2.20}$$

$$\hat{\Delta}^{l,c}_{t,s} := \Theta_{t,l,c}\overline{V}_{t,s,c} \tag{2.21}$$

where $1-\varepsilon$ is the level of confidence for the confidence interval $[\Delta^{l,c,-}_{t,s}, \Delta^{l,c,+}_{t,s}]$. Lemma 3 demonstrates that $\overline{V}$ remains optimal after adding constraint (2.18) to problem (2.1).

Lemma 3. *The solution $\overline{V}$ satisfies constraint* (2.18).

Proof. We will first show that the lower bounding part of constraint (2.18) is satisfied. Namely,

$$\Delta^{\min}_{l,c} = \sup_{\xi\in\hat{\Xi}} \sum_{(t,s)\in\mathbb{T}\times\mathbb{S}} \Delta^{l,c,-}_{t,s} + (\hat{\Delta}^{l,c}_{t,s} - \Delta^{l,c,-}_{t,s})\xi_{t,s}$$

$$
\begin{aligned}
&= \sup_{\xi \in \hat{\Xi}} \sum_{(t,s)\in \mathbb{T}\times\mathbb{S}} \Theta_{t,l,c}\overline{V}_{t,s,c} - \Theta_{t,l,c}(1-\varepsilon)(1-\xi_{t,s})\beta_{t,s,c} \\
&= \sum_{(t,s)\in \mathbb{T}\times\mathbb{S}} \Theta_{t,l,c}\overline{V}_{t,s,c} - \inf_{\xi \in \hat{\Xi}} \sum_{t,s} \Theta_{t,l,c}(1-\varepsilon)(1-\xi_{t,s})\beta_{t,s,c} \\
&\le \sum_{(t,s)\in \mathbb{T}\times\mathbb{S}} \Theta_{t,l,c}\overline{V}_{t,s,c}\,,
\end{aligned}
$$

where $\hat{\Xi} := \{\xi \in [0,\,1]^{\mathbb{T}\times\mathbb{S}} \sum_{(t,s)\in\mathbb{T}\times\mathbb{S}} \xi_{t,s} \le \Gamma\}$, and which would confirm that $\overline{V}$ satisfies the lower bound. In details, the first two equalities follow from the definition of $\Delta_{l,c}^{\min}$ and $\Delta_{t,s}^{l,c,-}$ (see equation (2.19)), while the first inequality follows from the fact that all terms in $\Theta_{t,l,c}(1-\varepsilon)(1-\xi_{t,s})\beta_{t,s,c}$ are non-negative. A similar analysis can be done to prove that $\overline{V}$ also satisfies the upper bound in constraint (2.18). □

Interestingly, Lemma 3 implies that the procedure proposed by Babonneau et al. (2020) will converge in the second iteration and prescribe the solution of the deterministic version of ETEM in this case study. As reported in Aliakbarisani et al. (2021), it therefore once again seems that Babonneau et al. (2020)'s approach is unable to immunize ETEM from demand response uncertainty.

2.8.2 Details on electricity generation structure

In this section we present a table format of Figures 2.10 and 2.11. Table 2.5 reports on the total installed capacity by type of power plant for each of DET, RMPCA, and SRM models. While, DET is proposing to build around 270 MW of power plant, RMPCA and RSM are proposing to build 513 and 800 MW of power plants. According to the capacity expansion strategy of all models, the wind power plant will prevail. The second technology is hydro power plant with around 23 MW by 2050. Finally, the capacity of other technologies, including photovoltaic, CHP, geothermal, fuel-cell, and municipal-waste power plants will be around only 9 MW. Table 2.6 reports on the average annual electricity production by each technology for RMPCA, SRM, and DET models. According to RMPCA strategy, Wind power plants will produce up to 88% of the total electricity generated in the region in 2050. Hydro power will produce 11%, and other technologies will produce only 0.2% of the total electricity produced in this region in 2050.

Table 2.5: Total installed capacity (in MW) by type of technology for RMPCA, SRM and DET models.

	2025			2030			2035			2040			2045			2050		
	RMPCA	SRM	DET	RMPCA	SRM	DET	RMPCA	SRM	DET	RMPCA	SRM	DET	RMPCA	SRM	DET	RMPCA	SRM	DET
Hydro-PP	21.3	21.3	18.9	22.4	22.4	22.4	22.4	22.4	22.4	22.6	22.6	22.6	22.8	22.8	22.8	23	23	23
PV-PP	0.2	0.2	0.2	0.2	0.2	0.2	0.8	0.8	0.8	1.8	1.8	1.8	1.8	1.8	1.8	1.8	1.8	1.8
Wind-PP	168.4	297.6	110.8	282.5	504.1	211.3	431.1	697.3	216.5	446.2	721.9	230.0	471.2	750.1	239.1	480.9	767.2	240.7
CHP	4.7	4.7	4.7	4.7	4.7	4.7	4.7	4.7	4.7	4.7	4.7	4.7	4.7	4.7	4.7	4.7	4.7	4.7
Other[1]	0.5	0.5	0.5	1.2	0.5	0.5	1.2	3.1	0.5	1.2	3.1	0.5	1.2	3.1	0.5	3.1	3.1	3.1

[1] Other technologies include geothermal,fuel-cell and municipal-waste power plants.

Table 2.6: Average annual electricity generation (in GWh) by type of technology for RMPCA, SRM and DET models over 1000 random scenarios.

	2025-2029			2030-2034			2035-2039			2040-2044			2045-2049			2050-2055		
	RMPCA	SRM	DET	RMPCA	SRM	DET	RMPCA	SRM	DET	RMPCA	SRM	DET	RMPCA	SRM	DET	RMPCA	SRM	DET
Hydro-PP	2010	1943.6	1642.8	2210.6	2086.8	2306	2153.4	2088	2146.1	2173.3	2108.7	2202.4	2188.5	2129.7	2244.5	2214.1	2152	2210.8
PV-PP	4.9	4.9	4.9	3.7	3.7	3.7	16.7	16.7	16.7	38.3	38.3	38.3	38.3	38.3	38.3	38.3	38.3	38.3
Wind-PP	9238	16323	6076	9506	21654	5744	14495	22233	6033	15233	23583	6537	16602	24892	7038	17137	25749	7124
CHP	12.5	0.5	40.3	10.2	0.0	39.4	1.6	0	15.8	1.6	0	15.8	1.5	0	16.6	1.5	0	16.6
Other[1]	16.2	0.7	32.5	13.8	0.0	29	2.4	0	0	2.3	0	0	2.2	0	6.8	2.3	0	8.9

[1] Other technologies include geothermal,fuel-cell and municipal-waste power plants.

References

Adelman, D. and Uçkun, C. (2019). Dynamic electricity pricing to smart homes. *Operations Research*, 67(6):1520–1542.

Aliakbarisani, S., Bahn, O., Delage, E., and Foguen, R. (2021). Robust integration of electric vehicles charging load in smart grid's capacity expansion planning. *Les Cahiers du GERAD*, G–2021–44.

Amjady, N., Attarha, A., Dehghan, S., and Conejo, A. J. (2018). Adaptive robust expansion planning for a distribution network with DERs. *IEEE Transactions on Power Systems*, 33(2):1698–1715.

Amrollahi, M. H. and Bathaee, S. M. T. (2017). Techno-economic optimization of hybrid photovoltaic/wind generation together with energy storage system in a stand-alone micro-grid subjected to demand response. *Applied Energy*, 202:66–77.

Arasteh, H., Sepasian, M., and Vahidinasab, V. (2015). Toward a smart distribution system expansion planning by considering demand response resources. *Journal of Operation and Automation in Power Engineering*, 3(2):116–130.

Ardestani-Jaafari, A. and Delage, E. (2018). The value of flexibility in robust location–transportation problems. *Transportation Science*, 52(1):189–209.

Ardestani-Jaafari, A. and Delage, E. (2020). Linearized robust counterparts of two-stage robust optimization problems with applications in operations management. *INFORMS Journal on Computing.*, Forthcoming.

Asensio, M., Meneses de Quevedo, P., Muñoz-Delgado, G., and Contreras, J. (2018). Joint distribution network and renewable energy expansion planning considering demand response and energy storage—part i: Stochastic programming model. *IEEE Transactions on Smart Grid*, 9(2):655–666.

Babonneau, F., Caramanis, M., and Haurie, A. (2016). A linear programming model for power distribution with demand response and variable renewable energy. *Applied Energy*, 181:83 – 95.

Babonneau, F., Caramanis, M., and Haurie, A. (2017). ETEM-SG: Optimizing regional smart energy system with power distribution constraints and options. *Environmental Modeling & Assessment*, 22(5):411–430.

Babonneau, F., Foguen, R., Haurie, A., and Malhame, R. (2020). Coupling a power dispatch model with a wardrop or mean-field-game equilibrium model. *Dynamic Games and Applications*.

Babonneau, F. and Haurie, A. (2019). Energy technology environment model with smart grid and robust nodal electricity prices. *Annals of Operations Research*, 274.

Babonneau, F., Haurie, A., Tarel, G., and Thénié, J. (2012). Assessing the future of renewable and smart grid technologies in regional energy systems. *Swiss J Economics Statistics*, 148:229–273.

Baringo, L. and Baringo, A. (2018). A stochastic adaptive robust optimization approach for the generation and transmission expansion planning. *IEEE Transactions on Power Systems*, 33(1):792–802.

Ben-Tal, A., den Hertog, D., and Vial, J. (2015). Deriving robust counterparts of nonlinear uncertain inequalities. *Math. Program*, 149:265–299.

Ben-Tal, A., Goryashko, A., Guslitzer, E., and Nemirovski, A. (2004). Adjustable robust solutions of uncertain linear programs. *Mathematical Programming*, 99(2):351–376.

Bertsimas, D., Brown, D. B., and Caramanis, C. (2011). Theory and applications of robust optimization. *SIAM Review*, 53(3):464–501.

Bertsimas, D. and Georghiou, A. (2018). Binary decision rules for multistage adaptive mixed-integer optimization. *Math. Program.*, 167:395–433.

Bertsimas, D. and Sim, M. (2004). The price of robustness. *Operations Research*, 52(1):35–53.

Bertsimas, D. and Thiele, A. (2006). A robust optimization approach to inventory theory. *Operations Research*, 54(1):150–168.

Birge, J. R. and Louveaux, F. (2011). *Introduction to Stochastic Programming*, chapter Solution methods, pages 102–180. Springer-Verlag, New York, NY, USA, second edition.

Bloom, J. A. (1983). Solving an electricity generating capacity expansion planning problem by generalized benders' decomposition. *Operations Research*, 31(1):84–100.

Bloom, J. A., Caramanis, M., and Charny, L. (1984). Long-range generation planning using generalized benders' decomposition: Implementation and experience. *Operations Research*, 32(2):290–313.

Chatterjee, N., Glick, R., and McNamee, B. (2018). Assessment of demand response and advanced metering. Technical report, Federal Energy Regulatory Commission.

Dehghan, S., Amjady, N., and Kazemi, A. (2014). Two-stage robust generation expansion planning: A mixed integer linear programming model. *IEEE Transactions on Power Systems*, 29(2):584–597.

DOE (2006). Benefits of demand response in electricity markets and recommendations for achieving them. Technical report, US Department of Energy, Washington DC.

Domínguez, R., Conejo, A. J., and Carrión, M. (2016). Investing in generation capacity: A multi-stage linear-decision-rule approach. *IEEE Transactions on Power Systems*, 31(6):4784–4794.

Dyson, M. E., Borgeson, S. D., Tabone, M. D., and Callaway, D. S. (2014). Using smart meter data to estimate demand response potential, with application to solar energy integration. *Energy Policy*, 73:607–619.

Georghiou, A., Tsoukalas, A., and Wiesemann, W. (2020). A primal–dual lifting scheme for two-stage robust optimization. *Operations Research*, 68(2):572–590.

Gärttner, J., Flath, C. M., and Weinhardt, C. (2018). Portfolio and contract design for demand response resources. *European Journal of Operational Research*, 266(1):340–353.

Han, D., Wu, W., Sun, W., and Yan, Z. (2018). A two-stage robust stochastic programming approach for generation expansion planning of smart grids under uncertainties. In *2018 IEEE Power Energy Society General Meeting (PESGM)*, pages 1–5.

He, S., Gao, H., Liu, J., and Liu, J. (2019). Distributionally robust optimal DG allocation model considering flexible adjustment of demand response. In *2019 IEEE Power Energy Society General Meeting (PESGM)*, pages 1–5.

Huang, J., Pan, K., and Guan, Y. (2020). Multistage stochastic power generation scheduling co-optimizing energy and ancillary services. *INFORMS Journal on Computing. Advance online publication.*

Iancu, D. A. and Trichakis, N. (2014). Pareto efficiency in robust optimization. *Management Science*, 60(1):130–147.

Knueven, B., Ostrowski, J., and Watson, J.-P. (2020). On mixed-integer programming formulations for the unit commitment problem. *INFORMS Journal on Computing. Advance online publication.*

Koltsaklis, N. E. and Dagoumas, A. S. (2018). State-of-the-art generation expansion planning: A review. *Applied Energy*, 230:563–589.

Li, C., Dong, Z., Chen, G., Luo, F., and Liu, J. (2015). Flexible transmission expansion planning associated with large-scale wind farms integration considering demand response. *IET Generation, Transmission Distribution*, 9(15):2276–2283.

Liu, C., Deng, K., Wen, G., and Yu, X. (2019). Optimal scheduling of electric vehicle charging with energy storage facility in smart grid. In *IECON 2019 - 45th Annual Conference of the IEEE Industrial Electronics Society*, volume 1, pages 6549–6554.

Lohmann, T. and Rebennack, S. (2017). Tailored benders decomposition for a long-term power expansion model with short-term demand response. *Management Science*, 63(6):2027–2048.

Magnanti, T. L. and Wong, R. T. (1981). Accelerating benders decomposition: Algorithmic enhancement and model selection criteria. *Operations Research*, 29(3):464–484.

Mejía-Giraldo, D. and McCalley, J. (2014). Adjustable decisions for reducing the price of robustness of capacity expansion planning. *IEEE Transactions on Power Systems*, 29(4):1573–1582.

Qi, N., Cheng, L., Xu, H., Wu, K., Li, X., Wang, Y., and Liu, R. (2020). Smart meter data-driven evaluation of operational demand response potential of residential air conditioning loads. *Applied Energy*, 279:115708.

Rahmaniani, R., Crainic, T. G., Gendreau, M., and Rei, W. (2017). The benders decomposition algorithm: A literature review. *European Journal of Operational Research*, 259(3):801–817.

Roveto, M., Mieth, R., and Dvorkin, Y. (2020). Co-optimization of VaR and CVaR for data-driven stochastic demand response auction. *IEEE Control Systems Letters*, 4(4):940–945.

Shariatzadeh, F., Mandal, P., and Srivastava, A. K. (2015). Demand response for sustainable energy systems: A review, application and implementation strategy. *Renewable and Sustainable Energy Reviews*, 45:343–350.

Sion, M. (1958). On general minimax theorems. *Pacific Journal of Mathematics*, 8(1):171–176.

Ströhle, P. and Flath, C. M. (2016). Local matching of flexible load in smart grids. *European Journal of Operational Research*, 253(3):811–824.

Vatani, B., Chowdhury, B., and Lin, J. (2017). The role of demand response as an alternative transmission expansion solution in a capacity market. In *2017 IEEE Industry Applications Society Annual Meeting*, pages 1–7.

Venizelou, V., Philippou, N., Hadjipanayi, M., Makrides, G., Efthymiou, V., and Georghiou, G. E. (2018). Development of a novel time-of-use tariff algorithm for residential prosumer price-based demand side management. *Energy*, 142:633–646.

Yanıkoğlu, I., Gorissen, B., and den Hertog, D. (2019). A survey of adjustable robust optimization. *European Journal of Operational Research*, 277(3):799–813.

Zhang, Q. and Zhang, S. (2019). Robust decision-making model for electricity retailers considering incentive-based demand response. In *2019 IEEE Sustainable Power and Energy Conference (iSPEC)*, pages 1157–1162.

Zhao, C., Wang, J., Watson, J., and Guan, Y. (2013). Multi-stage robust unit commitment considering wind and demand response uncertainties. *IEEE Transactions on Power Systems*, 28(3):2708–2717.

Zou, J., Ahmed, S., and Sun, X. A. (2018). Partially adaptive stochastic optimization for electric power generation expansion planning. *INFORMS Journal on Computing*, 30(2):388–401.

Chapter 3

Robust Integration of Electric Vehicles Charging Load in Smart Grid's Capacity Expansion Planning

Chapter information

This article is a joint work with my supervisors, Olivier Bahn and Erick Delage, and the other co-author is Rinel Foguen Tchuendom. It is submitted to Dynamic Games and Applications journal.

Abstract

Battery charging of electric vehicles (EVs) needs to be properly coordinated by electricity producers to maintain the network reliability. In this paper, we propose a robust approach to model the interaction between a large fleet of EV users and utilities in a long-term generation expansion planning problem. In doing so, we employ a robust multi-period adjustable generation expansion planning problem, called R-ETEM, in which demand responses of EV users are uncertain. Then, we employ a linear quadratic game to simulate the average charging behavior of the EV users. The two models are coupled through a

dynamic price signal broadcasted by the utility. Mean field game theory is used to solve the linear quadratic game model. Finally, we develop a new coupling algorithm between R-ETEM and the linear quadratic game with the purpose of adjusting in R-ETEM the uncertainty level of EV demand responses. The performance of our approach is evaluated on a realistic case study that represents the energy system of the Swiss "Arc Lémanique" region. Results show that a robust behaviorally-consistent generation expansion plan can potentially reduce the total actual cost of the system by 6.2% compared to a behaviorally-inconsistent expansion plan.

3.1 Introduction

Modeling the interaction between electric vehicles (EVs) and utilities (electricity producers) is an important problem in smart grid (SG) management because utilities need to properly coordinate the EVs load. On the one hand, EVs are a mobile load that is highly spatial and temporally uncertain, on the other hand, due to their vehicle-to-grid (V2G) features, EVs can provide the network with ancillary services and distributed storage if they are properly coordinated. In other words, utilities need to partially control the EV load profile to prevent network congestions and load imbalances. In addition, since EVs run on battery, utilities can take advantage of this distributed storage in order to increase the reliability of the network by valley-filling and peak-shaving of the power consumption profile. Usually, utilities use incentive pricing as a leverage to coordinate EV load in so-called demand response (DR) programs. Nevertheless, the operational planning is still challenging because the response of EV users to the price signals is uncertain. This uncertainty becomes even more important in a generation expansion planning (GEP) problem, where the planner needs to estimate the reserved capacity provided by DR programs over a long-term horizon. Let us recall here that GEP is the problem of determining the required capacity of a power network to satisfy demand at minimum cost, while also satisfying economic, environmental and technical constraints (see for a recent review Koltsaklis and Dagoumas, 2018).

Game theory and bi-level optimization are the main mathematical tools used to model the interaction between EV users, or consumers/prosumers in a broader perspective, and the electricity network (for example, see Mohsenian-Rad et al., 2010; Zugno et al., 2013; Wang et al., 2019; Zeng et al., 2020). In this literature, EV users play a non-cooperative game to decide on i) when and how much to consume electricity to charge the battery, and ii) when and how much to provide service to the network. Their behavior is impacted by the electricity price broadcasted by a utility or a local DR aggregator. Whereas the utility solves its own problem to maximize its profit from generating electricity or buying it from a wholesale market. This implies that the utility needs to design a dynamic price signal to induce consumers/prosumers to behave in such a way that their aggregated behavior maximizes its profit. To solve these models, a complementarity problem or Karush–Kuhn–Tucker conditions are usually used to reformulate the original problem into a mixed integer linear programming (MILP) problem, which is solved using column and constraint generation techniques. This approach works well when the number of players is small. From an application point of view, these problems model a short-term interaction between a local utility and a limited number of EVs connected to its network. But when the number of players increases, finding some equilibrium becomes computationally challenging. For example, to model the effect of EV interactions on the strategic long-term GEP problem, one needs to model the behavior of a fleet of EVs with a very large number of players connected to the whole network. To circumvent this issue, the theory of mean field games (MFG), introduced simultaneously by Huang et al. (2006) and Lasry and Lions (2006), provides a methodology to obtain some ε-Nash equilibrium, with vanishing errors as the pool size goes to infinity.

While there are many papers that address the interaction between a local utility and a small group of EVs over a short-term horizon, there is only a limited number of papers that address the influence of charging behavior of a large fleet of EVs on a long-term GEP problem (see Babonneau et al., 2016, 2020, as two examples). Babonneau et al. (2016) model the influence of the aggregated EV charging on GEP using a large-scale LP problem. In order to to do so, it is necessary to assume that i) all EVs share the same constraints concerning their utilization, ii) EV users are only seeking to minimize their cost, and iii) the latter is a convex function with respect to the total load. Moreover, the analysis in Babonneau et al. (2016) is limited to a deterministic setting. In a more realistic formulation of the interaction between a large population of EVs connected to a distribution network and a GEP problem, Babonneau et al. (2020) couple a long-term GEP problem, called ETEM, with a Wardrop equilibrium-based model. Moreover, in order to analyze the interaction in a stochastic setting, they develop a MFG model of battery charging and couple it with a robust version of ETEM.

In this paper, we propose a new scheme for robustly integrating the average collective charging behavior of a fleet of EVs in a long-term GEP problem. Specifically, we use the approach in Aliakbarisani et al. (2020) to robustify a specific GEP problem, called ETEM, against the perturbations of the demand response of a fleet of EVs connected to the network. We have chosen ETEM because, compared to other GEP problems: i) it provides a detailed description of useful demand technologies, ii) it models demand response by end-use technologies, and iii) it is an open-source commercially-used GEP model. The proposed robust ETEM (R-ETEM) is a multi-stage robust optimization problem, where in a first stage one decides on the capacity expansion and planned demand response, then after observing the actual demand response one can decide on the optimal procurement of energy in each period. It is well known that the adjustability of the decisions in multi-stage RO problem provides less conservative optimal solutions (compared to a static robust model). Similar to Aliakbarisani et al. (2020), we apply the affinely adjustable robust optimization technique, introduced by Ben-Tal et al. (2004), to solve R-ETEM. To model the EV users' behavior, we employ the linear quadratic game (LQG) presented in Tchuendom et al. (2019). This LQG is a finite horizon game among a large number of EV users, who selfishly optimize a cost function that accounts for their daily usage, desired level of charge of the EV battery, its degradation due fast charging, and regional dynamic electricity prices that correspond to the marginal costs of electricity in R-ETEM. Because of the very large population of small interacting EVs in the game, MFG theory is used to formulate and solve the LQG.

The main contribution of this paper consists in developing a new coupling algorithm between a long-term risk averse expansion planning model (R-ETEM) and a short-term higher-precision consumer behavior model (LQG). The aim of this coupling is to identify a robust optimal capacity expansion plan that is immunized against the demand response deviations observed in the behavioral model when it is implemented. Such optimal robust plans will be referred to as being behaviorally-consistent and will be optimized using a bisection method that converges in $O(\log(1/\varepsilon))$ iterations. We further provide a numerical illustration that highlights the impact of our approach on the expansion planning of electricity generation capacities in the real context of the Arc Lémanique region (in Switzerland), where our robust strategy significantly reduces the realized total cost.

The remainder of the paper is organized as follows. In Section 3.2, we present an overview of different methods to model the interaction between consumers, prosumers (and EV users in particular), and utilities. Moreover, we position our work with respect to closely related studies that address uncertainty in a GEP problem, with a special focus on ETEM. In Section 3.3, we present the formulation of R-ETEM. Section 3.4 formulates the LQG and describes how MFG theory is used to identify an ε-Nash equilibrium. Section 3.5 presents the new coupling algorithm that identifies behaviorally-consistent robust capacity expansion plans. Section 3.6 presents and discusses numerical results for our case study. Finally, Section 3.7 provides concluding remarks.

3.2 Literature review

In this section we briefly review the methods that are used in the literature to formulate the interaction between EV users, or other consumers/prosumers, and the electricity network. In a more general perspective, we then review papers that integrate short-term operational characteristics of the power network into a long-term GEP problem. Finally, we summarize some closely related studies that address uncertainties in a GEP problem.

Modeling the interaction between EV users and the electricy network has been addressed in many studies. Zeng et al. (2020) develop a bi-level robust optimization to model the effect of charging behavior of a number of EVs on the configuration of a charging station. The charging station is connected to the network and dynamically decides on the amount of energy to be purchased from, and injected to the network. They apply a complementarity theory to reformulate the so-called adversarial problem into a MILP and use a column-and-constraint generation algorithm to solve it. Zugno et al. (2013) propose a bi-level optimization model to formulate the interaction between the energy retailer and a number of partially flexible consumers. The retailer faces uncertainties in market price and in demand (due to weather conditions). They reformulate the problem to be cast as a single-level MILP problem. Wang et al. (2019) develop a stackelberg game between an electricity aggregator and EV users. The upper level optimization problem maximizes the profit of the aggregator who purchases electricity from the wholesale market and signals a dynamic price to a group of EV users. The lower level problem, on the other hand, minimizes the charging cost of each EV. They use an iterative algorithm to solve the problem. Mohsenian-Rad et al. (2010) propose a game theoretic approach for modeling the interaction between N prosumers who want to schedule a set of flexible loads in response to the dynamic tariffs which are broadcasted by the utility. They show that under some assumptions, including that the prosumers would be only cost minimizer and their total cost function would be convex, a unique Nash equilibrium can be obtained from solving a MILP problem. They propose a distributed algorithm as well in order to find the Nash equilibrium and solve an example with N=20 players. As discussed before, these papers use a game theoretic approach to formulate the interactions. They then use complementarity condition to turn the problem into a single optimization problem. From a computational point of view, this type of approach works well with a limited number of players. However, when the number of players increases, other methodologies, like MFG, become more appropriate (see, for example, Couillet et al., 2012; Ma et al., 2013; Chen et al., 2014; Zhu et al., 2016; Lindholm et al., 2017; Gomes and Saude, 2018; Tchuendom et al., 2019).

The current paper, in a broader perspective, contributes to a stream of research that investigates the integration of short-term operational decisions into a long-term GEP problem. Power systems planning requires decision making in two different timescales: short-term operational decisions and long-term strategic capacity expansion decisions. While the GEP problem addresses long-term investment decisions, due to the large size of the problem, it overlooks some important details of short-term operational characteristics of the network. Short-term operational decisions in power networks deal with issues such as unit commitment, demand response management, ancillary service operations, power flow, and economic dispatching. Poncelet et al. (2016) and Helistö et al. (2021) discuss how and to what extent the simplification of the short-term operational details in a long-term GEP problem affects the quality of the results. To address this drawback, a group of studies has developed methods to link a short-term power network operational model and a GEP problem. For example, a widespread practice is to link a short-term unit commitment problem with a GEP problem (Deane et al., 2012; Collins et al., 2017; Gaur et al., 2019; de Queiroz et al., 2019; Wyrwa et al., 2022). Koltsaklis and Georgiadis (2015) couple a short-term unit commitment problem that considers maintenance scheduling with a GEP problem. Ringkjøb et al. (2020) study the integration of short-term wind and solar production variability in the long-term GEP problem of TIMES. Short-term demand response management is an influential operation decision that is neglected in the traditional GEP problems. These problems assumed that, since consumers cannot see and immediately respond to prices, electricity demand is inelastic in the short term. However, with the penetration of smart meters that makes it possible to respond to real-time prices, this assumption is not valid anymore. To address this issue, a related stream of papers studies the integration of a short-term demand response model into the GEP problem (De Jonghe et al., 2011; Lohmann and Rebennack, 2017). In doing so, they introduce price-elastic demand response alongside dynamic operational constraints into GEP problems in order to enhance their solutions. The current study contributes to this literature by coupling a high-resolution demand response predicting model into a long-term GEP problem. We propose an original approach to integrate the information of the demand response model in the uncertainty model of a robust GEP problem.

GEP is a classical power system problem that plans the capacity expansion strategy of the entire electricity network over a long-term horizon to satisfy demand at minimum cost (see Koltsaklis and Dagoumas (2018) for a recent review). With the advent of smart grids, recent versions of the GEP problem consider DR as a reserved capacity (see e.g. Babonneau et al., 2017; Lohmann and Rebennack, 2017). Because of the long-term horizon of the planning in a GEP, this problem is plagued with many uncertainties. To tackle this issue, multi-stage versions of Robust Optimization (RO) and Stochastic Programming (SP) have been widely used (Dehghan et al., 2014; Mejía-Giraldo and McCalley, 2014; Han et al., 2018; Zou et al., 2018; Aliakbarisani et al., 2020). Specifically, Bloom (1983) and Bloom et al. (1984) are among the first papers to propose a two-stage SP formulation for the GEP problem with uncertain demand and supply. In Dehghan et al. (2014), the uncertainties of demand and investment cost are modeled in a two-stage RO model, while Mejía-Giraldo and McCalley (2014) uses such a formulation to address uncertainty in fuel price, demand and transmission capacity. Han et al. (2018) model the uncertainty of load demand and wind output in a GEP using a two-stage SP. Zou et al. (2018) propose a partially adaptive multi-stage SP GEP problem, where fuel price and demand are the two sources of uncertain.

Recently, Aliakbarisani et al. (2020) developed a robust multi-period conservative approximation formulation to address the uncertainty of DR in the ETEM model. This is the formulation that will be used in this paper for handling demand response uncertainty caused by a large fleet of EV users. Unlike Aliakbarisani et al. (2020), who simply assumed that DR deviations were exogenous to the expansion plan and thus that the size of the uncertainty set could be calibrated using historical data, our proposed approach will consider DR deviations to be endogenous, i.e. that they are affected by the marginal cost of useful energy production under the optimized expansion plan. Such endogeneity will be modeled using a continuous time linear quadratic game played by the EV users. The novelty in our approach consists in designing a procedure that will ensure that the robust expansion plan is both minimal with respect to worst-case cost and immunized against EV users' behavior as they react to the resulting marginal cost of energy.

Our work is similar in spirit to Babonneau et al. (2020), who were the first to attempt to integrate EV charging behavior in a robust version of ETEM. There are however crucial distinctions between the two works. First, the robust expansion planning model in Babonneau et al. (2020) only considers "here and now" decisions (a.k.a. static policies) and accounts for uncertainty about the maximum and minimum value that the demand response decision can take. They also take an optimistic view on robustness by robustifying only the sum of demand responses over the horizon instead of on a period by period basis. Secondly, the nature of the solution that they obtain when reaching a solution at equilibrium between the R-ETEM formulation and the LQGs is very different. To the best of our knowledge, their "robust" solution is only guaranteed to prescribe a **plausible** demand response plan, i.e. within the range of the more likely demand response profiles produced by the LQGs under market clearing prices. Such a solution actually has no guarantees regarding worst-case cost when the actual demand response deviates from the optimally selected plausible one. In opposition, our solution will provide (and minimize) a guarantee on the worst-case cost achieved by the expansion plan under all demand response deviation profiles produced by the LQGs under market clearing prices. We refer interested readers to Appendix 3.8.2 for more details about these distinctions. Finally, unlike Babonneau et al. (2020), which only present a simple step by step illustration of their algorithm, we perform a more detailed numerical investigation of how our new robust modeling approach affects the expansion planning of the electricity network of the Arc Lémanique region.

3.3 A robust multi-period ETEM model

In this work we consider the ETEM model proposed in Babonneau et al. (2017) (and summarized in Appendix 3.8.1). ETEM is a multi-regional multi-commodity GEP problem, and it is a member of the bottom-up family of energy models that integrates the entire energy value chains, from the resources to useful demands, aiming to obtain the best combination of supply and demand technologies at minimum cost. One salient feature of ETEM is a detailed description of demand technologies and the modeling of demand response by end-use technologies. This feature, alongside with the fact that ETEM is an open-source model, makes it well suited to the purpose of this study.

The description in ETEM is based on a list of geographical regions indexed by $l \in \mathbb{L}$, a list of energy commodities $c \in \mathbb{C}$, and a list of technologies $p \in \mathbb{P}$. The planning horizon, which typically spans over 40 years or more, is divided into different decision making periods, denoted as $t \in \mathbb{T}$, that are themselves divided into several time-slices in each period that capture the pattern of production and consumption i.e., $s \in \mathbb{S} := \mathbb{H} \times \mathbb{J}$ based on the hour of the day $h \in \mathbb{H}$ and season of the year $j \in \mathbb{J}$. ETEM is able to model both consumers and prosumers on the demand side, but in this paper we focus on consumers. The reason is that considering EVs as prosumers requires a detailed modeling of battery degradation as a result of additional discharge cycling in V2G operations, and designing an appropriate compensation scheme (Dubarry et al., 2017; Uddin et al., 2018), which is beyond the scope of this research. Our implementation will consider a $T = 8$ decision making periods each representing 5 years, while the time-slices will model the differences in consumption at a seasonal level ($\mathbb{J} := \{\text{winter, summer, intermediate seasons}\}$) and hourly level (with 4 different hour blocks as shown in Table 3.1). In total, there are 12 time-slices in a year $|\mathbb{S}| = 12$ (see Figure 3.1). Decisions in ETEM include (i) annual installation of each technology in each region, (ii) energy production by each technology in each region and each period and time slice, (iii) import of energy commodity from outside of the energy system, (iv) export of energy to outside of the energy system, (v) transmission of energy from one region to another region inside the boundary of the energy system, and finally (vi) planned demand response for the useful demand. In this paper, in order to simplify the presentation, we use a similar vector representation as used in Aliakbarisani et al. (2020), where $\boldsymbol{x} \in \mathbb{R}^m$ captures the technology installation decisions (i) in all periods and all regions while $\boldsymbol{y}_i$ captures the procurement decisions (ii-v) of all commodities, in all regions and time slices that belong to season $i \in \mathbb{I} := \mathbb{T} \times \mathbb{J}$, the set of seasonal periods. We depart from the notation in Aliakbarisani et al. (2020) by using a dedicated $\boldsymbol{s}_i$ to relate to demand response decisions in order to permit us to define the interaction with the consumption behavior model. Overall, the deterministic version of

ETEM takes the form:

$$\min_{\boldsymbol{x},\{\boldsymbol{y}_i,\boldsymbol{s}_i\}_{i=1}^{|\mathbb{I}|}} f^\top \boldsymbol{x} + \sum_{i\in\mathbb{I}} h_i^\top \boldsymbol{y}_i \tag{3.1a}$$

$$\text{s.t.} \quad A_i\boldsymbol{x} + E_i\boldsymbol{s}_i + B_i\boldsymbol{y}_i \le b_i,\ \forall i \in \mathbb{I} \tag{3.1b}$$

$$F_i\boldsymbol{s}_i \le U_i,\ \boldsymbol{s}_i \ge 0 \quad \forall i \in \mathbb{I} \tag{3.1c}$$

$$D\boldsymbol{x} \le e\,, \tag{3.1d}$$

where constraint (3.1b) represents the set of constraints on capacity, seasonal procurement and useful demand. For example, these constraints include, but are not limited to, energy balance, minimum required reserve capacity for peak periods, demand, and capacity factor constraints (see Appendix 3.8.1). On the other hand, constraint (3.1c) limits the feasible space for demand response and constraint (3.1d) imposes technical and economical constraints on the newly installed capacity. More importantly for what will follow, in terms of demand response modeling, constraint (3.1b) includes:

$$\sum_{p\in\mathbb{P}_c^P} \boldsymbol{P}_{t,s,l,p,c} \ge \Theta_{t,l,c}\boldsymbol{V}_{t,s,l,c} \qquad \forall t,s,l,c \in \mathbb{C}^{\mathscr{D}} \tag{3.2}$$

while (3.1c) contains:

$$\upsilon_{t,s,l,c}(1-\nu_{t,s,l,c}) \le \boldsymbol{V}_{t,s,l,c} \le \upsilon_{t,s,l,c}(1+\nu_{t,s,l,c}) \quad \forall t,s,l,c \in \mathbb{C}^{\mathscr{D}} \tag{3.3}$$

$$\sum_{s\in\mathbb{S}_j} \boldsymbol{V}_{t,s,l,c} = \sum_{s\in\mathbb{S}_j} \upsilon_{t,s,l,c} \qquad \forall t,l,c \in \mathbb{C}^{\mathscr{D}}, j \in \mathbb{J} \tag{3.4}$$

Together, these constraints model the idea that for each commodity c in the set of useful demand $\mathbb{C}^{\mathscr{D}}$, the total production of useful energy accounted for by $\boldsymbol{P}$ must satisfy the demand in each time-slice and region. The latter demand is a result of relative demand response plan denoted by $\boldsymbol{V}$ that attempts to optimally distribute the total demand of period t into all time-slices s inside period t, while staying within a certain ν margin from the nominal demand distribution υ. Finally, note that $\boldsymbol{s}_i$ captures all $\boldsymbol{V}_{t,s,l,c}$ with $i=(t,j)$, $l \in \mathbb{L}$, $s \in \mathbb{S}_j$, and all $c \in \mathbb{C}^{\mathscr{D}}$.

As described previously, beside the optimal expansion of the generation technologies, the planner decides in ETEM of the optimal level of DR contributions. It is therefore

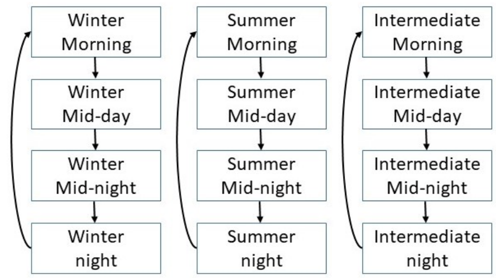

Figure 3.1: Sequence of time-slices

Table 3.1: Definition of hourly blocks $\mathbb{H}$

h_1	23 pm - 6 am
h_2	6 am - 12 pm
h_3	12 pm - 17 pm
h_4	17 pm- 23 pm

assumed that the consumers can be convinced to behave according to the planned demand response by using incentive programs such as real-time pricing. While, in long-term planning problem such as GEPs, there are necessarily many uncertainties that may affect the performance of the expansion plans, in this paper we focus on the influence of consumer behavioral uncertainties on the performance that can be expected from planned demand response. In particular, we assume that the planner wishes to immunize his expansion plan against possible deviations between the planned and actual DR. As shown in Aliakbarisani et al. (2020), this can be done by employing a R-ETEM model, which offers a protection against relative demand response deviations (RDRDs) in ETEM. More specifically, R-ETEM is a multi-period adjustable RO formulation of ETEM, which is a standard technique to model uncertainties in long term planning problems. R-ETEM also exploits affinely adjustable policies, a widely used approximation technique introduced by Ben-Tal et al. (2004) to efficiently identify conservative solutions to multi-stage robust optimization problem.

Mathematically speaking, R-ETEM considers that the total demand of final energy is perturbed by a relative demand response deviation (RDRD) denoted by $\boldsymbol{\delta}_{t,s,l,c}$, i.e that $\Theta_{t,l,c}\boldsymbol{V}_{t,s,l,c}$ in constraint (3.2) is replaced with $\Theta_{t,l,c}(\boldsymbol{V}_{t,s,l,c}+\boldsymbol{\delta}_{t,s,l,c})$ with $\boldsymbol{\delta}$ in some

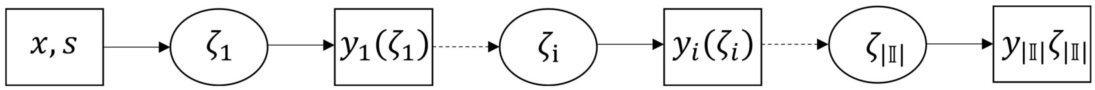

Figure 3.2: Sequence of decisions and uncertainty observations in our multi-period problem

uncertainty set $\Xi(\eta)$ defined as:

$$\Xi(\eta) = \left\{ \boldsymbol{\delta} \in \mathbb{R}^d \,\middle|\, \begin{array}{c} \exists \boldsymbol{\zeta} \in [-1,\, 1]^d \\ \boldsymbol{\delta}_{t,s,l,c} = \eta \boldsymbol{\zeta}_{t,s,l,c},\ \forall t,s,l,c \in \mathbb{C}^U \\ \sum_{s \in \mathbb{S}^j} \sum_{l \in \mathbb{L}} \sum_{c \in \mathbb{C}^U} |\boldsymbol{\zeta}_{t,s,l,c}| \leq \sqrt{|\mathbb{S}^j||\mathbb{C}^U||\mathbb{L}|}\ \forall t, j \in \mathbb{J} \end{array} \right\}, \tag{3.5}$$

where d is the total number of perturbations while η captures the level of uncertainty in Ξ and can be used to model the level of robustness (or conservatism) of the R-ETEM formulation. Note that unlike the budgeted uncertainty set used in Aliakbarisani et al. (2020), which assumes a known bounded support, our choice of Ξ encodes the Cartesian product of polyhedral outer approximations of norm-2 balls of radius η, which can be adjusted to include any arbitrarily large perturbation. Furthermore, based on constraints (3.3) and (3.4), one can establish the largest possible amount of deviation implied by the ETEM model to be:

$$\bar{\eta} := \max_{\boldsymbol{\delta}} \quad \min_{\eta : \boldsymbol{\delta} \in \Xi(\eta)} \eta \tag{3.6a}$$

$$\text{s.t.} \quad \boldsymbol{V}_{t,s,l,c} + \boldsymbol{\delta}_{t,s,l,c} \geq \upsilon_{t,s,l,c}(1 - \nu_{t,s,l,c}) \quad \forall t,s,l,c \in \mathbb{C}^{\mathscr{D}} \tag{3.6b}$$

$$\boldsymbol{V}_{t,s,l,c} + \boldsymbol{\delta}_{t,s,l,c} \leq \upsilon_{t,s,l,c}(1 + \nu_{t,s,l,c}) \quad \forall t,s,l,c \in \mathbb{C}^{\mathscr{D}} \tag{3.6c}$$

$$\sum_{s \in \mathbb{S}_j} \boldsymbol{V}_{t,s,l,c} + \boldsymbol{\delta}_{t,s,l,c} = \sum_{s \in \mathbb{S}_j} \upsilon_{t,s,l,c} \qquad \forall t,l,c \in \mathbb{C}^{\mathscr{D}}, j \in \mathbb{J}. \tag{3.6d}$$

This in turns motivates to restrict the attention to levels of robustness in the range $[0,\ \bar{\eta}]$.

In response to this observed demand deviation, the R-ETEM in Aliakbarisani et al. (2020) assumes that the planner is able to adjust his procurement decisions. The chronology of decision making is presented in Figure 3.2 and the general formulation of R-ETEM can be summarized as follows:

$$\min_{\boldsymbol{x},\{\boldsymbol{y}_i(\cdot),\boldsymbol{s}_i\}_{i=1}^{|\mathbb{I}|}} \max_{\{\boldsymbol{\zeta}_i\in\mathscr{Z}_i(\Gamma_i)\}_{i=1}^{|\mathbb{I}|}} f^\top\boldsymbol{x}+\sum_{i\in\mathbb{I}} h_i^\top\boldsymbol{y}_i(\boldsymbol{\zeta}_i) \tag{3.7a}$$

$$\text{s.t.}\quad A_i\boldsymbol{x}+E_i\boldsymbol{s}_i+B_i\boldsymbol{y}_i(\boldsymbol{\zeta}_i)\le b_i+C_i\boldsymbol{\zeta}_i \quad \forall\boldsymbol{\zeta}_i\in\mathscr{Z}_i(\Gamma_i),\,\forall i\in\mathbb{I} \tag{3.7b}$$

$$F_i\boldsymbol{s}_i\le U_i,\ \boldsymbol{s}_i\ge 0\quad \forall i\in\mathbb{I} \tag{3.7c}$$

$$D\boldsymbol{x}\le e\,, \tag{3.7d}$$

where $\mathscr{Z}_i(\Gamma_i) := \{\boldsymbol{\zeta}_i\,|\,\|\boldsymbol{\zeta}_i\|_\infty\le 1,\ \|\boldsymbol{\zeta}_i\|_1\le\Gamma_i\}$, $\Gamma_i=\sqrt{|\mathbb{S}^j|\times|\mathbb{C}^U|\times|\mathbb{L}|}$ with $i=(t,j)$, and where the seasonal procurement variable $\boldsymbol{y}_i(\cdot)$ is adjustable with respect to the realized uncertain parameter in the same time period and season $\boldsymbol{\zeta}_i$. Because such a multi-stage robust optimization problem is generally intractable (see Ben-Tal et al., 2004), Aliakbarisani et al. (2020) proposes a conservative approximation where the adjustable variable $\boldsymbol{y}_i(\boldsymbol{\zeta}_i)$ are affine functions of $\bar{\boldsymbol{\zeta}}_i$, i.e., $\boldsymbol{y}_i(\boldsymbol{\zeta}_i)=\boldsymbol{y}_i+\boldsymbol{Y}_i\bar{\boldsymbol{\zeta}}_i$, where $\boldsymbol{y}_i$ and $\boldsymbol{Y}_i$ become the decision variables, and $\bar{\boldsymbol{\zeta}}_i\in\bar{\mathscr{Z}}_i$ is a lifted representation of $\boldsymbol{\zeta}_i$ that distinguishes between positive and negative deviations and such that $\mathscr{Z}_i(\Gamma_i)=P_i\bar{\mathscr{Z}}_i$ for some projection matrix P_i. The final conservative approximation of the R-ETEM takes the form:

$$\min_{\boldsymbol{x},\{\boldsymbol{y}_i,\boldsymbol{Y}_i,\boldsymbol{s}_i\}_{i=1}^{|\mathbb{I}|}} \max_{\{\bar{\boldsymbol{\zeta}}_i\in\bar{\mathscr{Z}}_i\}_{i=1}^{|\mathbb{I}|}} f^\top\boldsymbol{x}+\sum_{i\in\mathbb{I}} h_i^\top(\boldsymbol{y}_i+\boldsymbol{Y}\bar{\boldsymbol{\zeta}}_i) \tag{3.8a}$$

$$\text{s.t.}\quad A_i\boldsymbol{x}+E_i\boldsymbol{s}_i+B_i(\boldsymbol{y}_i+\boldsymbol{Y}\bar{\boldsymbol{\zeta}}_i)\le b_i+C_iP_i\bar{\boldsymbol{\zeta}}_i \quad \forall\bar{\boldsymbol{\zeta}}_i\in\bar{\mathscr{Z}}_i,\,\forall i\in\mathbb{I} \tag{3.8b}$$

$$F_i\boldsymbol{s}_i\le U_i,\ \boldsymbol{s}_i\ge 0\quad \forall i\in\mathbb{I} \tag{3.8c}$$

$$D\boldsymbol{x}\le e\,, \tag{3.8d}$$

After applying standard robust reformulation technique, problem (3.7) is conservatively approximated using a single finite-dimensional linear program that can be solved using either off-the-shelf solvers, or more efficiently using a Bender's decomposition scheme. We refer interested readers to Aliakbarisani et al. (2020) for more technical details and to Appendix 3.8.2 for a formal summary of the differences between R-ETEM and the robust model proposed in Babonneau and Haurie (2019).

3.4 A behavioral model for exchangeable EVs

Inspired by Tchuendom et al. (2019), we employ a LQG to model the charging/discharging behavior of a fleet of N exchangeable EVs. Each EV user is a price taker, but the aggregated charging profile affects the real time electricity price. EV users choose their charging profile rationally (i.e. they seek to minimize a given cost function). The cost function, beside the price of energy consumption, takes into account that i) EV users have a preferable state of the charge during the day, and any deviation from it is costly, and ii) EV users want to protect their batteries from the consequences of fast charging. Therefore the cost function is the summation of energy price, cost of deviation from the Desired Level of Charge (DLC) and cost of fast charging. In the limit as the fleet's size N goes to infinity, the LQG becomes a Mean Field Game (MFG) model. MFG theory is a well known technique to study the strategic behavior of large population of exchangeable interacting agents and can be used to approximate the solution of the LQG model when N is large.

3.4.1 Linear quadratic game formulation

Consider a N-player stochastic game of exchangeable EV users who want to charge their batteries in a finite horizon ($T > 0$) at minimum cost. We consider $T = 1$ represents one day, $\tau \in [0, T]$ is the continuous index for all time slots inside this day. It is assumed that the discharge profile i.e., $(\nu_\tau)_{\tau\in[0,T]}$, is estimated from the mobility data and exogenously given to the model, and it is common to all EV users. But, vehicle specific Brownian motions, i.e., $W^i := (W^i_\tau)_{\tau\in[0,T]}, i \in \{1,\dots,N\}$, account for driver to driver independent idiosyncratic deviations from the common discharge profile.

Every EV user's control consists in the charging rate at time τ denoted by $(u^i_\tau)_{\tau\in[0,T]}, i \in \{1,\dots,N\}$. Also, the process $(X^i_\tau)_{\tau\in[0,T]}, i \in \{1,\dots,N\}$ denotes fleet's states of charge which dynamics are captured by the following linear stochastic system of equations:

$$X_\tau^i = x_0 + \int_0^\tau (u_r^i - v_r)dr + \varepsilon W_\tau^i \quad \forall i \in \{1,\dots,N\}, \tau \in [0,T],$$

where ε is a strictly positive constant and the initial state x_0 is a random parameter with a normal distribution $\mathscr{N}(a_0, s^2)$. We also denote by a_τ the preferrable/comfortable state of the charge profile common to all agents, which is exogenously defined.

Because the EV users are exchangeable, we can highlight a representative EV user, which we identify by $i \in \{1,..,N\}$. The study of the finite behavioral game model is formulated as a stochastic linear system with quadratic cost function, reveals that, any rationally chosen control by the representative EV user must be an affine function of its state of the charge process, which is modelled as a Gaussian process. Thus, thanks to the Gaussian nature of the state of charge, the control process u_τ^i, for any $i \in \{1,..,N\}$, and their sample mean process, will also be Gaussian.

Given the set of N players control processes, one can define the sample mean of the finite fleet of EVs, denoted $\Delta^N(U_\tau)$, where $U_\tau := \{u_\tau^i, i = 1,\dots,N\}$, as:

$$\Delta^N(U_\tau) := \frac{1}{N}\sum_{i=1}^N u_\tau^i, \quad \forall \tau \in [0,T].$$

The finite behavioral game model assumes that the charging/discharging marginal price is a function of the fleet's aggregate demand profile through its mean demand as below:

$$p_\tau := \lambda(\tau)\Delta^N(U_\tau),\ \forall \tau \in [0,T], \tag{3.9}$$

where $\lambda : [0, T] \to [0, \infty)$ is a function, smooth outside of a set of measure zero. (Note that, we consider functions that are smooth outside of a set of measure zero because we will solve the associated MFG model numerically).

Given the fixed marginal price function defined above, each player $i = 1,\dots,N$ minimizes the following cost function:

$$J^i(u^i, u^{-i}) = \mathbb{E}\Big[\frac{\overline{q}}{2}(X_T^i - a_T)^2 + \int_0^T \Big(\frac{\kappa}{2}(u_\tau^i)^2 + u_\tau^i p_\tau + \frac{q}{2}(X_\tau^i - a_\tau)^2\Big)d\tau\Big]. \tag{3.10}$$

Observe that the cost function of any player $i \in \{1,..,N\}$ depends on the controls of all other players, denoted $u^{-i} := (u^1,\ldots,u^{i-1},u^{i+1},\ldots,u^N)$, through the marginal price which is a function of the fleet's aggregate demand profile.

In the cost function, the constants $\overline{q} > 0$ and $q > 0$ model the cost associated to the deviation from the desired level of charge $(a_\tau)_{\tau\in[0,T]}$, and the term $\frac{\kappa}{2}(u^i_\tau)^2$ represents the cost of battery deterioration from fast charging/discharging (the quadratic term, i.e. $(u^i_t)^2$, penalizes large charging rates hence fast charging). Even in this linear quadratic Gaussian setting, finding a Nash equilibrium to such a behavioral game model quickly becomes intractable as the number of players increases.

3.4.2 Mean field game formulation and solvability

To circumvent the problem that finding the Nash equilibrium in the formulated linear quadratic game becomes intractable when N becomes very large, we consider the MFG model as a method to find an approximate Nash equilibrium, for which the approximation error decreases as N goes to infinity. In a nutshell, the solution of a MFG model, referred to as a MFG equilibrium corresponds to the exact Nash equilibrium of the game with infinitely many players.

We define a Brownian motion $(W_\tau)_{\tau\in[0,T]}$ on a complete probability space denoted $(\Omega,\mathbb{F} = (\mathscr{F}_\tau)_{\tau\in[0,T]},\mathbb{P})$ satisfying the usual conditions, where, $\mathscr{F}_\tau = \sigma\{x_0,W_s,\ 0 \le s \le \tau\}$, defines the filtration at time $\tau \in [0,T]$. Consider the set of admissible controls, denoted by $\mathscr{A}([0,T])$, below:

$$\mathscr{A}([0,T]) = \left\{x : \Omega\times[0,T] \longrightarrow \mathbb{R} \quad | \quad \mathbb{E}\left[\int_0^T |x_t|^2 dt\right] < \infty\right\}. \tag{3.11}$$

Below, we define the mean field game associated to the finite behavioral game model above, in three steps :

1. Fix a candidate average aggregate (mean) demand profile $\Delta := (\Delta_\tau)_{\tau\in[0,T]}$

2. Solve the control problem of finding $u^* \in \mathscr{A}([0,T])$ such that it is a minimizer of:

$$\min_{u\in\mathscr{A}([0,T])} \mathbb{E}\left[\frac{\overline{q}}{2}(X_T - a_T)^2 + \int_0^T \left(\frac{\kappa}{2}(u_\tau)^2 + u_\tau p_\tau(\Delta_\tau) + \frac{q}{2}(X_\tau - a_\tau)^2\right) d\tau\right], \tag{3.12}$$

where, $p_\tau(\Delta) := \lambda(\tau)\Delta_\tau$, and

$$X_\tau = x_0 + \int_0^\tau (u_s - v_s)ds + \varepsilon W_\tau, \quad x_0 = \mathscr{N}(a_0, s^2).$$

3. Show that, the MFG equilibrium is achieved. That is:

$$\Delta_\tau := \mathbb{E}[u^*_\tau],\ \forall \tau \in [0,T]. \tag{3.13}$$

Observe that the MFG model defined above consists of a control problem coupled with a fixed-point problem. The MFG equilibrium, denoted by $(u^*_\tau, \Delta_\tau)_{\tau\in[0,T]}$, is composed of the optimal demand profile of the representative player and the mean demand profile of the infinite population of players.

The following theorem, recalled from Tchuendom et al. (2019), characterizes the solution to the mean field game defined above.

Theorem 4. *There is a solution $(u^*_\tau, \Delta_\tau)_{\tau\in[0,T]}$ to the mean field game defined above if and only if there is a solution $(\eta_\tau, w_\tau, \Phi_\tau, \Delta_\tau)_{\tau\in[0,T]}$ for the following Forward-Backward Ordinary Differential Equations (FBODE):*

$$\frac{d\eta_\tau}{d\tau} = \frac{\eta_\tau^2}{\kappa} - q,\ \eta_T = \overline{q}, \tag{3.14}$$

$$\frac{dw_\tau}{d\tau} = \left(\frac{\varepsilon^2\eta_\tau^2}{\kappa^2} - \frac{2q}{\eta_\tau}w_\tau\right),\ w_0 = \frac{s^2\eta_0^2}{\kappa^2}, \tag{3.15}$$

$$\frac{d\Delta_\tau}{d\tau} = -F_1(\tau)\Phi_\tau - F_2(\tau)\Delta_\tau + F_3(\tau), \tag{3.16}$$

$$\frac{d\Phi_\tau}{d\tau} = B_1(\tau)\Phi_\tau + B_2(\tau)\Delta_\tau + B_3(\tau), \tag{3.17}$$

$$\Delta_0 = I_1(0)\Phi_0 + I_2(0),\ \Phi_T = -\overline{q}a_T. \tag{3.18}$$

The coefficients of the FBODEs are defined as:

$$I_1(\tau) = \frac{-1}{\kappa + \lambda(\tau)}, \qquad I_2(\tau) = -I_1(\tau)\Big(\eta_\tau(sF^{-1}[0.5;0,1] - a_0)\Big),$$

$$
\begin{aligned}
&B_1(\tau) = \frac{\eta_\tau}{\kappa}, \quad B_2(\tau) = \frac{\eta_\tau \lambda(\tau)}{\kappa}, \quad B_3(\tau) = q a_\tau + \frac{\eta_\tau(\kappa v_\tau)}{\kappa},\\
&F_1(\tau) = -\frac{q}{\eta_\tau} I_1(\tau), \quad F_2(\tau) = -I_1(\tau)\Big(\frac{d\lambda(\tau)}{d\tau} + \frac{q}{\eta_\tau}[\lambda(\tau)+\kappa]\Big),\\
&F_3(\tau) = -\kappa I_1(\tau)\Big(\frac{\varepsilon^2 \eta_\tau^2 F^{-1}[0.5;0,1]}{2\kappa^2\sqrt{w_\tau}} - \frac{q}{\kappa}[a_\tau + \frac{\lambda(\tau)}{\eta_\tau}]\Big).
\end{aligned}
$$

where $F[r;0,1]$ denotes the Cumulative Distribution Function of a standard normal random variable with mean 0 and variance 1.

Theorem 4 states that solving the mean field game above is equivalent to solving the FBODEs (3.14-3.15-3.16-3.17). Existence and uniqueness of solutions to the FBODEs (3.14-3.15-3.16-3.17), is garanteed under contraction type conditions (see Tchuendom et al. (2019)).

We recall that in this setting, the process $(u^*_\tau)_{\tau\in[0,T]}$ denotes to the optimal demand of the representative EV user at equilibrium and $(\Delta_\tau)_{\tau\in[0,T]}$ denotes the average optimal demand of all EV users at equilibrium (i.e $\Delta_\tau = \mathbb{E}[u^*_\tau],\ \tau\in[0,T]$).

Thanks to the linear-quadratic nature of the control problem, the optimal state of the charge and demand of the representative EV user at equilibrium $(u^*_\tau)_{\tau\in[0,T]}$, is given by the feedback formula below:

$$
X^*_\tau = x_0 - \int_0^\tau \frac{1}{\kappa}\big[\eta_r X^*_r + \Phi_r + \lambda(r)\Delta_r + \kappa v_r\big]dr + \varepsilon W_\tau, \quad \tau\in[0,T], \tag{3.19}
$$

$$
u^*_\tau = -\frac{1}{\kappa}\big[\eta_\tau X^*_\tau + \Phi_\tau + \lambda(\tau)\Delta_\tau\big], \quad \tau\in[0,T]. \tag{3.20}
$$

We note that, solving the FBODEs (3.14-3.15-3.16-3.17) is not straightforward, even in our linear setting. The difficulty stems from the fact that the associated initial and terminal conditions. Observe that, the initial mean demand profile (Δ_0) depends on the initial value (Φ_0), which is not available at time $\tau = 0$. To circumvent this difficulty, the following proposition exploits the linear structure of the FBODEs (3.14-3.15-3.16-3.17), to obtain a representation of the deterministic profile $(\Phi_\tau)_{\tau\in[0,T]}$ as a linear function of the average optimal demand of EV users, $(\Delta_\tau)_{\tau\in[0,T]}$.

Proposition 5. *Assume that there is a unique solution, $(\eta_\tau, w_\tau, \Phi_\tau, \Delta_\tau)_{\tau\in[0,T]}$, to the the FBODEs (3.14-3.15-3.16-3.17) and a unique solution $(\Psi_\tau, \Pi_\tau)_{\tau\in[0,T]}$, to the backwards ordinary differential equations (BODEs) below: $\forall\tau[0,T]$*

$$\frac{d\Psi_\tau}{d\tau} = F_1(\tau)\Psi_\tau^2 + F_2(\tau)\Psi_\tau + B_1(\tau)\Psi_\tau + B_2(\tau), \;\; \Psi_T = 0, \tag{3.21}$$

$$\frac{d\Pi_\tau}{d\tau} = F_1(\tau)\Psi_\tau\Pi_\tau - F_3(\tau)\Psi_\tau + B_1(\tau)\Pi_\tau + B_3(\tau), \;\; \Pi_\tau = -\bar{q}a_T, \tag{3.22}$$

then, the following representation formula holds:

$$\Phi_\tau = \Psi_\tau\Delta_\tau + \Pi_\tau, \;\; \forall\tau \in [0,T]. \tag{3.23}$$

Proof. We prove the proposition by applying a chain differentiation rule to representation formula (3.23) and obtaining the ODE (3.17).

$$\begin{aligned}
\frac{d\Phi_\tau}{d\tau} &= \Delta_\tau\frac{d\Psi_\tau}{d\tau} + \Psi_\tau\frac{d\Delta_\tau}{d\tau} + \frac{d\Pi_\tau}{d\tau} \quad \forall\tau \in [0,T], \\
&= \Delta_\tau\Big[F_1(\tau)\Psi_\tau^2 + F_2(\tau)\Psi_\tau + B_1(\tau)\Psi_\tau + B_2(\tau)\Big] \\
&\quad + \Psi_\tau\Big[-F_1(\tau)(\Psi_\tau\Delta_\tau + \Pi_\tau) - F_2(\tau)\Delta_\tau + F_3(\tau)\Big] \\
&\quad + \Big[F_1(\tau)\Psi_\tau\Pi_\tau - F_3(\tau)\Psi_\tau + B_1(\tau)\Pi_\tau + B_3(\tau)\Big], \quad \forall\tau \in [0,T], \\
&= B_1(\tau)\Phi_\tau + B_2(\tau)\Delta_\tau + B_3(\tau), \quad \forall\tau \in [0,T],
\end{aligned}$$

and at terminal condition, $\tau = T$, we have:

$$\Phi_T = \Psi_T\Delta_T + \Pi_T = 0 \times \Delta_T + (-\bar{q}a_T) = -\bar{q}a_T. \qquad \square \tag{3.24}$$

□

As a direct consequence of the proposition 5, and equation (3.20), the representative EV user's optimal demand at equilibrium can be rewritten as follows:

$$u_\tau^* = -\frac{1}{\kappa}\big[\eta_\tau X_\tau^* + \Phi_\tau + \lambda(\tau)\Delta_\tau\big], \quad \forall\tau \in [0,T], \tag{3.25}$$

$$= -\frac{1}{\kappa}\big[\eta_\tau X_\tau^* + (\Psi_\tau\Delta_\tau + \Pi_\tau) + \lambda(\tau)\Delta_\tau\big], \quad \forall\tau \in [0,T]. \tag{3.26}$$

From this updated formula for the representative EV user's optimal demand, we can derive another formula for the representative EV user's mean optimal demand.

Indeed, since at MFG equilibrium it holds that $\mathbb{E}[u^*_\tau] = \Delta_\tau,\ \forall \tau \in [0,T]$, it follows that:

$$\begin{aligned}
\Delta_\tau &= \mathbb{E}[u^*_\tau],\ \forall \tau \in [0,T],\\
&\iff \Delta_\tau = -\frac{1}{\kappa}\left[\eta_\tau \mathbb{E}[X^*_\tau] + (\Psi_\tau + \lambda(\tau))\Delta_\tau + \Pi_\tau\right],\ \forall \tau \in [0,T],\\
&\iff \Delta_\tau\big(-\kappa - \Psi_\tau - \lambda(\tau)\big) = \eta_\tau \mathbb{E}[X^*_\tau] + \Pi_\tau,\ \forall \tau \in [0,T],\\
&\iff \Delta_\tau = -\frac{\eta_\tau \mathbb{E}[X^*_\tau] + \Pi_\tau}{\kappa + \Psi_\tau + \lambda(\tau)},\ \forall \tau \in [0,T],
\end{aligned} \tag{3.27}$$

where the process $\big(\mathbb{E}[X^*_\tau]\big)_{\tau\in[0,T]}$ denotes the EV users' average optimal state of charge :

$$\begin{aligned}
\mathbb{E}[X^*_\tau] &= \mathbb{E}[x_0] - \int_0^\tau \frac{1}{\kappa}\left[\eta_r \mathbb{E}[X^*_r] - \big(\Psi_r + \lambda(r)\big)\frac{\eta_r \mathbb{E}[X^*_r] + \Pi_r}{\kappa + \Psi_r + \lambda(r)} + \Pi_r + \kappa v_r\right] dr\\
&= \mathbb{E}[x_0] - \int_0^\tau \left[\frac{\eta_r \mathbb{E}[X^*_r] + \Pi_r}{\kappa + \Psi_r + \lambda(r)} + v_r\right] dr, \quad ,
\end{aligned} \tag{3.28}$$

for all $\tau \in [0,\, T]$.

Finally, to compute the EV users' average optimal state of charge and average demand, it is enough to compute the solution, (η_τ, w_τ) to FBODEs $(3.14-3.15)$, and the solution, $(\Psi_\tau, \Pi_\tau)_{\tau\in[0,T]}$, to the FBODEs $(3.21-3.22)$. Then evaluate the feedback formulas (3.28) and (3.27). A detailed implementation algorithm is presented in Appendix 3.8.3.

3.5 Coupling R-ETEM and LQGs

Up to this point, we have proposed a R-ETEM model that immunizes the expansion plan against possible behavioral deviations from the planned response over a 40+ years horizon. We also presented a linear quadratic game that can be used to simulate the continuous time charging behavior of EV users on a typical day. Focusing on the case where EV charging is the only useful demand with behavioral uncertainty (i.e. $\mathbb{C}^U := \{\bar{c}\}$ with $\bar{c}$ as electricity used to charge EVs, we are left with the task of describing the interactions between the two types of models. Specifically, for each time-season $i \in \mathbb{I}$ and region $l \in \mathbb{L}$, one can envision having recourse to the linear quadratic game formulation to simulate the behaviour of EV users on a typical day of this period based on available information regarding N, a, q, and κ. In doing so, we first will ensure that the price function used in the LQG is consistent with the market clearing price (i.e. marginal cost) implied by the solution of R-ETEM. We will also propose a bisection algorithm that calibrates the level of uncertainty in R-ETEM in a way that ensures R-ETEM produces a robust expansion plan that is behaviorally-consistent with the LQG models. In simple terms, the final robust plan should be immunized against the demand response deviations observed in the ensemble of behavioral model when it is implemented.

3.5.1 Extracting the marginal cost in R-ETEM

In this subsection, we indicate how to extract marginal costs for the procurement of useful energy $c \in \mathbb{C}^{\mathscr{D}}$. In particular, in the deterministic model (3.1), this can be done by looking at the dual variable associated to the demand satisfaction constraint (3.2). In the conservative approximation of R-ETEM, this is not as straightforward. This section proposes a general procedure for doing so.

Specifically, we start by observing that (3.8) can be equivalently formulated as:

$$\min_{\boldsymbol{x},\{\boldsymbol{y}_i,\boldsymbol{Y}_i,\boldsymbol{s}_i,\bar{\boldsymbol{s}}_i\}_{i=1}^{|\mathbb{I}|}} \max_{\{\bar{\boldsymbol{\zeta}}_i \in \bar{\mathscr{Z}}\}_{i=1}^{|\mathbb{I}|}} f^\top \boldsymbol{x} + \sum_{i\in\mathbb{I}} h_i^\top (\boldsymbol{y}_i + \boldsymbol{Y}\bar{\boldsymbol{\zeta}}_i) \tag{3.29a}$$

$$\text{s.t.} \quad A_i\boldsymbol{x} + E_i\boldsymbol{s}_i + B_i(\boldsymbol{y}_i + \boldsymbol{Y}\bar{\boldsymbol{\zeta}}_i) \leq b_i + C_iP_i\bar{\boldsymbol{\zeta}}_i \quad \forall \bar{\boldsymbol{\zeta}}_i \in \bar{\mathscr{Z}}_i,\ \forall i \in \mathbb{I} \tag{3.29b}$$

$$F_i\bar{\boldsymbol{s}}_i \leq U_i,\ \bar{\boldsymbol{s}}_i \geq 0 \quad \forall i \in \mathbb{I} \tag{3.29c}$$

$$D\boldsymbol{x} \leq e\,, \tag{3.29d}$$

$$\boldsymbol{s}_i = \bar{\boldsymbol{s}}_i \quad \forall i \in \mathbb{I} \tag{3.29e}$$

Recall that $\boldsymbol{s}_i$ was capturing all the relative demand responses $\boldsymbol{V}_{t,s,l,c}$ with $i = (t,j)$, $s \in \mathbb{S}_j$, and $c \in \mathbb{C}^{\mathscr{D}}$. Hence, when the minimum of problem (3.29) is finite, the optimal assignment $\{\boldsymbol{\gamma}_i^*\}_{i\in\mathbb{I}}$ of dual variables associated to (3.29e) captures the marginal effect of increasing the relative demand responses on the optimal cost. We are left with converting marginal cost of relative demand response in units of marginal cost of absolute demand response.

In particular, the marginal energy cost for final demand c, in region l, in time period t and time-slice s according to the conservative R-ETEM model (3.8) is $\bar{\gamma}^*_{t,s,l,c} := [\boldsymbol{\gamma}^*_i]_{t,s,l,c}/\Theta_{t,l,c}$ with $i = (t, j) : s \in \mathbb{S}^j$, and where $[\boldsymbol{\gamma}^*_i]_{t,s,l,c}$ takes the element of the dual vector associated to constraint $\boldsymbol{V}_{t,s,l,c} = \bar{\boldsymbol{V}}_{t,s,l,c}$.

3.5.2 Calibrating the marginal price function in MFG

In order to calibrate the price function in the MFG behavioral model, we employ a similar approach as in Babonneau et al. (2020). Namely, the marginal price p_τ should reflect the marginal cost of production when the average charging amount is equal to the planned response. In time-season period $i = (t, j)$, and for region l, this is done using:

$$\lambda^{i,l}(\tau) := \sum_{s \in \mathbb{S}^j} \mathbf{1}\{\tau \in \mathcal{T}_s\} \frac{\bar{\gamma}^*_{t,s,l,\bar{c}}}{\Theta_{t,l,\bar{c}} \boldsymbol{V}_{t,s,l,\bar{c}}/(N^l D_i)} \tag{3.30}$$

where $\mathbf{1}\{\cdot\}$ is the indicator function, N^l is the number of vehicles in region l, $\bar{c}$ is the index of the final demand of electricity for charging EVs, $\mathcal{T}_s$ indicates the period of the day associated to time slice s, and where D_i is the total number of days in time-season period $i = (t, j)$, Indeed, one can check that with this definition if for any $\tau \in \mathcal{T}_s$ we have that the average charging amount and the planned response are the same, i.e. $\Delta^N(U_\tau) = \Theta_{t,l,\bar{c}} \boldsymbol{V}_{t,s,l,\bar{c}}/(ND_i)$, then it follows that the marginal price reduces to:

$$\begin{aligned} p_\tau &= \lambda^{i,l}(\tau)\Delta^N(U_\tau) = \lambda^{i,l}(\tau)\, \Theta_{t,l,\bar{c}} \boldsymbol{V}_{t,s,l,\bar{c}}/(ND_i) \\ &= \sum_{s' \in \mathbb{S}^j} \mathbf{1}\{\tau \in \mathcal{T}_{s'}\} \bar{\gamma}^*_{t,s',l,\bar{c}} = \bar{\gamma}^*_{t,s,l,\bar{c}}\,. \end{aligned}$$

3.5.3 Optimizing behaviorally-consistent robust expansion plans

Once the marginal price functions used in each LQG are well calibrated, the question remains of whether the behavioral uncertainty that is modeled in R-ETEM is consistent with the simulations produced by the behavioral LQG models. A very natural condition to impose on R-ETEM is that it should produce a plan, which once implemented leads to consumers behaviors that fall within the range for which the plan is immunized against.

Definition 1. *The optimal robust expansion strategy* $\boldsymbol{x}^*$ *and planned demand response* $\boldsymbol{s}^*$ *are "behaviorally-consistent" if when the operator charges consumers according to the price function* (3.9)*, the actual relative demand response deviation measured by the behavioral model of Section 3.4 falls within the uncertainty set* $\Xi(\eta)$ *defined in* (3.5)*.*

Practically speaking, given any fixed uncertainty set $\Xi(\eta)$, verifying whether $\boldsymbol{x}^*(\eta)$ and $\boldsymbol{s}^*(\eta)$, i.e. the optimal solutions of problem (3.8) under $\Xi(\eta)$, are behaviorally-consistent involves solving the MFGs for each $i \in \mathbb{I}$ and $l \in \mathbb{L}$ with the price function (3.9), obtaining $\Delta^{i,l}$ based on equation (3.27) and verifying whether the realized relative demand vector $\hat{\boldsymbol{s}}$ defined as:

$$[\hat{\boldsymbol{s}}_i]_{t,s,l,\bar{c}} := \frac{\int_{\tau \in \mathscr{T}_s} \Delta_\tau^{i,l} d\tau}{\sum_{s \in \mathbb{S}_j} \int_{\tau \in \mathscr{T}_s} \Delta_\tau^{i,l} d\tau}, \ \forall s \in \mathbb{S}_j, \ \forall l \in \mathbb{L}, \forall (t,j) = i, \ \forall i \in \mathbb{I}, \tag{3.31}$$

is such that $\boldsymbol{\delta} = \hat{\boldsymbol{s}} - \boldsymbol{s}^*(\eta) \in \Xi(\eta)$.

Conceptually, our calibration procedure for η aims at finding the minimal worst-case cost expansion plan that is behaviorally-consistent with the LQG models. As such, given that the optimal value of problem (3.8) is non-decreasing in η, Algorithm 2 will equivalently aim at identifying the smallest level of robustness η that leads to a robust solution that is behaviorally consistent.

Lemma 6. *Algorithm 2 is guaranteed to terminate in* $\log_2(\bar{\eta}/\varepsilon)$ *iterations, where* ε *as the required level of precision and* $\bar{\eta}$ *the largest level of robustness considered (see equation* (3.6)*).*

Proof. This follows straightforwardly from the fact that Algorithm 2 is a bisection algorithm on interval $[0, \ \bar{\zeta}]$ that terminates when the interval has a length smaller than ε. □

3.6 Case study and numerical results

The proposed approach to obtain robust behaviorally consistent expansion strategy is implemented on a realistic case study based on the energy system of the Arc Lémanique

Algorithme 2 : A bisection algorithm to find a minimal worst-case optimal behaviorally-consistent expansion plan

Set a desired level of tolerance ε;
Set $\eta_{\mathrm{LB}} = 0$, $\eta_{\mathrm{UB}} = \bar{\eta}$;
while $\eta_{UB} - \eta_{LB} > \varepsilon$ **do**
  Set $\eta = (\eta_{\mathrm{LB}} + \eta_{UB})/2$;
  Solve problem (3.29) with $\Xi(\eta)$ to obtain $\boldsymbol{s}^*$ and $\bar{\gamma}^*$;
  for $(i,l) \in \mathbb{I} \times \mathbb{L}$ **do**
    Set $\lambda^{i,l}(\tau)$ according to equation (3.30);
    Solve the MFG in Section 3.4 for region l and time-season period i using $\lambda^{i,l}(\tau)$ to obtain $\Delta^{i,l}$;
  end
  Set $\hat{\boldsymbol{s}}$ as defined in (3.31);
  if $\hat{\boldsymbol{s}} - \boldsymbol{s} \in \Xi(\eta)$ **then**
    $\eta_{\mathrm{UB}} \leftarrow \eta$;
  else
    $\eta_{\mathrm{LB}} \leftarrow \eta$;
  end
  Solve problem (3.29) with $\Xi(\eta_{\mathrm{UB}})$ and return $\boldsymbol{x}^*$;
end

region (Cantons of Geneva and Vaud, in Switzerland). Studies show that by 2050 up to 70% of the total transportation demand in the region can potentially be satisfied by electric vehicles (Babonneau et al., 2017). ETEM covers three regional buses and 142 different technologies including central electricity and heat production and distributed energy resources. We model 21 types of final demands which are categorized into industrial, residential and transportation. Based on the optimum annual share of EVs in satisfying useful transportation demand reported in Babonneau et al. (2017), we have calculated the annual final demand for electricity to charge EVs. Figure 3.3 shows the reference energy system (RES) modeled by ETEM. All data regarding ETEM model is from Babonneau and Haurie (2019) and for a more detailed description of the energy system in the Arc Lémanique region, we refer interested readers to this paper.

The purpose of this numerical study is i) to estimate the level of contribution of EV users in demand response programs by a LQG models, and ii) to obtain the robust capacity expansion policies that are behaviorally consistent. To do so, first we calibrate the LQG model with our available data. Then using Algorithm 2 we calibrate $\Xi(\eta)$ in order to estimate the required level of uncertainty in the R-ETEM to have behaviorally consistent expansion policies. In addition, we perform a sensitivity analysis on the cost parameter q in the LQG model. Finally, we analyze the influence of demand response and demand response uncertainty on expansion strategies and asses the price of robustness.

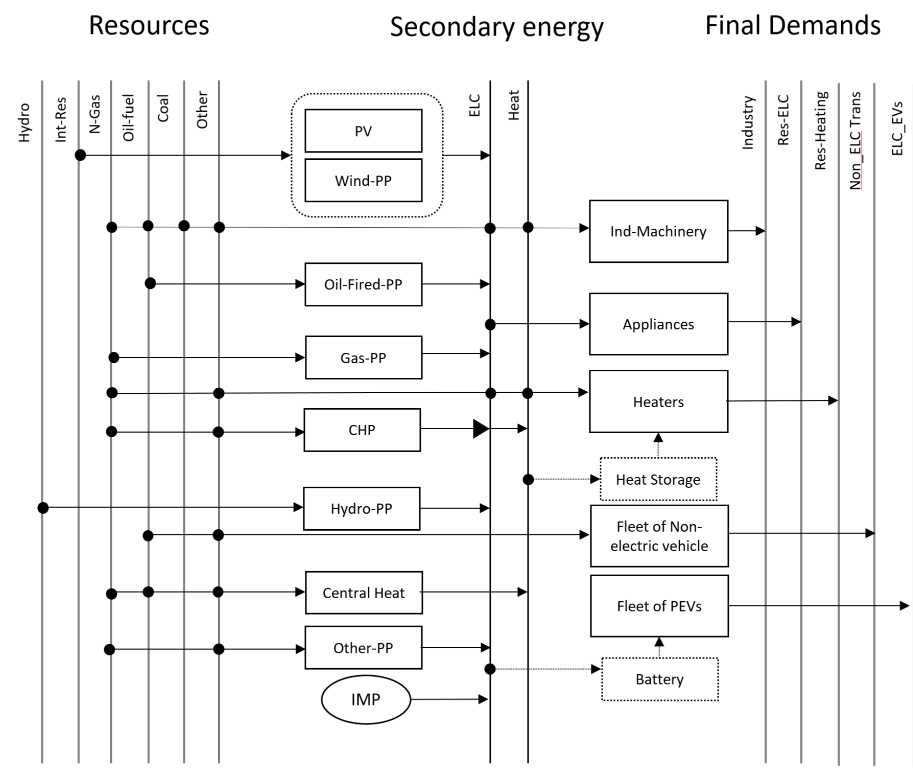

Figure 3.3: Arc Lémanique reference energy system, where Int-Res stands for intermittent resources (solar and wind), N-Gas for natural gas, Oil-fuel for processed oil products, Other for hydrogen and additional sources of energy (such as solid waste and wood and geothermal), ELC for electricity, RES for residential, PP for power plant, CHP for combined heat and power plant, IMP for electricity import, Ind-Machinery for industrial machinery. Other-PP includes geothermal, fuel-cell and municipal waste power plants. ELC_EVs is the perturbed useful demand (i.e. $\bar{c}$) for electricity to charge the battery of EVs.

3.6.1 Calibrating the LQG models

In order to calibrate the LQG models, we use the useful demand of transportation which is satisfied by EVs, optimally calculated in Babonneau and Haurie (2019), as the aggregated discharge. In other words, we fix the demand to the actual demand in the deterministic ETEM model. Then ETEM calculates the marginal cost of electricity production given the already available mix of technologies in the energy system. The marginal cost is passed to LQG model and we calibrate the range of LQG parameters, i.e., q, $\overline{q}$ and κ so that it replicates actual demand responses close to the aggregated discharge. Figure 3.4a represents the average charging and discharging of a EV users in the fleet in a specific season and region $(i,l) = (1,1)$. The average state of charge (SOC) for this control is also presented in Figure 3.4b. After aggregating the results of the LQG models, Figure 3.5 compares the nominal versus actual (i.e. simulated using LQG models) DR for the base period in the model.

3.6.2 Algorithm convergence and q-sensitivity on a 15-years horizon

In this section, we illustrate the convergence of Algorithm 2 when R-ETEM considers a 15-years horizon from 2015 to 2030.

Algorithm convergence

Figure 3.6 displays the convergence of Algorithm 2 in terms of upper and lower bounds for the optimal level of uncertainty η^*. We observe that the algorithm converges after 6 iterations to within a tolerance of $\varepsilon = 0.01$ and that the optimal level of uncertainty is $\eta^* \approx 0.26$. It means that at optimum, the R-ETEM model needs to be immunized against a 26% deviation of the actual demand response from the planned demand response. We note that when $\eta < \eta^*$ the obtained policies are not behaviorally consistent, while for $\eta > \eta^*$ the model is too conservative thus leading to larger worst-case total cost than necessary. Therefore, when $\eta > \eta^*$, one can consider the optimal value of R-ETEM as an upper bound on the the minimal behaviorally consistent worst-case cost of the system,

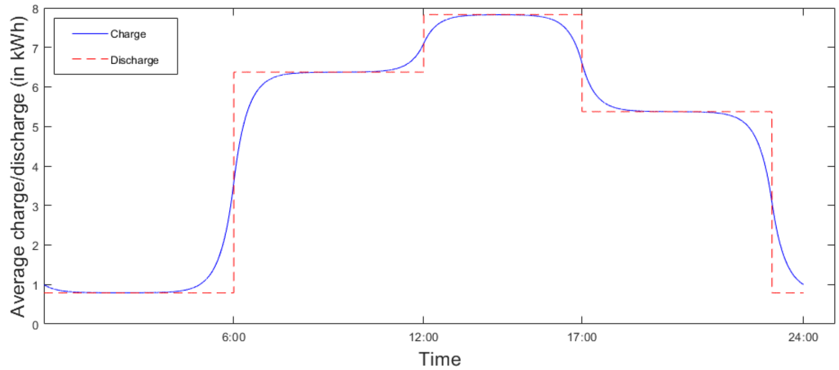

(a)

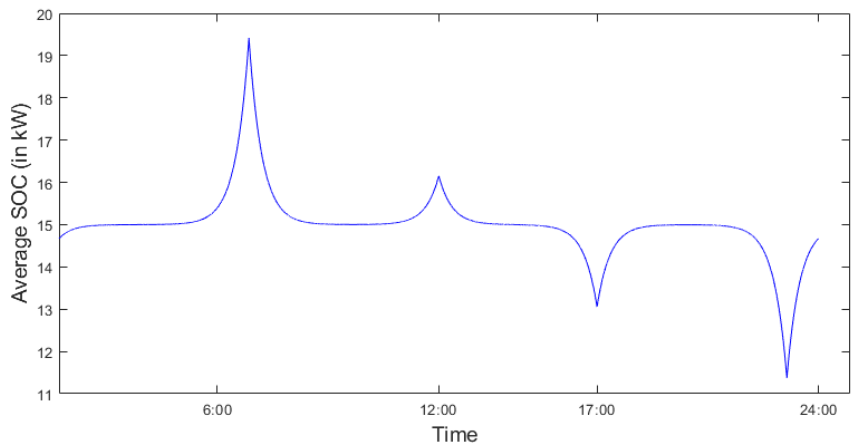

(b)

Figure 3.4: (a) Average charge and discharge and (b) average state of the charge (SOC) of batteries in the whole fleet for one day in a representative region and time period after LQG calibration.

and similarly as a lower bound when $\eta < \eta^*$. These two bounds are presented in Figure 3.6.

Preliminary analysis of sensitivity to cost of deviation from DLC

In this section, we tested the sensitivity of the minimal behaviorally-consistent level of uncertainty η^*, and its associated worst case total cost of the system, with respect to the cost of deviation from the fleet desired level of charge (DLC) and present the results in Figure 3.7. When the cost of deviation from the DLC is higher, the minimal level of uncertainty is reduced. Indeed, when this cost is high, EV users are less responsive to

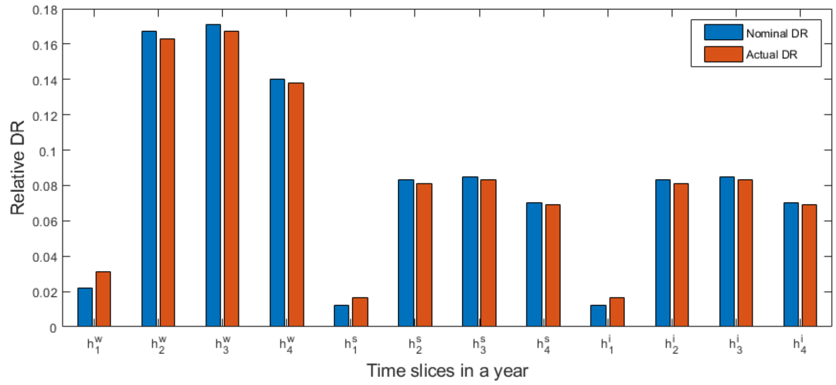

Figure 3.5: Actual versus nominal relative demand responses for all time slices in a year. h_1^w - h_4^w refer to four time slices in a winter day, h_1^s - h_4^s refer to four time slices in a summer day, and h_1^i - h_4^i refer to four time slices in a intermediate day (see table 3.1 for a definition of each time slice).

the electricity price. In other words, they are willing to charge their battery at any price in order to reach their desired level of charge. In this situation, the charging behaviour becomes easier to predict based on mobility data. This in turns allows the model to employ a lower level of uncertainty in the planning phase.

3.6.3 Robustness of optimal capacity expansion plans for a 40-years horizon

In this section, we numerically show how robust behaviorally-consistent solutions affect the electricity generation capacities in the long-term R-ETEM covering 40 years from 2015 to 2055. Moreover, we compare the actual, planned and nominal DRs. Finally, we discuss the performance of robust behaviorally-consistent solutions. In summary, we observed that the behaviorally-consistent expansion model builds more capacity to avoid the high cost of the worst-case scenario.

Electricity generation capacity and planned DR

We now turn to studying the effect of accounting for demand response robustness on the capacity expansion strategy. Specifically, we will compare the strategies obtained

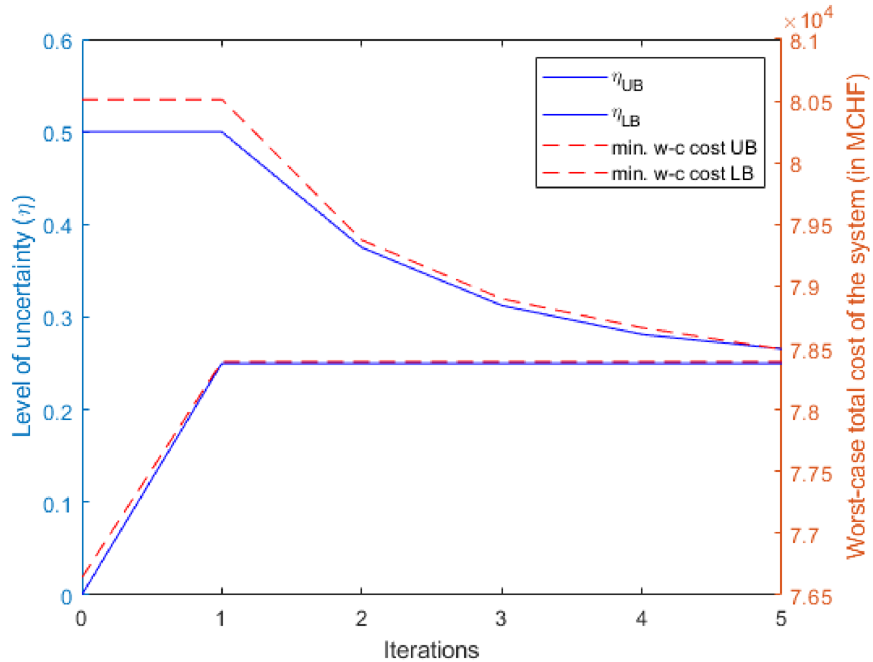

Figure 3.6: Convergence of the bisection algorithm (with $\varepsilon = 0.01$) in terms of the upper and lower bounds for the behaviorally-consistent level of uncertainty η (left axis) and the minimal worst-case total cost of the system (right axis).

for three different models: i) a model (referred to as No-DR) that assumes EV users do not participate in DR programs; (ii) a model (BI-DR) that assumes that EV users participate in DR programs and their contribution is fully predictable, hence is behaviorally inconsistent; and (iii) a model (RBC-DR) that assumes that EV users participate in DR programs and accounts for behavioral DR divergences. Numerically, the No-DR plan is obtained from solving (3.1) with $v_{t,s,l,c} = 0$ in constraint (3.3), the BI-DR plan is obtained from solving (3.1), and finally, the RBC-DR plan is obtained from solving (3.8) with η^* calibrated using Algorithm 2.

Remark 2. *We note that, in the context of this work, one can theoretically demonstrate that the approach proposed in Babonneau et al. (2020) for coupling a "robustified" version of ETEM with an LQG model produces the same solutions as the BI-DR model. These theoretical findings might explain the empirical observations made in Babonneau et al. (2020) that their coupling scheme would terminate after a single iteration, thus returning*

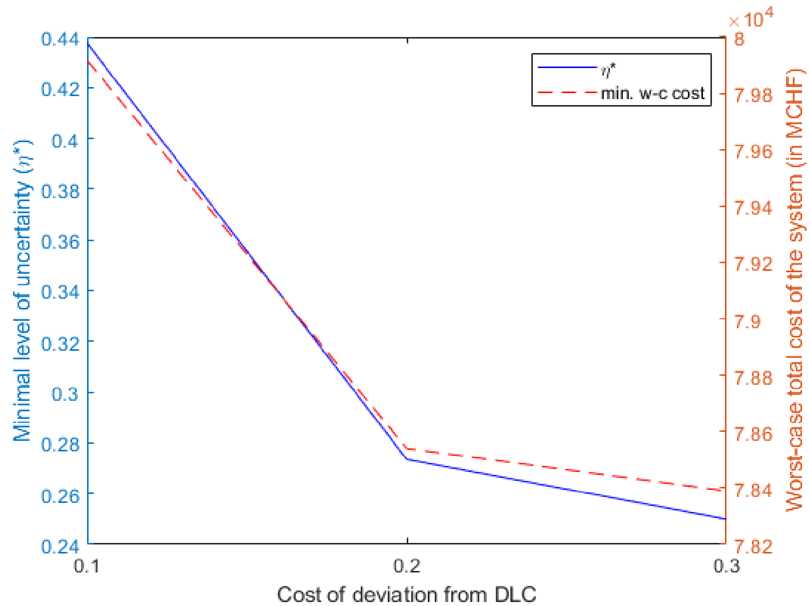

Figure 3.7: Sensitivity analysis of the minimal behaviorally-consistent level of uncertainty $\eta*$ (left axis) and and worst-case total cost of the system on the cost of deviation from the desired level of the charge (DLC).

the solution of the nominal ETEM model. We encourage interested readers to Appendix 3.8.4 for more details.

Figure 3.8 shows the total installed capacity proposed by these three models. We observe that BI-DR installs the least amount of capacity compared to the other two models. This is because this model expects that peak loads will be significantly reduced using DR programs. By contrast, the No-DR is installing more gas power plant (around 39% more than BI-DR) to meet the peak load. Finally, RBC-DR builds extra capacity compared to BI-DR to immunize against deviations from planned EV user behaviors. The extra capacity is mostly provided by CHP technologies.

Figure 3.9 compares the actual, planned and nominal DRs. The LQG model suggests, for all seasons, to charge more during time-slice h_1 (between 11:00 p.m. and 6:00 a.m.) as the marginal price of electricity is cheaper during these hours following lower network loads. Note that as the differences between the actual DR and the planned DR in all time-slices are always less that $\eta* \approx 0.26$, the expansion planning of the R-ETEM is indeed

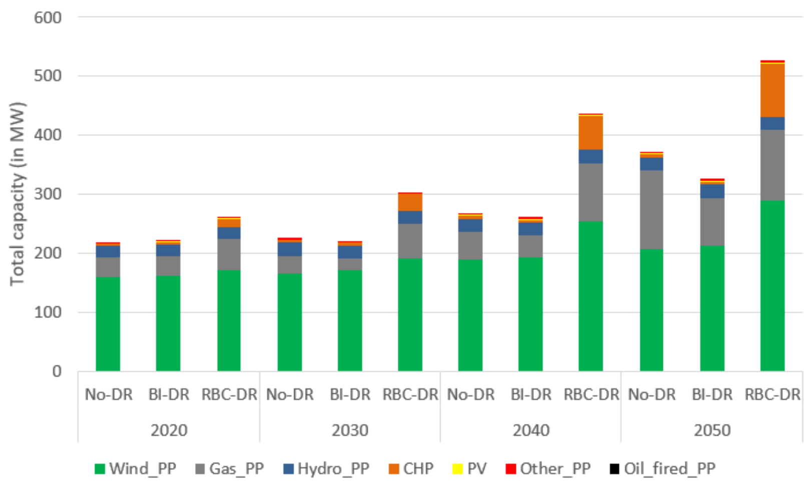

Figure 3.8: Evolution of the electricity generation capacity plan for 3 types of models: an optimal plan with no demand response (No-DR), an optimal plan with DR but behaviorally-inconsistent (BI-DR), and a robustly optimal behaviorally-consistent plan with DR (RBC-DR).

remains behaviorally consistent.

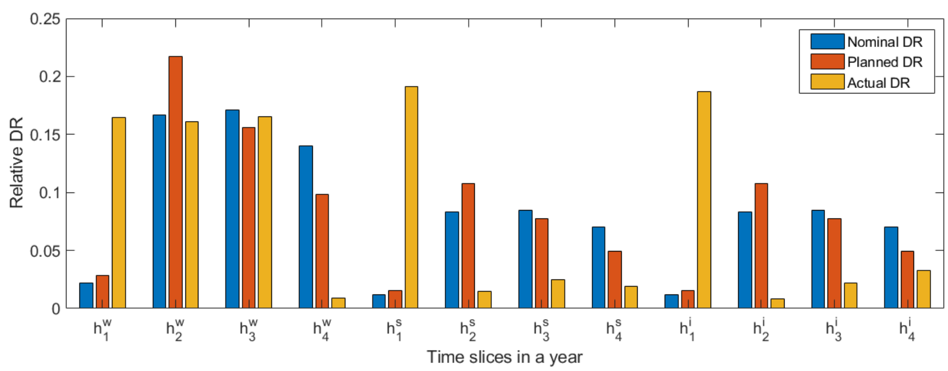

Figure 3.9: Nominal, actual and planned demand responses over all time-slices in a period. h_1^w to h_4^w refer to four time slices in a winter day, h_1^s to h_4^s refer to four time slices in a summer day, and h_1^i to h_4^i refer to four time slices in an intermediate day (see Table 3.1 for a definition of each time slice).

Robust performance

In this section, we evaluate the performance of the solutions of the three models introduced in Section 3.6.3, i.e., No-DR, BI-DR and RBC-DR. In doing so, we define two measures: i) the total cost of the system if we assume the scenario proposed by LQG

Table 3.2: Comparison of actual and nominal costs of No-DR, BI-DR and RBC-DR solutions.

	Actual cost MCHF	Rel diff[1] %	Nominal cost MCHF	Rel diff[1] %
RBC-DR	177,182.5	-	174,245.5	-
BI-DR	188,238.6	6.2%	170,328.3	-2.2%
No-DR	184,059.7	3.9%	170,931.5	-1.9%

[1] Relative difference with RBC-DR

happens (referred to as "actual cost"), and ii) the total cost of the system if we assume the planned DR happens with zero deviation (referred to as "nominal cost"). In order to obtain the actual and nominal costs, first we solve the three models and store the value of variable $\boldsymbol{x}$ and $\boldsymbol{s}_i$ in $(\boldsymbol{x}^{No-DR}, \boldsymbol{s}_i^{No-DR})$,$(\boldsymbol{x}^{BI-DR}, \boldsymbol{s}_i^{BI-DR})$, and $(\boldsymbol{x}^{RBC-DR}, \boldsymbol{s}_i^{RBC-DR})$. Then, we plug these values in problem (3.7) and re-optimize it fixing the value of $\boldsymbol{\zeta}_i$ to $\boldsymbol{s}_i - \hat{\boldsymbol{s}}_i$ and 0 for actual and nominal costs respectively. $\hat{\boldsymbol{s}}_i$ is the solution of LQG as is calculated in (3.31). Table 3.2 shows that RBC-DR reduces the actual cost of the system by 3.9% compared to No-DR model, and 6.2% compared to BI-DR model. Indeed, by installing more generation capacities (see again Figure 3.8), RBC-DR solutions are better protected against the realization of the actual DR calculated using the LQG models. But, in a case that there would be zero deviation between the actual DR and the planned DR, the cost of RBC-DR is 1.9% and 2.2% more than No-DR and BI-DR costs, respectively. This loss in performance under the nominal model can be interpreted as the price of robustness.

3.7 Conclusion

In this paper, we develop a robust approach to evaluate the interaction between electric vehicle (EV) users and utilities on a long-term generation expansion planning (GEP) problem for a smart grid. Namely, we employ a specific robust multi-period adjustable GEP problem, called R-ETEM, where the EV user demand responses are uncertain. In R-ETEM, one decides first on the optimal capacity expansion of the network and the planned demand responses. Then, on a seasonal basis, after observing the actual demand responses, the procurement decisions are taken. In our case study, we choose to immunize

R-ETEM against perturbations of the demand response of a large fleet of EVs. To do so, we employ a linear quadratic game (LQG) to simulate the average charging behavior of the fleet. The utility broadcasts a real-time price which depends on the marginal cost of electricity production (calculated by solving R-ETEM) and the aggregated charging demand of the fleet. In response, EV users minimize a cost function consisting of the price paid for electricity and the cost of deviation from a comfort zone. We propose a novel coupling algorithm between R-ETEM and the LQG with the purpose of adjusting the level of uncertainty in R-ETEM and obtaining behaviorally-consistent expansion plans. The coupling algorithm necessarily converges in finite iterations. We test our algorithm on a real-world case study based on the energy system of the "Arc Lémanique" region (Cantons of Geneva and Vaud, in Switzerland). The results reinforce that a behaviorally-consistent expansion plan can significantly reduce the total actual cost of the system (e.g., by 6.2% in our case study). One interesting direction to extend the results of this paper is to model EV users as being prosumers. In this scenario, EVs can provide the grid with power and ancillary services, such as providing reserved capacity and frequency control. However, it is also necessary to consider the mechanism of battery degradation and designing a compensation plan. Another direction could be to consider additional operational details in the GEP problem, such as supply uncertainty, to obtain more precise capacity expansion policies.

3.8 Appendix

3.8.1 Formulation of the ETEM energy model

In this appendix, we present the formulation of the deterministic ETEM energy model. We mostly use a similar notation as in Aliakbarisani et al. (2020). However, we slightly depart from Aliakbarisani et al. (2020) where we use a regional demand response variable $\boldsymbol{V}$. Let us start with the definition of the sets. Set $\mathbb{T}$ indicates time periods, and $\mathbb{S}$ is the set of time slices inside a period. Set $\mathbb{C}$ is for energy commodities, and $\mathbb{P}$ identifies

Table 3.3: Nomenclature used in ETEM formulation

$t \in \mathbb{T}$	Index for time period	$\beta_{t,s,p}$	Capacity factor
$s \in \mathbb{S}$	Index for time-slices	η_c	Network efficiency
$p \in \mathbb{P}$	Index for technologies	$\eta^t_{f,f'}$	Technology efficiency
$c \in \mathbb{C}$	Index for energy commodities	$\lambda''_{t,s,l,l',c}$	Transmission cost
$c_s \in \mathbb{CS}$	Index for energy storage	$\lambda'_{t,s,c}$	Export cost
$f \in \mathbb{F}$	Index for energy flows	$\lambda_{t,s,c}$	Import cost
$l \in \mathbb{L}$	Index for buses (geographical zones)	$\nu_{t,s,c}$	Maximum deviation from nominal demand response
$j \in \mathbb{J}$	Index for seasons		
$i \in \mathbb{I}$	Index for period-seasons (t,j)	$\nu_{t,p}$	Variable cost
$\mathbb{P}^C_c \subseteq \mathbb{P}$	Set of technologies consuming c	$\Omega_{t,l,p}$	Available capacity of technology p
$\mathbb{P}^P_c \subseteq \mathbb{P}$	Set of technologies producing c	$\pi_{t,p}$	Fixed production cost
$\mathbb{P}^R \subseteq \mathbb{P}$	Set of intermittent technologies	ρ	Discount factor
$\mathbb{C}^I \subseteq \mathbb{C}$	Set of imported commodities	θ^c_p	Proportion of output c from technology p that can be used in peak period
$\mathbb{C}^{\mathscr{D}} \subseteq \mathbb{C}$	Set of useful demands		
$\mathbb{C}^{EX} \subseteq \mathbb{C}$	Set of exported commodities	l_p	Life duration of technology p
$\mathbb{C}^{TR} \subseteq \mathbb{C}$	Set of transmitted commodities	$\Theta_{t,l,d}$	Annual final demand
$\mathbb{C}_f \subseteq \mathbb{C}$	Set of commodities linked to flow f	$\upsilon_{t,s,c}$	Nominal demand response
$\mathbb{C}^{\mathscr{G}} \subseteq \mathbb{C}$	Set of commodities with margin reserve	$\rho_{t,s,c}$	Required reserve for commodity $c \in \mathbb{C}^{\mathscr{G}}$
$\mathbb{S}^j \subseteq \mathbb{S}$	Set of time-slices s in season j	$\boldsymbol{C}_{t,l,p}$	Variable for new capacity addition
$\mathbb{S}^s \subseteq \mathbb{S}$	Set of successive time-slices of s	$\boldsymbol{C}^T_{t,l,p}$	Total installed capacity
$\mathbb{S}^{\mathscr{G}} \subseteq \mathbb{S}$	Set of time-slices in peak period	$\boldsymbol{P}_{t,s,l,p,c}$	Variable for activity of technology p
$\mathbb{FI}_p \subseteq \mathbb{F}$	Set of inputs to technology p	$\boldsymbol{I}_{t,s,l,c}$	Variable for import
$\mathbb{FO}_p \subseteq \mathbb{F}$	Set of outputs from technology p	$\boldsymbol{E}_{t,s,l,c}$	Variable for export
$\alpha_{t,p}$	Investment cost	$\boldsymbol{T}_{t,s,l,l',c}$	Variable for regional transmission
		$\boldsymbol{V}_{t,s,l,d}$	Variable for demand response

technologies. Input-output energy flows are shown in set $\mathbb{F}$. Finally, set $\mathbb{L}$ identifies buses in different geographical zones. A full nomenclature is presented Table 3.3.

$$\min \sum_{t,l} \rho^t \cdot \Bigg(\sum_p \alpha_{t,p} \boldsymbol{C}_{t,l,p} + \pi_{t,p} \Big(\sum_{k=0}^{l_p-1} \boldsymbol{C}_{t-k,l,p} + \Omega_{t,l,p} \Big) + \sum_{s,c} \nu_{t,p} \boldsymbol{P}_{t,s,l,p,c} + \sum_{s,c} (\lambda_{t,s,c} \boldsymbol{I}_{t,s,l,c} - \lambda'_{t,s,c} \boldsymbol{E}_{t,s,l,c}) + \sum_{s,l',c} \lambda''_{t,s,l,l',c} \boldsymbol{T}_{t,s,l,l',c} \Bigg), \tag{3.32a}$$

s.t.

$$\Big(\sum_{p \in \mathbb{P}^P_c} \boldsymbol{P}_{t,s,l,p,c} + \boldsymbol{I}_{t,s,l,c} \Big) \eta_c + \sum_{l' \neq l} (\eta_c \boldsymbol{T}_{t,s,l',l,c} - \boldsymbol{T}_{t,s,l,l',c}) \geq \sum_{p \in \mathbb{P}^C_c} \boldsymbol{P}_{t,s,l,p,c} + \boldsymbol{E}_{t,s,l,c}$$
$$\forall\, t,s,l,c \in \mathbb{C}/\mathbb{C}^{\mathscr{D}} \tag{3.32b}$$

$$\Big(\sum_{l,p \in \mathbb{P}^c} \theta^c_p \cdot \beta_{t,s,p} \Big(\sum_{k=0}^{l_p-1} \boldsymbol{C}_{t-k,l,p} + \Omega_{t,l,p} \Big) + \sum_{l,p \in \mathbb{P}^P_c/\mathbb{P}_c} \theta^c_p \cdot \boldsymbol{P}_{t,s,l,p,c} + \boldsymbol{I}_{t,s,l,c} \Big) \cdot \rho_{t,s,c}$$

$$\geq \sum_{l,p\in\mathbb{P}^C_c} \boldsymbol{P}_{t,s,l,p,c} + \boldsymbol{E}_{t,s,l,c} \quad \forall t, s \in \mathbb{S}^{\mathscr{G}}, c \in \mathbb{C}^{\mathscr{G}} \tag{3.32c}$$

$$\eta_c \sum_{p\in\mathbb{P}^{P_c}} \boldsymbol{P}_{t,s,l,p,c} = \sum_{p\in\mathbb{P}^{C_c}, s'\in\mathbb{S}^s} \boldsymbol{P}_{t,s',l,p,c} \quad \forall t,s,l,c \in \mathbb{CS} \tag{3.32d}$$

$$\sum_{p\in\mathbb{P}^P_c} \boldsymbol{P}_{t,s,l,p,c} \geq \Theta_{t,l,c} \boldsymbol{V}_{t,s,l,c} \qquad \forall t,s,l,c \in \mathbb{C}^{\mathscr{D}} \tag{3.32e}$$

$$\upsilon_{t,s,l,c}(1-\nu_{t,s,l,c}) \leq \boldsymbol{V}_{t,s,l,c} \leq \upsilon_{t,s,l,c}(1+\nu_{t,s,l,c}) \quad \forall t,s,l,c \in \mathbb{C}^{\mathscr{D}} \tag{3.32f}$$

$$\sum_{s\in\mathscr{S}_j} \boldsymbol{V}_{t,s,l,c} = \sum_{s\in\mathscr{S}_j} \upsilon_{t,s,l,c} \qquad \forall t,l,c \in \mathbb{C}^{\mathscr{D}}, j \in \mathbb{J} \tag{3.32g}$$

$$\sum_{c:p\in\mathbb{P}^P_c} \boldsymbol{P}_{t,s,l,p,c} \leq \beta_{t,s,p} \left(\sum_{k=0}^{l_p-1} \boldsymbol{C}_{t-k,l,p} + \Omega_{t,l,p} \right) \qquad \forall t,s,l,p \notin \mathbb{P}^R, \tag{3.32h}$$

$$\sum_{c\in\mathbb{C}^p_m} \boldsymbol{P}_{t,s,l,p,c} = \beta_{t,s,p} \left(\sum_{k=0}^{l_p-1} \boldsymbol{C}_{t-k,l,p} + \Omega_{t,l,p} \right) \qquad \forall t,s,l,p \in \mathbb{P}^R \tag{3.32i}$$

$$\sum_{c\in\mathbb{C}_{f'}} \boldsymbol{P}_{t,s,l,p,c} = \eta^t_{f,f'} \cdot \sum_{c\in\mathbb{C}_f} \boldsymbol{P}_{t,s,l,p,c} \quad \forall f \in \mathbb{FI}_p, f' \in \mathbb{FO}_p, t,s,l,p \tag{3.32j}$$

$$(\boldsymbol{P},\boldsymbol{I},\boldsymbol{E},\boldsymbol{T}) \in \mathscr{Y}, \ \boldsymbol{C} \in \mathscr{X}, \ \boldsymbol{P} \geq 0, \boldsymbol{I} \geq 0, \boldsymbol{E} \geq 0, \boldsymbol{T} \geq 0, \boldsymbol{C} \geq 0, \boldsymbol{V} \geq 0. \tag{3.32k}$$

Equation (3.32a) is the objective function which minimizes a discounted sum of all costs of the system over all regions ($l \in \mathbb{L}$) and time periods ($t \in \mathbb{T}$). The total cost include investment, fixed and operational costs of technologies, import, export and transmission costs of energy commodities. Variables $\boldsymbol{C},\boldsymbol{P},\boldsymbol{I},\boldsymbol{E},\boldsymbol{T}$ are capacity installation, energy production, import, export and regional transmission of energy, respectively. Parameters $\alpha_{t,p}$, $\nu_{t,p}$, $\lambda_{t,s,c}$, $\lambda'_{t,s,c}$, $\lambda''_{t,s,l,l',c}$, and $\pi_{t,p}$ are unit costs of the associated variables.

A commodity balance constraint is presented in (3.32b). It assures that during each period t and time-slice s, the regional procurement of energy commodity c is more or equal to the overall consumption. Total regional procurement, the left-hand side of the constraint, includes i) total production of commodity c in region l by all technologies producing it ($\mathbb{P}^P_c$), ii) import of commodity c, and iii) net transmission of commodity c into region l. It is worth mentioning that while import and export refers to the transfer of energy from outside of the boundary of the energy system, energy transmission is the amount of energy which is produced in one region and transmitted to another region inside the energy system. Input energy c is multiplied by parameter η_c, which is the efficiency of the network with respect to commodity c, e.g., the efficiency of electricity transmission lines. On the right-hand side, the overall consumption of commodity c is equal to internal consumption by technologies $\mathbb{P}_c^C$, added to the amount of commodity that is exported.

In addition to the energy balance constraint (3.32b), for commodities in set $\mathbb{C}^{\mathscr{G}}$ constraint (3.32c) provides a safety margin, during peak time-slices $s \in \mathbb{S}^{\mathscr{G}}$, to protect against random events not explicitly represented in the model. Parameter $\rho_{t,s,c} \in [0,\ 1]$ represents the fraction of reserved capacity needed to ensure covering the peak load. The left-hand side of this constraint models the maximum amount of commodity $c \in \mathbb{C}^{\mathscr{G}}$ that can be procured in period t and time-slice s. This amount is equal to the sum of i) the maximum production capacity of commodity c by technologies that produce it as their main output ($\mathbb{P}_c$), ii) the production of commodity c by technologies that produce c as their by-product of their main activity, and iii) the import of commodity c. The left-hand side is the total consumption similar to constraint (3.32b). Parameter θ_p^c is the proportion of technology production that can be used during the peak period. Constraint (3.32d) is a balance constraint for storage commodities. Namely, depending on the efficiency of the storage technology i.e., η_c, a fixed portion of the amount of storage at time-slice s can be restored at subsequent time-slice s'. Constraints (3.32e) - (3.32g) together are modeling the notion of demand response. Specifically, constraint (3.32e) ensures that for each commodity c in the set of useful demand $\mathbb{C}^{\mathscr{D}}$, the total production accounted for by variable $\boldsymbol{P}$ must satisfy the demand in each time slice and region. Parameter $\Theta_{t,l,c}$ is the total demand and variable $\boldsymbol{V}_{t,s,l,c}$ attempts to optimally distribute the total demand of period t into all time-slices $s \in \mathbb{S}$ inside period t and region l. Constraint (3.32f) limits the demand response to vary within a certain margin $\nu_{t,s,l,c}$ from the nominal value, i.e., $\upsilon_{t,s,l,c}$. In addition, since the shift of the demand is only possible between time slices in a day, constraint (3.32g) limits the sum of the demand response to be equal to the sum of the nominal values in each season.

Constraint (3.32h), known as capacity factor constraint, limits the maximum activity of each technology to the available capacity of that technology. Parameter $\beta_{t,s,p}$ is the capacity factor and simply represents the fraction of the total capacity which is available at each time-slice. In addition, constraint (3.32i) enforces that the production by renewable technologies take their maximum possible value considering the total available capacity of these technologies. Constraint (3.32j) defines the efficiency of technology p. Parameter $\eta^{t}_{f,f'}$ is the efficiency of technology p with output flow $f^{'} \in \mathbb{FO}_p$ and input flow $f \in \mathbb{FI}_p$.

Finally, space $\mathscr{X}$ and $\mathscr{Y}$ represent operational, technical, and economical constraints that define the structure of the energy network and a desirable space for capacity and procurement decisions. For example, constraints on CO_2 emissions, technology market penetration, technology ramping, total energy import and export are among the constraints that form up the space $\mathscr{X}$ and $\mathscr{Y}$. Since these constraints do not affect our analysis in this paper, we omit to report them and refer the reader to Babonneau et al. (2017) for a complete list of constraints.

3.8.2 Differences between R-ETEM and Babonneau et al. (2020)

In Babonneau et al. (2020), the authors propose to robustify the deterministic version of ETEM presented in (3.1) by replacing constraint (3.3) with the robust constraint:

$$\Delta^{\min}_{l,c} \leq \sum_{t\in\mathbb{T}}\sum_{s\in\mathbb{S}} \Theta_{t,l,c}\boldsymbol{V}_{t,s,l,c} \leq \Delta^{\max}_{l,c}\,, \forall\, l \in \mathbb{L}, c \in \mathbb{C}^{\mathscr{D}} \tag{3.33}$$

with

$$\Delta^{\min}_{l,c} := \sup_{\xi\in\hat{\Xi}} \sum_{(t,s)\in\mathbb{T}\times\mathbb{S}} \Delta^{l,c,-}_{t} + (\bar{\Delta}^{l,c}_{t} - \Delta^{l,c,-}_{t})\xi_t$$

and

$$\Delta^{\max}_{l,c} := \inf_{\xi\in\hat{\Xi}} \sum_{(t,s)\in\mathbb{T}\times\mathbb{S}} \Delta^{l,c,+}_{t} + (\bar{\Delta}^{l,c}_{t} - \Delta^{l,c,+}_{t})\xi_t$$

where $\hat{\Xi}$ is a budgeted uncertainty set in the non-negative orthant, while $[\Delta^{l,c,-}_{t}, \Delta^{l,c,+}_{t}]$ is a confidence region for the demand response at time t, and $\bar{\Delta}^{l,c}_{t}$ is the average value. We first note that (3.33) is a relaxation (therefore an optimistic approximation) of:

$$\Delta^{l,c,-}_{t} + (\bar{\Delta}^{l,c}_{t} - \Delta^{l,c,-}_{t})\xi_t \leq \Theta_{t,l,c}\boldsymbol{V}_{t,s,l,c}\,, \forall\, \xi \in \hat{\Xi}, \forall\, (s,t,l,c) \in \mathbb{S}\times\mathbb{T}\times\mathbb{L}\times\mathbb{C}^{\mathscr{D}} \tag{3.34a}$$

$$\Theta_{t,l,c}\boldsymbol{V}_{t,s,l,c} \leq \Delta^{l,c,+}_{t} + (\bar{\Delta}^{l,c}_{t} - \Delta^{l,c,+}_{t})\xi_t\,, \forall\, \xi \in \hat{\Xi}, \forall\, (s,t,l,c) \in \mathbb{S}\times\mathbb{T}\times\mathbb{L}\times\mathbb{C}^{\mathscr{D}}, \tag{3.34b}$$

which imposes a robust set of upper and lower bonds on the demand response plan in each time-slice. Thus, we can interpret any feasible solution of constraint (3.34) (and approximately (3.33)) as identifying a demand response that has a robust potential of being plausible with respect to the distribution that generated the statistics captured in $(\Delta_t^{l,c,-}, \bar{\Delta}_t, \Delta_t^{l,c,+})$. In particular, the constraint offers no protection against the demand response deviations captured by $(\Delta_t^{l,c,-}, \bar{\Delta}_t, \Delta_t^{l,c,+})$. This is especially noticeable when considering that $\Delta_{l,c}^{\min}$ and $\Delta_{l,c}^{\max}$ are both non-increasing and non-decreasing with respect to $\Delta_t^{l,c,-}$ and $\Delta_t^{l,c,+}$ respectively. This implies that has the observed demand response becomes more uncertain, constraint (3.33) actually becomes less restrictive for $\Theta_{t,l,c}$.

3.8.3 Numerical algorithm to obtain the average optimal state of charge and demand

To compute the representative EV user's average optimal state of charge and average demand, one needs to numerically solve FBODEs $(3.14-3.15)$ to obtain (η_τ, w_τ). Then, the solution, $(\Psi_\tau, \Pi_\tau)_{\tau\in[0,T]}$ is obtained by solving the FBODEs $(3.21-3.22)$. Finally, we the average optimal state of charge and average demand is calculated with the feedback formula (3.28) and (3.27). This procedure is done with a simple implementation of the Euler Scheme. Algorithm 3 presents the detail of this implementation.

3.8.4 Babonneau et al. (2020) returns the solution of BI-DR model (3.1)

In the following, we identify weak conditions under which the approach proposed in Babonneau et al. (2020) converges in one iteration simply recommending the solution of the behaviorally inconsistent demand response model (3.1).

Assumption 2. *The aggregate mean demand profile $\mathbb{E}[u_\tau^*]$ observed at equilibrium in the mean field game integrates to the total discharge captured by the discharge profile, i.e.*

$$\int_0^T \Delta_\tau d\tau = \int_0^T v_\tau d\tau. \tag{3.35}$$

Algorithme 3 : Euler Scheme for numerical computation of the MFG equilibrium

Discretize [0,T], into points $\tau \in \mathscr{T}$, with uniform gap $d\tau$;
Set $\eta_T = \bar{q}$;
for $\tau \in \mathscr{T}$ **do**
  $\eta_{\tau-d\tau} \leftarrow \eta_\tau - \big(\frac{\eta_\tau^2}{\kappa} - q\big)d\tau$
end
Set $w_0 = \frac{s^2\eta_0^2}{\kappa^2}$
for $\tau \in \mathscr{T}$ **do**
  $w_{\tau+d\tau} \leftarrow w_\tau + \big(\frac{\varepsilon^2\eta_\tau^2}{\kappa^2} - w_\tau\frac{2q}{\eta_\tau}\big)d\tau$
end
Set $\Psi_T = 0$
for $\tau \in \mathscr{T}$ **do**
  $\Psi_{\tau-d\tau} \leftarrow \Psi_\tau - \big(F_1(\tau)\Psi_\tau^2 + F_2(\tau)\Psi_\tau + B_1(\tau)\Psi_\tau + B_2(\tau)\big)d\tau$
end
Set $\Pi_T = -\bar{q}a_T$
for $\tau \in \mathscr{T}$ **do**
  $\Pi_{\tau-d\tau} \leftarrow \Pi_\tau - \big(F_1(\tau)\Psi_\tau\Pi_\tau - F_3(\tau)\Psi_\tau + B_1(\tau)\Pi_\tau + B_3(\tau)\big)d\tau$
end
Set $m_0 = a_0$
for $\tau \in \mathscr{T}$ **do**
  $m_{\tau+d\tau} \leftarrow m_\tau + \big(-\frac{\eta_\tau m_\tau + \Pi_\tau}{\kappa+\Psi_\tau+\lambda(\tau)} - v_\tau\big)d\tau$
end
for $\tau \in \mathscr{T}$ **do**
  $\Delta_\tau \leftarrow -\frac{\eta_\tau m_\tau + \Pi_\tau}{\kappa+\Psi_\tau+\lambda(\tau)}$
end

This assumption is for instance satisfied when the mean field game captures the stationary behavior of agents over a repeated period of length T. Indeed, in this context the optimal average state of charge at the beginning and end of the horizon must be equal, i.e. $\mathbb{E}[X_0^*] = \mathbb{E}[X_T^*]$. Specifically,

$$0 = \mathbb{E}[X_T^*] - \mathbb{E}[X_0^*] = \mathbb{E}\left[x_0 + \int_0^T (u_\tau^* - v_\tau)d\tau + \varepsilon W_T\right] - \mathbb{E}[X_0^*]$$
$$= \int_0^T \mathbb{E}[u_\tau^*]d\tau - \int_0^T v_\tau d\tau \Rightarrow \int_0^T \Delta_\tau d\tau = \int_0^T v_\tau d\tau$$

Proposition 7. *Let Assumption 2 be satisfied and the discharge profile of all linear quadratic game models be consistent with the total demand of the season that it describes* *in ETEM, namely:*

$$\sum_{s\in\mathscr{S}} \Theta_{t,l,c}\upsilon_{t,s,l,c} = \int_0^T v_\tau^{l,c,t} d\tau\,, \forall t \tag{3.36}$$

Then, the solution $\overline{V}$ *of the non-robust ETEM* (3.1) *satisfies constraint* (3.33) *formulated using the equilibrium of the mean field games.*

Proof. We will first show that the lower bounding part of constraint (3.33) is satisfied. Namely,

$$\Delta_{l,c}^{\min} = \sup_{\xi\in\hat{\Xi}} \sum_{(t,s)\in\mathbb{T}\times\mathbb{S}} \Delta_{t,s}^{l,c,-} + (\hat{\Delta}_{t,s}^{l,c} - \Delta_{t,s}^{l,c,-})\xi_{t,s} \tag{3.37a}$$

$$= \sup_{\xi\in\hat{\Xi}} \sum_{(t,s)\in\mathbb{T}\times\mathbb{S}} \hat{\Delta}_{t,s}^{l,c} - (\hat{\Delta}_{t,s}^{l,c} - \Delta_{t,s}^{l,c,-})(1-\xi_{t,s}) \tag{3.37b}$$

$$= \sum_{(t,s)\in\mathbb{T}\times\mathbb{S}} \hat{\Delta}_{t,s}^{l,c} - \inf_{\xi\in\hat{\Xi}} \sum_{(t,s)\in\mathbb{T}\times\mathbb{S}} (\hat{\Delta}_{t,s}^{l,c} - \Delta_{t,s}^{l,c,-})(1-\xi_{t,s}) \tag{3.37c}$$

$$\leq \sum_{(t,s)\in\mathbb{T}\times\mathbb{S}} \hat{\Delta}_{t,s}^{l,c} \tag{3.37d}$$

$$= \sum_{t\in\mathbb{T}} \left(\int_0^T \Delta_\tau^{l,c,t} d\tau\right) \tag{3.37e}$$

$$= \sum_{t\in\mathbb{T}} \left(\int_0^T v_\tau^{l,c,t} d\tau\right) \tag{3.37f}$$

$$= \sum_{t\in\mathbb{T}} \left(\sum_{s\in\mathbb{S}} \Theta_{t,l,c}\upsilon_{t,s,l,c}\right) \tag{3.37g}$$

$$= \sum_{t\in\mathbb{T}} \left(\sum_{s\in\mathbb{S}} \Theta_{t,l,c}\overline{V}_{t,s,l,c}\right) \tag{3.37h}$$

where $\hat{\Xi} := \{\xi \in [0,\,1]^{\mathbb{T}\times\mathbb{S}} | \sum_{(t,s)\in\mathbb{T}\times\mathbb{S}} \xi_{t,s} \leq \Gamma\}$, and which would confirm that $\overline{V}$ satisfies the lower bound. In details, the inequality in (3.37d) follows from the infimum being greater or equal to zero due to $\hat{\Xi} \subseteq [0,\,1]^{\mathbb{T}\times\mathbb{S}}$ and $\hat{\Delta}_{t,s}^{l,c} \geq \Delta_{t,s}^{l,c,-}$. The equality in (3.37d) follows from $\int_0^T \Delta_\tau^{l,c,t} d\tau = \sum_{s\in\mathbb{S}} \hat{\Delta}_{t,s}^{l,c}$ based on the definition of $\hat{\Delta}_{t,s}^{l,c}$. Equalities (3.37f) and (3.37g) follows from Assumption 2 and (3.36) respectively. Finally, (3.37g) follows from the fact that $\overline{V}$ satisfies constraint (3.4).

A similar analysis can be done to prove that $\overline{V}$ also satisfies the upper bound in constraint (3.33). □

The following corollary follows directly from Proposition 7 given the nature of the procedure described in Babonneau et al. (2020), which consists in 1) solving model (3.1); 2) communicating the price information to the LQG model; 3) identifying the equilibrium using the limiting MFG; 4) adding (or updating) constraint (3.33) to model (3.1) based on MFG solution; 5) iterating until convergence.

Corollary 8. *Given that Assumption 2 is satisfied and that the discharge profile of all linear quadratic game models be consistent with the total demand of the season that it describes in ETEM, then the procedure described in Babonneau et al. (2020) will converge in one iteration prescribing the expansion plan that minimizes model* (3.1).

We note that Appendix A.2 of Aliakbarisani et al. (2020) also recently demonstrated that the same behavior occurs for Babonneau et al. (2020)'s approach when the behavioral model is such that its expected demand response matches the demand response prescribed by model (3.1). Comparatively speaking, Assumption 2 is weaker as it only requires that this match occurs for the total demand response over all the time slices of each period t.

References

Aliakbarisani, S., Bahn, O., and Delage, E. (2020). Affine decision rule approximation to immunize against demand response uncertainty in smart grids capacity planning. *Les Cahiers du GERAD*, G–2020–62.

Babonneau, F., Caramanis, M., and Haurie, A. (2016). A linear programming model for power distribution with demand response and variable renewable energy. *Applied Energy*, 181:83 – 95.

Babonneau, F., Caramanis, M., and Haurie, A. (2017). ETEM-SG: Optimizing regional smart energy system with power distribution constraints and options. *Environmental Modeling & Assessment*, 22(5):411–430.

Babonneau, F., Foguen, R., Haurie, A., and Malhame, R. (2020). Coupling a power dispatch model with a wardrop or mean-field-game equilibrium model. *Dyn Games Appl*.

Babonneau, F. and Haurie, A. (2019). Energy technology environment model with smart grid and robust nodal electricity prices. *Annals of Operations Research*, 274.

Ben-Tal, A., Goryashko, A., Guslitzer, E., and Nemirovski, A. (2004). Adjustable robust solutions of uncertain linear programs. *Mathematical Programming*, 99(2):351–376.

Bloom, J. A. (1983). Solving an electricity generating capacity expansion planning problem by generalized benders' decomposition. *Operations Research*, 31(1):84–100.

Bloom, J. A., Caramanis, M., and Charny, L. (1984). Long-range generation planning using generalized benders' decomposition: Implementation and experience. *Operations Research*, 32(2):290–313.

Chen, Y., Bušić, A., and Meyn, S. (2014). Individual risk in mean field control with application to automated demand response. In *53rd IEEE Conference on Decision and Control*, pages 6425–6432.

Collins, S., Deane, J. P., Poncelet, K., Panos, E., Pietzcker, R. C., Delarue, E., and Ó Gallachóir, B. P. (2017). Integrating short term variations of the power system into integrated energy system models: A methodological review. *Renewable and Sustainable Energy Reviews*, 76:839–856.

Couillet, R., Perlaza, S. M., Tembine, H., and Debbah, M. (2012). A mean field game analysis of electric vehicles in the smart grid. In *2012 Proceedings IEEE INFOCOM Workshops*, pages 79–84.

De Jonghe, C., Hobbs, B. F., and Belmans, R. (2011). Integrating short-term demand response into long-term investment planning. *Cambridge Working Paper in Economics*.

de Queiroz, A., Mulcahy, D., Sankarasubramanian, A., Deane, J., Mahinthakumar, G., Lu, N., and DeCarolis, J. (2019). Repurposing an energy system optimization model for seasonal power generation planning. *Energy*, 181:1321–1330.

Deane, J., Chiodi, A., Gargiulo, M., and Ó Gallachóir, B. P. (2012). Soft-linking of a power systems model to an energy systems model. *Energy*, 42(1):303–312. 8th World Energy System Conference, WESC 2010.

Dehghan, S., Amjady, N., and Kazemi, A. (2014). Two-stage robust generation expansion planning: A mixed integer linear programming model. *IEEE Transactions on Power Systems*, 29(2):584–597.

Dubarry, M., Devie, A., and McKenzie, K. (2017). Durability and reliability of electric vehicle batteries under electric utility grid operations: Bidirectional charging impact analysis. *Journal of Power Sources*, 358:39–49.

Gaur, A. S., Das, P., Jain, A., Bhakar, R., and Mathur, J. (2019). Long-term energy system planning considering short-term operational constraints. *Energy Strategy Reviews*, 26:100383.

Gomes, D. and Saude, J. (2018). A mean-field game approach to price formation in electricity markets. *arXiv:1807.07088v1*.

Han, D., Wu, W., Sun, W., and Yan, Z. (2018). A two-stage robust stochastic programming approach for generation expansion planning of smart grids under uncertainties. In *2018 IEEE Power Energy Society General Meeting (PESGM)*, pages 1–5.

Helistö, N., Kiviluoma, J., Morales-España, G., and O'Dwyer, C. (2021). Impact of operational details and temporal representations on investment planning in energy systems dominated by wind and solar. *Applied Energy*, 290. Funding Information: N.H. has received funding from the Jenny and Antti Wihuri Foundation. This work has been supported by the Strategic Research Council at the Academy of Finland, project ?Transition to a Resource Efficient and Climate Neutral Electricity System (EL-TRAN)?

(grant number 314319). This project has received funding from the European Union's Horizon 2020 research and innovation programme under grant agreement No 864276. Ciara O'Dwyer has received funding from the European Union Horizon 2020 research and innovation programme under grant agreement No 774629. Publisher Copyright: © 2021 The Authors Copyright: Copyright 2021 Elsevier B.V., All rights reserved.

Huang, M., Malhamé, R. P., and Caines, P. E. (2006). Large population stochastic dynamic games: closed-loop McKean-Vlasov systems and the Nash certainty equivalence principle. *Commun. Inf. Syst.*, 6(3):221–251.

Koltsaklis, N. E. and Dagoumas, A. S. (2018). State-of-the-art generation expansion planning: A review. *Applied Energy*, 230:563 – 589.

Koltsaklis, N. E. and Georgiadis, M. C. (2015). A multi-period, multi-regional generation expansion planning model incorporating unit commitment constraints. *Applied energy*, 158:310–331.

Lasry, J.-M. and Lions, P.-L. (2006). Jeux à champ moyen. I. Le cas stationnaire. *C. R. Math. Acad. Sci. Paris*, 343(9):619–625.

Lindholm, L., Sandberg, M., and Szepessy, A. (2017). A mean field game model of an electricity market with consumers minimizing energy cost through dynamic battery usage. *Digitala Vetenskapliga Arkivet*.

Lohmann, T. and Rebennack, S. (2017). Tailored benders decomposition for a long-term power expansion model with short-term demand response. *Management Science*, 63(6):2027–2048.

Ma, Z., Callaway, D. S., and Hiskens, I. A. (2013). Decentralized charging control of large populations of plug-in electric vehicles. *IEEE Transactions on Control Systems Technology*, 21(1):67–78.

Mejía-Giraldo, D. and McCalley, J. (2014). Adjustable decisions for reducing the price of robustness of capacity expansion planning. *IEEE Transactions on Power Systems*, 29(4):1573–1582.

Mohsenian-Rad, A.-H., Wong, V. W. S., Jatskevich, J., Schober, R., and Leon-Garcia, A. (2010). Autonomous demand-side management based on game-theoretic energy consumption scheduling for the future smart grid. *IEEE Transactions on Smart Grid*, 1(3):320–331.

Poncelet, K., Delarue, E., Six, D., Duerinck, J., and D'haeseleer, W. (2016). Impact of the level of temporal and operational detail in energy-system planning models. *Applied Energy*, 162:631–643.

Ringkjøb, H.-K., Haugan, P. M., Seljom, P., Lind, A., Wagner, F., and Mesfun, S. (2020). Short-term solar and wind variability in long-term energy system models - a european case study. *Energy*, 209:118377.

Tchuendom, R., Malhame, R., and Caines, P. (2019). A quantilized mean field game approach to energy pricing with application to fleets of plug-in electric vehicles. *Communication présentée à 58th IEEE Conference on Decision and Control (CDC 2019)*, pages 299–304.

Uddin, K., Dubarry, M., and Glick, M. B. (2018). The viability of vehicle-to-grid operations from a battery technology and policy perspective. *Energy Policy*, 113:342–347.

Wang, Z., Yue, D., Liu, J., and Xu, Z. (2019). A stackelberg game modelling approach for aggregator pricing and electric vehicle charging. In *2019 IEEE 28th International Symposium on Industrial Electronics (ISIE)*, pages 2209–2213.

Wyrwa, A., Suwała, W., Pluta, M., Raczyński, M., Zyśk, J., and Tokarski, S. (2022). A new approach for coupling the short- and long-term planning models to design a pathway to carbon neutrality in a coal-based power system. *Energy*, 239:122438.

Zeng, B., Dong, H., Sioshansi, R., Xu, F., and Zeng, M. (2020). Bilevel robust optimization of electric vehicle charging stations with distributed energy resources. *IEEE Transactions on Industry Applications*, 56(5):5836–5847.

Zhu, Z., Lambotharan, S., Chin, W. H., and Fan, Z. (2016). A mean field game theoretic approach to electric vehicles charging. *IEEE Access*, 4:3501–3510.

Zou, J., Ahmed, S., and Sun, X. A. (2018). Partially adaptive stochastic optimization for electric power generation expansion planning. *INFORMS Journal on Computing*, 30(2):388–401.

Zugno, M., Morales, J. M., Pinson, P., and Madsen, H. (2013). A bilevel model for electricity retailers' participation in a demand response market environment. *Energy Economics*, 36:182–197.

General Conclusion

The growing share of renewable energies (RE) in electricity production networks increases the intermittency in the supply of electricity. Therefore, to maintain the reliability and stability of electricity networks, it is necessary to add further flexibility in the demand side by exploiting demand response (DR) programs. On the other hand, with the emergence of electric vehicles (EVs) in the urban transportation sector, a large scale implementation of DR programs becomes more easily achievable by electricity network operators. However, integrating DR of EV charging loads into the electricity grid is challenging because the level of the contribution by EV users in the DR programs is uncertain. The objective of this dissertation was to develop new cross-disciplinary decision making models that can provide interesting managerial insights on how to optimally and robustly integrate DR resources into the long-term capacity expansion of the smart grids. In doing so, we provided optimization models, advanced solution algorithms, and practical expansion policies for urban-scale energy systems in the presence of REs, in the supply side, and DR in the demand side. Our contributions was presented as three scientific articles. Specifically, in the first article, we adopted the formulation of the open-source capacity expansion planning problem, called Energy-Technology-Environment-Model (ETEM), to model the entire chain of energy system in the greater Montreal region. We analyzed the impact of different decarbonization pathways on the residential, commercial and transportation sectors, and provided insights on major technological shifts in each sector to achieve the decarbonization target. In addition, we quantified the optimal share of each sector in the total greenhouse gas (GHG) reduction target for the region. This article highlighted the importance of electrification of the transportation sector through the replacement of fossil fuels cars with EVs.

In the first article, the assumption was the energy planner has accurately estimated all the influential parameters of the planning problem. However, in a long-term planning problem there are many uncertainties. In the second and third articles, we addressed the demand response uncertainty (DRU). Specifically, in the second article, we introduced DRU as an implementation error of the DR variable in ETEM. We cast the resulting model as an adjustable multi-period robust optimization problem. In this setting, the planner first decides on the capacity expansion and the planned demand response. Then, periodically, after observing the actual level of DR in each season, the optimal energy procurement is determined. To solve the problem, we derive a Robust Multi-Period Conservative Approximation (RMPCA) of the problem, and develop a new Benders decomposition algorithm (inspired from Ardestani-Jaafari and Delage, 2018) to solve it. We numerically adjusted the level of uncertainty in the developed robust ETEM (R-ETEM) by implementing an out-of-sample simulation.

In the third article, we turn our focus on the uncertainty of DR exclusively provided by EV users. In this article we adopted a linear-quadratic game (LQG) model, originally developed by Tchuendom et al. (2019), to simulate the average battery charging behavior of a large fleet of EVs. Then, we designed a new coupling algorithm between the charging behavior model and the R-ETEM with the objective of adjusting the level of uncertainty in R-ETEM. In other words, contrary to the second article, where the level of uncertainty was determined by an out-of-sample simulation, in the third article, information on the actual charging behavior was used to adjust the level of uncertainty in R-ETEM.

The results of this research is useful for policy-makers who want to plan for the expansion of the energy network, while considering i) interconnection between energy networks and advanced technological and socio-economic innovations in other sectors, specifically the transportation sector, and ii) environmental issues associated to the expansion of energy networks. The developed robust generation expansion planning (GEP) problem could be run on a rolling horizon basis, in order to generate more realistic expansion solutions that takes into account the future technological innovations. Although the focus in this research was on the demand response provided by the EV users, the modeling framework could be easily extended to other DR providers, such as prosumers in residential and commercial sectors who uses smart technologies to satisfy space heating demand.

Finally, we present a few interesting research avenues that might be worth exploring to expand on the content of this dissertation. First, one can consider other sources of uncertainty, such as supply uncertainty, fuel price, etc. in a capacity expansion planning to identify more robust capacity expansion strategies. To handle the resulting large-scale problem, a heuristic greedy algorithm could be utilized. A second interesting direction could be to develop a joint energy-transportation optimization problem, where the mobility behavior could be endogenously modeled. In these types of problem, the estimation of DR contribution by EVs would be more realistic because they consider more details of the dynamic of mobility decisions. Developing similar models to the charging behavior model of the third article, in order to estimate the DR contribution of the residential sector could be another interesting direction to explore. In the third article, we have modeled the interaction between the electricity network and individual EV users. In another interesting setting, one could consider DR aggregators and large players. Specifically, with the advent of car-sharing companies, and fleet of autonomous shared electric vehicles, these large players may start playing an important role, and it will become important to evaluate their impact on the electricity networks.

Bibliography

Acha, S., Mariaud, A., Shah, N., and Markides, C. N. (2018). Optimal design and operation of distributed low-carbon energy technologies in commercial buildings. *Energy*, 142:578–591.

Adelman, D. and Uçkun, C. (2019). Dynamic electricity pricing to smart homes. *Operations Research*, 67(6):1520–1542.

Albana, K., Giulia, M., Paolo, Z., Andreea, I., Greet, J.-M., Brigitte, K., Rivas, C. S., Fabio, M.-F., and Paolo, B. (2016). Covenant of mayors: Greenhouse gas emissions achievements and projections. Technical report, European Commission.

Aliakbarisani, S., Bahn, O., and Delage, E. (2020a). Affine decision rule approximation to immunize against demand response uncertainty in smart grids capacity planning. *Les Cahiers du GERAD*, G–2020–62.

Aliakbarisani, S., Bahn, O., and Delage, E. (2020b). Affine decision rule approximation to immunize against demand response uncertainty in smart grids capacity planning. *Les Cahiers du GERAD*, G–2020–62.

Aliakbarisani, S., Bahn, O., Delage, E., and Foguen, R. (2021). Robust integration of electric vehicles charging load in smart grid's capacity expansion planning. *Les Cahiers du GERAD*, G-2021-44.

Amjady, N., Attarha, A., Dehghan, S., and Conejo, A. J. (2018). Adaptive robust expansion planning for a distribution network with DERs. *IEEE Transactions on Power Systems*, 33(2):1698–1715.

Amrollahi, M. H. and Bathaee, S. M. T. (2017). Techno-economic optimization of hybrid photovoltaic/wind generation together with energy storage system in a stand-alone micro-grid subjected to demand response. *Applied Energy*, 202:66–77.

Andrey, Christopher, Babonneau, Frédéric, Haurie, Alain, and Labriet, Maryse (2015). Modélisation stochastique et robuste de l´atténuation et de l´adaptation dans un système énergétique régional. application à la région midi-pyrénées. *Nat. Sci. Soc.*, 23(2):133–149.

Arasteh, H., Sepasian, M., and Vahidinasab, V. (2015). Toward a smart distribution system expansion planning by considering demand response resources. *Journal of Operation and Automation in Power Engineering*, 3(2):116–130.

Ardestani-Jaafari, A. and Delage, E. (2017). Linearized robust counterparts of two-stage robust optimization problems with applications in operations management. Technical report, Cahier du GERAD G-2016-69.

Ardestani-Jaafari, A. and Delage, E. (2018). The value of flexibility in robust location–transportation problems. *Transportation Science*, 52(1):189–209.

Asensio, M., Meneses de Quevedo, P., Muñoz-Delgado, G., and Contreras, J. (2018). Joint distribution network and renewable energy expansion planning considering demand response and energy storage—part i: Stochastic programming model. *IEEE Transactions on Smart Grid*, 9(2):655–666.

Babonneau, F., Caramanis, M., and Haurie, A. (2016). A linear programming model for power distribution with demand response and variable renewable energy. *Applied Energy*, 181:83 – 95.

Babonneau, F., Caramanis, M., and Haurie, A. (2017). ETEM-SG: Optimizing regional smart energy system with power distribution constraints and options. *Environmental Modeling & Assessment*, 22(5):411–430.

Babonneau, F., Foguen, R., Haurie, A., and Malhame, R. (2020). Coupling a power dispatch model with a wardrop or mean-field-game equilibrium model. *Dynamic Games and Applications*.

Babonneau, F. and Haurie, A. (2019). Energy technology environment model with smart grid and robust nodal electricity prices. *Annals of Operations Research*, 274.

Babonneau, F., Haurie, A., Tarel, G., and Thénié, J. (2012). Assessing the future of renewable and smart grid technologies in regional energy systems. *Swiss J Economics Statistics*, 148:229–273.

Baringo, L. and Baringo, A. (2018). A stochastic adaptive robust optimization approach for the generation and transmission expansion planning. *IEEE Transactions on Power Systems*, 33(1):792–802.

Ben-Tal, A., den Hertog, D., and Vial, J. (2015). Deriving robust counterparts of nonlinear uncertain inequalities. *Math. Program*, 149:265–299.

Ben-Tal, A., Goryashko, A., Guslitzer, E., and Nemirovski, A. (2004). Adjustable robust solutions of uncertain linear programs. *Mathematical Programming*, 99(2):351–376.

Bertsimas, D., Brown, D. B., and Caramanis, C. (2011). Theory and applications of robust optimization. *SIAM Review*, 53(3):464–501.

Bertsimas, D. and Georghiou, A. (2018). Binary decision rules for multistage adaptive mixed-integer optimization. *Math. Program.*, 167:395–433.

Bertsimas, D. and Sim, M. (2004). The price of robustness. *Operations Research*, 52(1):35–53.

Bertsimas, D. and Thiele, A. (2006). A robust optimization approach to inventory theory. *Operations Research*, 54(1):150–168.

Birge, J. R. and Louveaux, F. (2011). *Introduction to Stochastic Programming*, chapter Solution methods, pages 102–180. Springer-Verlag, New York, NY, USA, second edition.

Bloom, J. A. (1983). Solving an electricity generating capacity expansion planning problem by generalized benders' decomposition. *Operations Research*, 31(1):84–100.

Bloom, J. A., Caramanis, M., and Charny, L. (1984). Long-range generation planning using generalized benders' decomposition: Implementation and experience. *Operations Research*, 32(2):290–313.

CFUT (2019). Climate emergency urban opportunity, how national governments can secure economic prosperity and avert climate catastrophe by transforming cities. Technical report, Coalition For Urban Transitions (CFUT).

Chatterjee, N., Glick, R., and McNamee, B. (2018). Assessment of demand response and advanced metering. Technical report, Federal Energy Regulatory Commission.

Chen, Y., Bušić, A., and Meyn, S. (2014). Individual risk in mean field control with application to automated demand response. In *53rd IEEE Conference on Decision and Control*, pages 6425–6432.

Coelho, S., Russo, M., Oliveira, R., Monteiro, A., Lopes, M., and Borrego, C. (2018). Sustainable energy action plans at city level: A portuguese experience and perception. *Journal of Cleaner Production*, 176:1223–1230.

Collins, S., Deane, J. P., Poncelet, K., Panos, E., Pietzcker, R. C., Delarue, E., and Ó Gallachóir, B. P. (2017). Integrating short term variations of the power system into integrated energy system models: A methodological review. *Renewable and Sustainable Energy Reviews*, 76:839–856.

Couillet, R., Perlaza, S. M., Tembine, H., and Debbah, M. (2012). A mean field game analysis of electric vehicles in the smart grid. In *2012 Proceedings IEEE INFOCOM Workshops*, pages 79–84.

Dagoumas, A. (2014). Modelling socio-economic and energy aspects of urban systems. *Sustainable Cities and Society*, 13:192–206.

De Jonghe, C., Hobbs, B. F., and Belmans, R. (2011). Integrating short-term demand response into long-term investment planning. *Cambridge Working Paper in Economics*.

de Queiroz, A., Mulcahy, D., Sankarasubramanian, A., Deane, J., Mahinthakumar, G., Lu, N., and DeCarolis, J. (2019). Repurposing an energy system optimization model for seasonal power generation planning. *Energy*, 181:1321–1330.

Deane, J., Chiodi, A., Gargiulo, M., and Ó Gallachóir, B. P. (2012). Soft-linking of a power systems model to an energy systems model. *Energy*, 42(1):303–312. 8th World Energy System Conference, WESC 2010.

DeAngelo, B., Edmonds, J., Fahey, D., and Sanderson, B. (2017). Perspectives on climate change mitigation. *Climate Science Special Report: Fourth National Climate Assessment*, 1:393–410.

Dehghan, S., Amjady, N., and Kazemi, A. (2014). Two-stage robust generation expansion planning: A mixed integer linear programming model. *IEEE Transactions on Power Systems*, 29(2):584–597.

Dias, L., Simões, S., Gouveia, J., and Seixas, J. (2019). City energy modelling - optimising local low carbon transitions with household budget constraints. *Energy Strategy Reviews*, 26:100387.

DOE (2006). Benefits of demand response in electricity markets and recommendations for achieving them. Technical report, US Department of Energy, Washington DC.

Domínguez, R., Conejo, A. J., and Carrión, M. (2016). Investing in generation capacity: A multi-stage linear-decision-rule approach. *IEEE Transactions on Power Systems*, 31(6):4784–4794.

Dubarry, M., Devie, A., and McKenzie, K. (2017). Durability and reliability of electric vehicle batteries under electric utility grid operations: Bidirectional charging impact analysis. *Journal of Power Sources*, 358:39–49.

Dyson, M. E., Borgeson, S. D., Tabone, M. D., and Callaway, D. S. (2014). Using smart meter data to estimate demand response potential, with application to solar energy integration. *Energy Policy*, 73:607–619.

Elizondo, A., Pérez-Cirera, V., Strapasson, A., Fernández, J. C., and Cruz-Cano, D. (2017). Mexico's low carbon futures: An integrated assessment for energy planning and climate change mitigation by 2050. *Futures*, 93:14–26.

Forsberg, J. (2021). Energy transition in transportation: Applying times-based energy system optimisation models to sub-national levels. Technical report, Licentiate dissertation, Luleå University of Technology.

Forsberg, J. and Krook-Riekkola, A. (2021). Recoupling climate change and air quality: Exploring low-emission options in urban transportation using the times-city model. *Energies*, 14(11).

Gaur, A. S., Das, P., Jain, A., Bhakar, R., and Mathur, J. (2019). Long-term energy system planning considering short-term operational constraints. *Energy Strategy Reviews*, 26:100383.

Georghiou, A., Tsoukalas, A., and Wiesemann, W. (2020). A primal–dual lifting scheme for two-stage robust optimization. *Operations Research*, 68(2):572–590.

Gomes, D. and Saude, J. (2018). A mean-field game approach to price formation in electricity markets. *arXiv:1807.07088v1*.

Gärttner, J., Flath, C. M., and Weinhardt, C. (2018). Portfolio and contract design for demand response resources. *European Journal of Operational Research*, 266(1):340–353.

Han, D., Wu, W., Sun, W., and Yan, Z. (2018). A two-stage robust stochastic programming approach for generation expansion planning of smart grids under uncertainties. In *2018 IEEE Power Energy Society General Meeting (PESGM)*, pages 1–5.

He, S., Gao, H., Liu, J., and Liu, J. (2019). Distributionally robust optimal DG allocation model considering flexible adjustment of demand response. In *2019 IEEE Power Energy Society General Meeting (PESGM)*, pages 1–5.

Heinisch, V., Göransson, L., Odenberg, M., and Johnsson, F. (2019). Interconnection of the electricity and heating sectors to support the energy transition in cities. *International Journal of Sustainable Energy Planning and Management*, 24:57–66. ID: unige:154440.

Helistö, N., Kiviluoma, J., Morales-España, G., and O'Dwyer, C. (2021). Impact of operational details and temporal representations on investment planning in energy systems dominated by wind and solar. *Applied Energy*, 290. Funding Information: N.H. has received funding from the Jenny and Antti Wihuri Foundation. This work has been supported by the Strategic Research Council at the Academy of Finland, project ?Transition to a Resource Efficient and Climate Neutral Electricity System (EL-TRAN)? (grant number 314319). This project has received funding from the European Union's Horizon 2020 research and innovation programme under grant agreement No 864276. Ciara O'Dwyer has received funding from the European Union Horizon 2020 research and innovation programme under grant agreement No 774629. Publisher Copyright: © 2021 The Authors Copyright: Copyright 2021 Elsevier B.V., All rights reserved.

Huang, J., Pan, K., and Guan, Y. (2020). Multistage stochastic power generation scheduling co-optimizing energy and ancillary services. *INFORMS Journal on Computing. Advance online publication.*

Huang, M., Malhamé, R. P., and Caines, P. E. (2006). Large population stochastic dynamic games: closed-loop McKean-Vlasov systems and the Nash certainty equivalence principle. *Commun. Inf. Syst.*, 6(3):221–251.

Iancu, D. A. and Trichakis, N. (2014). Pareto efficiency in robust optimization. *Management Science*, 60(1):130–147.

IEA (2021). Empowering cities for a net zero future. Technical report, IEA, Paris.

Knueven, B., Ostrowski, J., and Watson, J.-P. (2020). On mixed-integer programming formulations for the unit commitment problem. *INFORMS Journal on Computing. Advance online publication.*

Koltsaklis, N. E. and Dagoumas, A. S. (2018). State-of-the-art generation expansion planning: A review. *Applied Energy*, 230:563–589.

Koltsaklis, N. E. and Georgiadis, M. C. (2015). A multi-period, multi-regional generation expansion planning model incorporating unit commitment constraints. *Applied energy*, 158:310–331.

Lasry, J.-M. and Lions, P.-L. (2006). Jeux à champ moyen. I. Le cas stationnaire. *C. R. Math. Acad. Sci. Paris*, 343(9):619–625.

Li, C., Dong, Z., Chen, G., Luo, F., and Liu, J. (2015). Flexible transmission expansion planning associated with large-scale wind farms integration considering demand response. *IET Generation, Transmission Distribution*, 9(15):2276–2283.

Lind, A. and Espegren, K. (2017). The use of energy system models for analysing the transition to low-carbon cities – the case of oslo. *Energy Strategy Reviews*, 15:44–56.

Lindholm, L., Sandberg, M., and Szepessy, A. (2017). A mean field game model of an electricity market with consumers minimizing energy cost through dynamic battery usage. *Digitala Vetenskapliga Arkivet*.

Liu, C., Deng, K., Wen, G., and Yu, X. (2019). Optimal scheduling of electric vehicle charging with energy storage facility in smart grid. In *IECON 2019 - 45th Annual Conference of the IEEE Industrial Electronics Society*, volume 1, pages 6549–6554.

Lohmann, T. and Rebennack, S. (2017). Tailored benders decomposition for a long-term power expansion model with short-term demand response. *Management Science*, 63(6):2027–2048.

Luss, H. (1984). Capacity expansion planning for a single facility product line. *European Journal of Operational Research*, 18(1):27–34.

Ma, Z., Callaway, D. S., and Hiskens, I. A. (2013). Decentralized charging control of large populations of plug-in electric vehicles. *IEEE Transactions on Control Systems Technology*, 21(1):67–78.

Magnanti, T. L. and Wong, R. T. (1981). Accelerating benders decomposition: Algorithmic enhancement and model selection criteria. *Operations Research*, 29(3):464–484.

Maroufmashat, A., Elkamel, A., Fowler, M., Sattari, S., Roshandel, R., Hajimiragha, A., Walker, S., and Entchev, E. (2015). Modeling and optimization of a network of energy hubs to improve economic and emission considerations. *Energy*, 93:2546–2558.

Maroufmashat, A., Sattari, S., Roshandel, R., Fowler, M., and Elkamel, A. (2016). Multi-objective optimization for design and operation of distributed energy systems through the multi-energy hub network approach. *Industrial & Engineering Chemistry Research*, 55(33):8950–8966.

Masson-Delmotte., P.Zhai, Pörtner, H.-O., Roberts, D., Skea, J., Shukla, P., Pirani, A., Moufouma-Okia, W., Péan, C., Pidcock, R., Connors, S., Matthews, J., Chen, Y., Zhou, X., Gomis, M., Lonnoy, E., T. Maycock, M. T., , and Waterfield, T. (2018). Summary for policymakers. in: Global warming of 1.5°c. an ipcc special report on the impacts of global warming of 1.5°c above pre-industrial levels and related global greenhouse gas emission pathways, in the context of strengthening the global response to the threat of climate change, sustainable development, and efforts to eradicate poverty. Technical report, Intergovernmental Panel on Climate Change.

Mehleri, E., Sarimveis, H., Markatos, N., and Papageorgiou, L. (2013). Optimal design and operation of distributed energy systems: Application to greek residential sector. *Renewable Energy*, 51:331–342.

Mejía-Giraldo, D. and McCalley, J. (2014). Adjustable decisions for reducing the price of robustness of capacity expansion planning. *IEEE Transactions on Power Systems*, 29(4):1573–1582.

Mirakyan, A. and De Guio, R. (2013). Integrated energy planning in cities and territories: A review of methods and tools. *Renewable and Sustainable Energy Reviews*, 22:289–297.

Mohsenian-Rad, A.-H., Wong, V. W. S., Jatskevich, J., Schober, R., and Leon-Garcia, A. (2010). Autonomous demand-side management based on game-theoretic energy consumption scheduling for the future smart grid. *IEEE Transactions on Smart Grid*, 1(3):320–331.

Municipal, M. (2020). Plan climat 2020-2030, pour une ville inclusive, résiliente et carboneutre. Technical report, Montreal Municipal.

Poncelet, K., Delarue, E., Six, D., Duerinck, J., and D'haeseleer, W. (2016). Impact of the level of temporal and operational detail in energy-system planning models. *Applied Energy*, 162:631–643.

Qi, N., Cheng, L., Xu, H., Wu, K., Li, X., Wang, Y., and Liu, R. (2020). Smart meter data-driven evaluation of operational demand response potential of residential air conditioning loads. *Applied Energy*, 279:115708.

Rahmaniani, R., Crainic, T. G., Gendreau, M., and Rei, W. (2017). The benders decomposition algorithm: A literature review. *European Journal of Operational Research*, 259(3):801–817.

Ringkjøb, H.-K., Haugan, P. M., Seljom, P., Lind, A., Wagner, F., and Mesfun, S. (2020). Short-term solar and wind variability in long-term energy system models - a european case study. *Energy*, 209:118377.

Roveto, M., Mieth, R., and Dvorkin, Y. (2020). Co-optimization of VaR and CVaR for data-driven stochastic demand response auction. *IEEE Control Systems Letters*, 4(4):940–945.

Scheller, F. and Bruckner, T. (2019). Energy system optimization at the municipal level: An analysis of modeling approaches and challenges. *Renewable and Sustainable Energy Reviews*, 105:444–461.

Shakouri, H. and Aliakbarisani, S. (2016). At what valuation of sustainability can we abandon fossil fuels? a comprehensive multistage decision support model for electricity planning. *Energy*, 107:60 – 77.

Shariatzadeh, F., Mandal, P., and Srivastava, A. K. (2015). Demand response for sustainable energy systems: A review, application and implementation strategy. *Renewable and Sustainable Energy Reviews*, 45:343–350.

Sion, M. (1958). On general minimax theorems. *Pacific Journal of Mathematics*, 8(1):171–176.

Ströhle, P. and Flath, C. M. (2016). Local matching of flexible load in smart grids. *European Journal of Operational Research*, 253(3):811–824.

Tchuendom, R., Malhame, R., and Caines, P. (2019). A quantilized mean field game approach to energy pricing with application to fleets of plug-in electric vehicles. *Communication présentée à 58th IEEE Conference on Decision and Control (CDC 2019)*, pages 299–304.

Uddin, K., Dubarry, M., and Glick, M. B. (2018). The viability of vehicle-to-grid operations from a battery technology and policy perspective. *Energy Policy*, 113:342–347.

Vaillancourt, K., Bahn, O., Frenette, E., and Sigvaldason, O. (2017). Exploring deep decarbonization pathways to 2050 for canada using an optimization energy model framework. *Applied Energy*, 195:774–785.

Vaillancourt, K., Bahn, O., and Sigvaldason, O. (2018). *The Canadian Contribution to Limiting Global Warming Below 2 °C: An Analysis of Technological Options and Regional Cooperation*, pages 227–244. Springer International Publishing, Cham.

Vatani, B., Chowdhury, B., and Lin, J. (2017). The role of demand response as an alternative transmission expansion solution in a capacity market. In *2017 IEEE Industry Applications Society Annual Meeting*, pages 1–7.

Venizelou, V., Philippou, N., Hadjipanayi, M., Makrides, G., Efthymiou, V., and Georghiou, G. E. (2018). Development of a novel time-of-use tariff algorithm for residential prosumer price-based demand side management. *Energy*, 142:633–646.

Wang, Z., Yue, D., Liu, J., and Xu, Z. (2019). A stackelberg game modelling approach for aggregator pricing and electric vehicle charging. In *2019 IEEE 28th International Symposium on Industrial Electronics (ISIE)*, pages 2209–2213.

Whitmore, J. and Pineau, P.-O. (2019). The state of energy in quebec -2019. Technical report, Chair of energy sector management, HEC Montreal.

Wuebbles, D., Easterling, D., Hayhoe, K., Knutson, T., Kopp, R., Kossin, J., Kunkel, K., LeGrande, A., Mears, C., Sweet, W., Taylor, P., Vose, R., and Wehner, M. (2017). Our globally changing climate. *Climate Science Special Report: Fourth National Climate Assessment*, 1:35–72.

Wyrwa, A., Suwała, W., Pluta, M., Raczyński, M., Zyśk, J., and Tokarski, S. (2022). A new approach for coupling the short- and long-term planning models to design a pathway to carbon neutrality in a coal-based power system. *Energy*, 239:122438.

Xydis, G. (2012). Development of an integrated methodology for the energy needs of a major urban city: The case study of athens, greece. *Renewable and Sustainable Energy Reviews*, 16(9):6705–6716.

Yanıkoğlu, I., Gorissen, B., and den Hertog, D. (2019). A survey of adjustable robust optimization. *European Journal of Operational Research*, 277(3):799–813.

Yuan, X.-C., Lyu, Y.-J., Wang, B., Liu, Q.-H., and Wu, Q. (2018). China's energy transition strategy at the city level: The role of renewable energy. *Journal of Cleaner Production*, 205:980–986.

Zeng, B., Dong, H., Sioshansi, R., Xu, F., and Zeng, M. (2020). Bilevel robust optimization of electric vehicle charging stations with distributed energy resources. *IEEE Transactions on Industry Applications*, 56(5):5836–5847.

Zhang, Q. and Zhang, S. (2019). Robust decision-making model for electricity retailers considering incentive-based demand response. In *2019 IEEE Sustainable Power and Energy Conference (iSPEC)*, pages 1157–1162.

Zhao, C., Wang, J., Watson, J., and Guan, Y. (2013). Multi-stage robust unit commitment considering wind and demand response uncertainties. *IEEE Transactions on Power Systems*, 28(3):2708–2717.

Zhu, Z., Lambotharan, S., Chin, W. H., and Fan, Z. (2016). A mean field game theoretic approach to electric vehicles charging. *IEEE Access*, 4:3501–3510.

Zou, J., Ahmed, S., and Sun, X. A. (2018). Partially adaptive stochastic optimization for electric power generation expansion planning. *INFORMS Journal on Computing*, 30(2):388–401.

Zugno, M., Morales, J. M., Pinson, P., and Madsen, H. (2013). A bilevel model for electricity retailers' participation in a demand response market environment. *Energy Economics*, 36:182–197.